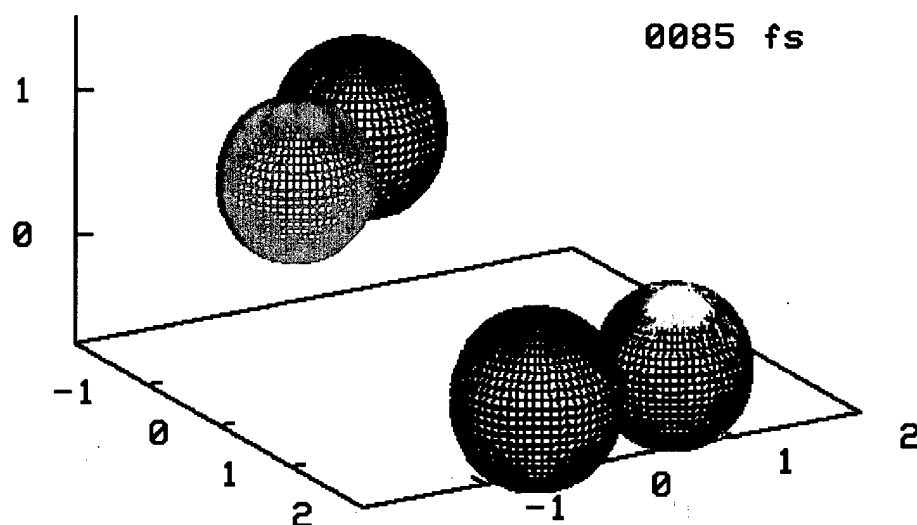


XVIIth Conference on the Dynamics of Molecular Collisions



**July 18-23, 1999
The Resort at Split Rock
Lake Harmony, PA**

**James J. Valentini, Chair
James T. Muckerman, Vice-Chair**

REPORT DOCUMENTATION PAGE

AFRL-SR-BL-TR-00-

Public reporting burden for this collection of information is estimated to average 1 hour per response, gathering and maintaining the data needed, and completing and reviewing the collection of information, including suggestions for reducing this burden, to Washington Headquarters Davis Highway, Suite 1204, Arlington, VA 22202-4302, and to the Office of Management and Budget

02046

ata sources,
spect of this
5 Jefferson
i03.

1. AGENCY USE ONLY (Leave blank)		2. REPORT DATE 25 Feb 00	3. REPORT TYPE AND DATES COVERED FINAL - 01 May 99 - 31 Aug 99	
4. TITLE AND SUBTITLE Co-Sponsorship of 1999 Conference on the Dynamics of Molecular Collision			5. FUNDING NUMBERS F49620-99-1-0225	
6. AUTHOR(S) Dr. James J. Valentini				
7. PERFORMING ORGANIZATION NAME(S) AND ADDRESS(ES) Columbia University 351 Engineering Terrace, Mail Code 2205 1210 Amsterdam Avenue New York NY 10027			8. PERFORMING ORGANIZATION REPORT NUMBER	
9. SPONSORING/MONITORING AGENCY NAME(S) AND ADDRESS(ES) AFOSR/NL 801 N. Randolph St., Rm 732 Arlington VA 22203-1977			10. SPONSORING/MONITORING AGENCY REPORT NUMBER	
11. SUPPLEMENTARY NOTES				
12a. DISTRIBUTION AVAILABILITY STATEMENT Approved for Public Release: Distribution Unlimited			12b. DISTRIBUTION CODE	
13. ABSTRACT (Maximum 200 words) This was the seventeenth edition of the Conference on the Dynamics of Molecular Collisions, which initially concentrated on molecular beams research but soon was broadened. Financial support for the conference was provided by the US Air Force Office of Scientific Research and Lambda Physik. Administrative support has been contributed by Columbia University. Printing of the meeting program was contributed by Brookhaven Science Associates, operators of Brookhaven National Laboratory under contract with the US Department of Energy.				
14. SUBJECT TERMS Molecular, Conference, Collisions			15. NUMBER OF PAGES 87	
			16. PRICE CODE	
17. SECURITY CLASSIFICATION OF REPORT UNCLASS	18. SECURITY CLASSIFICATION OF THIS PAGE UNCLASS	19. SECURITY CLASSIFICATION OF ABSTRACT UNCLASS	20. LIMITATION OF ABSTRACT	

**XIIth CONFERENCE ON THE
DYNAMICS OF MOLECULAR COLLISIONS**

July 18-23, 1999

**The Resort at Split Rock
Lake Harmony, Pennsylvania**

Chairman: James J. Valentini, Columbia University
**Vice-Chairman: James T. Muckerman, Brookhaven National
Laboratory**
**Treasurers: Donald G. Truhlar and W. Ronald Gentry,
University of Minnesota**

HISTORY OF THE CONFERENCE

This will be the seventeenth edition of the Conference on the Dynamics of Molecular Collisions, which initially concentrated on molecular beams research but soon was broadened. A brief history is provided by the following list, which includes the location and the chairman, with the chairman's institutional affiliation:

- I. 1965, New Hampton, New Hampshire; John Fenn (Yale University)
- II. 1968, Andover, New Hampshire; John C. Polanyi (University of Toronto)
- III. 1970, Oak Ridge, Tennessee; E. F. Green (Brown University)
- IV. 1972, Plymouth, New Hampshire; Sheldon Datz (Oak Ridge National Laboratory)
- V. 1974, Santa Cruz, California; James L. Kinsey (Massachusetts Institute of Technology)
- VI. 1976, Plymouth, New Hampshire; Bruce E. Mahan (University of California, Berkeley)
- VII. 1978, Pacific Grove, California; Yuan T. Lee (University of California, Berkeley)
- VIII. 1981, Plymouth, New Hampshire; R. James Cross (Yale University)
- IX. 1983, Gull Lake, Minnesota; W. Ronald Gentry (University of Minnesota)
- X. 1985, Snowbird, Utah; Donald G. Truhlar (University of Minnesota)
- XI. 1987, Wheeling, West Virginia; Paul Dagdigian (The Johns Hopkins University)
- XII. 1989, Pacific Grove, California; William H. Miller (University of California, Berkeley)
- XIII. 1991, Lake George, New York; James M. Farrar (University of Rochester)
- XIV. 1993, Helen, Georgia; Joel M. Bowman (Emory University)
- XV. 1995, Pacific Grove, California; Daniel Neumark (University of California, Berkeley)
- XIV. 1997, Gull Lake, Minnesota; George Schatz (Northwestern University)

ACKNOWLEDGMENT

Financial support for the conference has been provided by the U.S. Air Force Office of Scientific Research and by Lambda Physik.

Administrative support has been contributed by Columbia University.

Printing of the meeting program was contributed by Brookhaven Science Associates, operators of Brookhaven National Laboratory under contract with the U.S. Department of Energy.

XVIIth Conference on the Dynamics of Molecular Collisions

The Resort at Split Rock, Lake Harmony, Pennsylvania

July 18-23, 1999

James J. Valentini, Chairman; James T. Muckerman, Vice Chairman

Conference Schedule

Monday July 19

7:30-8:30 a.m. BREAKFAST

8:30-8:35 a.m. Announcements

Session I: Bimolecular Reaction Dynamics-Experiment

8:35-8:55 a.m. Paul Dagdigian, "Reactive Scattering: Overview"

8:55-9:35 a.m. Hansjürgen Loesch "A Systematic Study of Steric Effects
in Reactive Scattering"

9:35-9:50 a.m. Discussion

9:50-10:10 a.m. BREAK

10:10-10:50 a.m. Arthur Suits, "New Directions in Radical Photochemistry
and Reaction Dynamics"

10:50-11:05 a.m. Discussion

11:05-11:45 a.m. Richard Zare, "Measuring State-Resolved Differential
Cross Sections Using the PHOTOLOC
Technique"

11:45-12:00 noon Discussion

12:00-1:30 p.m. LUNCH

5:30-7:00 p.m. DINNER

Session II: Collisions at Ultralow Temperatures

7:00-7:20 p.m. Daniel Heinzen, "Ultralow Temperature Collisions:
Overview"

7:20-8:00 p.m. William Stwalley, "Making Molecules at MicroKelvin"

8:00-8:15 p.m. Discussion

- 8:15-8:55 p.m. Paul Julienne, "Collisions and the Dynamics of Cold Atomic Gases"
- 8:55-9:10 p.m. Discussion
- 9:10-11:00 p.m. Poster Session A (Odd Numbers C1-C51)

Tuesday, July 20

- 7:30-8:30 a.m. BREAKFAST
- 8:30-8:35 a.m. Announcements

Session III: Bimolecular Reaction Dynamics-Theory

- 8:35-8:55 a.m. Russell Pack "Exciting Developments in the Theory of Reaction Dynamics"
- 8:55-9:35 a.m. John Zhang, "The SVRT Model for Quantum Polyatomic Reaction Dynamics"
- 9:35-9:50 a.m. Discussion
- 9:50-10:10 a.m. BREAK
- 10:10-10:50 a.m. Antonio Varandas, "Current Issues In Potential Energy Surfaces: The Challenge Of Conical Intersections"
- 10:50-11:05 a.m. Discussion
- 11:05-11:45 a.m. Stephen Gray, "Quantum Studies of Nonadiabatic Effects in $O(^1D) + H_2 \rightarrow OH + H$ "
- 11:45-12:00 noon Discussion
- 12:00-1:30 p.m. LUNCH
- 5:30-7:00 p.m. DINNER

Session IV: Eigenstate Resolved Dynamics

- 7:00-7:20 p.m. Thomas Rizzo, "Eigenstate Resolved Chemical Reaction Dynamics"
- 7:20-8:00 p.m. Patrick Vaccaro, "Holographic Probes of Molecular Structure and Dynamics: Nonlinear Optical Spectroscopy as a Probe of Proton Transfer and Hydrogen Bonding in Malonaldehyde"
- 8:00-8:15 p.m. Discussion
- 8:15-8:55 p.m. Amit Sinha, "State Selected Unimolecular Dissociation of HOCl Near Threshold: $6\nu_{OH}$ Vibrational State"

- 8:55-9:10 p.m. Discussion
- 9:10-11:00 p.m. Poster Session B (Even Numbers C2-C50)

Wednesday, July 21

- 7:30-8:30 a.m. BREAKFAST
- 8:30-8:35 a.m. Announcements

Session V: Control of Molecular Dynamics

- 8:35-8:55 a.m. David Tannor, "Control of Molecular Dynamics: A Historical and Conceptual Overview"
- 8:55-9:35 a.m. Gustav Gerber, "Coherent Control of Quantum Dynamics by Feedback-Optimized Femtosecond Laser Pulses"
- 9:35-9:50 a.m. Discussion
- 9:50-10:10 a.m. BREAK
- 10:10-10:50 a.m. Robert Gordon, "Exploring the Continuum with Phase Lag Spectroscopy"
- 10:50-11:05 a.m. Discussion
- 11:05-11:45 a.m. Stephen Leone, "Phase and Amplitude Control of Molecular Wave Packets"
- 11:45-12:00 noon Discussion
- 12:00-1:30 p.m. LUNCH
- 5:30-7:00 p.m. DINNER

Session VI: Non-Adiabatic Processes

- 7:00-7:20 p.m. Robert Parson, "Nonadiabaticity in Multidimensional Systems"
- 7:20-8:00 p.m. Sharon Hammes-Schiffer, "Nonadiabatic Molecular Dynamics of Charge Transfer Reactions"
- 8:00-8:15 p.m. Discussion
- 8:15-8:55 p.m. Laurie Butler "How the Electronic Wavefunction Can (and Can't) Evolve During Chemical Reaction Dynamics"
- 8:55-9:10 p.m. Discussion
- 9:10-11:00 p.m. Poster Session C (Odd Numbers C53-C101)

Thursday, July 22

7:30-8:30 a.m. BREAKFAST

8:30-8:35 a.m. Announcements

Session VII: Dynamics in Clusters

8:35-8:55 a.m. James Lisý, "The Interplay of Dynamics and Structure in Cluster Ions"

8:55-9:35 a.m. Michael Heaven, "Spectroscopy and Dynamics of the CN-H₂/D₂ van der Waals Complex"

9:35-9:50 a.m. Discussion

9:50-10:10 a.m. BREAK

10:10-10:50 a.m. Zlatko Bacic, "Vibration-Tunneling Dynamics in Highly Quantum Clusters: He-Large Molecule Dimers and Small Metal/Hydrogen Clusters"

10:50-11:05 a.m. Discussion

11:05-11:45 a.m. Koichi Yamashita, "Superfluidity and Spectroscopy of Na-Doped Quantum Helium Clusters: a Path Integral Monte Carlo Study"

11:45-12:00 noon Discussion

12:00-1:30 p.m. LUNCH

5:30-7:00 p.m. CONFERENCE BANQUET

Session VIII: Collisions at Surfaces

7:00-7:20 p.m. Barbara Garrison, "Diversity of Reactions at Surfaces"

7:20-8:00 p.m. J. Michael White, "State-Resolved Dynamics of NO Produced by 248 nm Photodissociation of t-butyl Nitrite on Ag(111)"

8:00-8:15 p.m. Discussion

8:15-8:55 p.m. Hua Guo, "Quantum Dissipative Dynamics of Surface Photoprocesses"

8:55-9:10 p.m. Discussion

9:10-11:00 p.m. Poster Session D (Even Numbers C52-C102)

Friday, July 23

7:30-8:30 a.m. BREAKFAST

8:30-8:35 a.m. Announcements

Session IX: Photodissociation Dynamics

8:35-8:55 a.m.	Reinhard Schinke, "Photodissociation Dynamics: New Developments and Challenges"
8:55-9:35 a.m.	Gregory Hall, "Multiple Surface Dynamics in ICN Dissociation"
9:35-9:50 a.m.	Discussion
9:50-10:10 a.m.	BREAK
10:10-10:50 a.m.	Gabriel Balint-Kurti, "Molecular Photodissociation Theory"
10:50-11:05 a.m.	Discussion
11:05-11:45 a.m.	Daniel Neumark, "Photodissociation Dynamics of Radicals and Ions"
11:45-12:00 noon	Discussion
12:00-1:30 p.m.	LUNCH

ABSTRACTS
OF
INVITED TALKS
(I1-I32)

Vibration-tunneling dynamics in highly quantum clusters:
He-large molecule dimers and small metal/hydrogen clusters

Zlatko Bačić

Department of Chemistry, New York University, New York, NY 10003. U.S.A.

Clusters containing one or more light atoms such as He or hydrogen display highly quantum mechanical behavior. Their excited vibrational eigenstates exhibit large-amplitude, strongly anharmonic motions of the light atom(s). The corresponding wave functions are extensively delocalized, often over multiple minima on the potential energy surface, giving rise to intricate vibration-tunneling dynamics. This will be illustrated by our recent multidimensional quantum calculations of the vibration-tunneling level structure of two very different types of quantum systems: van der Waals (vdW) M-He dimers where He atom is bound to a large aromatic molecule M, and small metal/hydrogen clusters. Extreme quantum dynamical character of the M-He dimers is evident from our results when M is 2,3-dimethylnaphthalene (2,3-DMN)¹ or tetracene/pentacene.² In the case of 2,3-DMN-He, energy levels $\approx 50 \text{ cm}^{-1}$ above the ground state are delocalized over the global minima above and below the molecular plane of 2,3-DMN, as well as the local minimum adjacent to the two methyl groups. We will also discuss the results of quantum bound state calculations for H/M_n clusters (M = Ni, Pd; $n = 2 - 4$).³ In metal/hydrogen clusters with four or more metal atoms, H atom can bind to different sites, resulting in isomeric structures with distinct vibration-tunneling level patterns.

[1] A. Bach, S. Leutwyler, D. Sabo, and Z. Bačić, *J. Chem. Phys.* **107**, 8781 (1997); [2] M. Xu, Z. Bačić, A. Bach, and S. Leutwyler, manuscript in preparation; [3] J. Dai and Z. Bačić, manuscript in preparation.

Molecular Photodissociation Theory

**Gabriel G. Balint-Kurti, Alexander Brown, László Füsti-Molnár and
Junia Melin**

University of Bristol

The theory of photodissociation processes using quantum wavepacket dynamics will be reviewed. Applications of the theory will be presented for several different systems. For H_2O the second absorption band, $\tilde{\text{B}}^1\text{A}_1 \leftarrow \tilde{\text{X}}^1\text{A}_1$, will be discussed where the electronically non-adiabatic transition occurs via a conical intersection in linear geometry. Detailed results will also be presented for the photodissociation of HI , where spin-orbit coupling leads to the production of two different electronic states of iodine, each with its own angular distribution. Current work on the photodissociation of N_2O will be reviewed.

The theory underlying the prediction of OH Λ -doublet product photofragment quantum state distributions in the photodissociation of H_2O and HOCl will be outlined. For HOCl new theory will be presented for the correlated scattering angle dependent polarised distributions of the OH Λ -doublet states and the spin-orbit states of the Cl atoms.

References:

- G.G. Balint-Kurti, "Dynamics of OH Lambda-Doublet Production through Photodissociation of Water in its first Absorption Band - Formal Theory (I)". *J. Chem. Phys.*, **84**, 4443 (1986).
- G.G. Balint-Kurti, R.N. Dixon and C.C. Marston "Grid Methods for Solving the Schrödinger Equation and Time Dependent Quantum Dynamics of Molecular Photofragmentation and reactive scattering Processes". *Internat. Rev. Phys. Chem.*, **11**, 317 (1992).
- A.R. Offer and G.G. Balint-Kurti, "Time-dependent quantum mechanical study of the photodissociation of HOCl and DOCl ", *J. Chem. Phys.*, **101**, 10416 (1994).
- A.R. Offer and G.G. Balint-Kurti, "Photodissociation of HOCl : A Model for the Prediction of the OH Λ -doublet and Cl Spin-Orbit Product State Distributions", *J. Chem. Phys.*, **104**, 563 (1996).
- L. Füsti-Molnár, P. Szalay and G.G. Balint-Kurti "Photodissociation of HOBr I. *Ab initio* Potential Energy Surfaces for the three lowest electronic states and calculation of rotational-vibrational energy levels and wavefunctions". *J. Chem. Phys.*, **110**, 8448 (1999).
- A. Pe'er, M. Shapiro and G.G. Balint-Kurti "The Breaking of the Backward-Forward Symmetry in the Angular Distribution of mj-Selected Photofragments", *J. Chem. Phys.*, in press (1999).

How the Electronic Wavefunction Can (and Can't) Evolve During Chemical Reaction Dynamics

I3

Laurie J. Butler, The University of Chicago

While we often try to understand chemical reactions by modeling them as occurring on a single Born-Oppenheimer potential energy surface, when the change in electronic wavefunction along the adiabatic reaction coordinate is large the dynamics can evolve on more than one potential energy surface. These experiments investigate how the breakdown of the Born-Oppenheimer approximation at a barrier or at a conical intersection along an adiabatic reaction coordinate can alter the dynamics of and expected branching between molecular dissociation pathways. We discuss two systems. In N_2O_4 photodissociation, the change in electronic wavefunction along the adiabatic reaction coordinate is $\pi_{nb}\pi^*$ to $n\sigma^*$, a two-electron change in electronic configuration analogous to that in nitric acid and nitromethane photodissociation at 193 nm. The long N-N bond length allows us Franck-Condon access to the region of the avoided crossing; our emission spectra of the dissociating molecules probes the electronic character of the excited state potential energy surface in the Franck-Condon region and the early dynamics. Our recent molecular beam photofragment scattering experiments examine the resulting competition between energetically allowed photodissociation channels. The second part of the talk discusses experiments on trimethylamine versus methylamine photodissociation. The work investigates the influence of intramolecular vibrational energy redistribution on the branching between two dissociation channels at a conical intersection analogous to that in ammonia.

Reactive Scattering: Overview

Paul J. Dagdigian
Department of Chemistry
The Johns Hopkins University
Baltimore, MD 21218

This talk will briefly summarize current work in reactive scattering with highlights of recent interesting experiments.

A number of experimental advances have allowed new kinds of experiments to be carried out. These include the measurement of product velocities with sub-Doppler resolution by sophisticated laser techniques, the development of pulsed and continuous beams of reactive and refractory reagents, and the application of traditional spectroscopic techniques such as direct absorption to dynamics studies. A crossed molecular beam apparatus with synchrotron photoionization mass spectrometric detection has been used for reactive scattering experiments.

The measurement of vector correlations through sub-Doppler laser experiments continues to be of particular interest, especially the interplay between the product angular distribution and the rotational polarization. Studies of reactions of open-shell reagents or products, involving multiple potential energy surfaces, can be significantly influenced by nonadiabatic effects. Experimental studies and theoretical treatments of exemplary reactions have provided considerable information on the importance of nonadiabatic dynamics in these systems.

The reaction of an atom with a diatomic molecule is the prototype of a chemical reaction. Attention is turning in recent years to the study of the dynamics of reactions involving larger molecules. The reaction of Cl atoms with small aliphatic hydrocarbons and the astrophysically important reactions of carbon atoms are examples of the kind of polyatomic reactions now being studied.

The idea of controlling the outcome of a chemical reaction by exciting a particular bond in a reagent has long had considerable appeal. Such bond-selected chemistry has been achieved for a triatomic molecule. Current interest is focused on the extension to larger reagents. This is more difficult than for triatomic reagents because of intramolecular redistribution of the initial excitation, which becomes more rapid in larger molecules.

The detailed understanding of the dynamics of exemplary reactions continues to depend on corresponding advances in the calculation of the potential energy surfaces and the treatment of the collision dynamics.

Gustav Gerber

Physikalisches Institut, Universität Würzburg, 97074 Würzburg, Germany

Using tailored femtosecond laser pulses from a computer-controlled pulse shaper the branching ratios of different organometallic photodissociation reaction channels were optimized. The optimization procedure is based upon the feedback from reaction product quantities in a learning evolutionary algorithm which iteratively improves the phase of the applied femtosecond laser pulse. It is shown that in the case of $\text{CpFe(CO)}_2\text{Cl}$ two different bond cleaving reactions can be selected, resulting in chemically different products. At least in this case, the method works automatically and finds optimal solutions without prior knowledge of the molecular system and the experimental environment.

The experiments reported here represent the first successful step towards synthesizing chemical substances with higher efficiencies while at the same time reducing unwanted byproducts. The method can be applied to the liquid phase as well. With this tool novel experiments can be realized simply by choosing the appropriate feedback. The technique is extremely useful in a wide range of fields and applications where specific temporal and spectral ultrashort laser pulses are required.

References

Femtosecond Pulse Shaping by an Evolutionary Algorithm with Feedback
Appl. Phys. B65, 779-782 (1997)

Automated Coherent Control of Chemical Reactions and Pulse Compression
by an Evolutionary Algorithm with Feedback
Ultrafast Phenomena XI, eds. T. Elsaesser, I.G. Fujimoto, D.A. Wiersma, W. Zinth
Springer Series in Chemical Physics, Vol. 63, 471-473 (1998)

Control of Chemical Reactions by Feedback-Optimized Phase-Shaped Femtosecond Laser Pulses
Science 282, 919-922 (1998)

Robert J. Gordon, Jeanette A. Fiss, Ani Khachatrian, Kaspars Truhins, and Langchi Zhu

Department of Chemistry, University of Illinois at Chicago (m/c 111), 845 West Taylor Street
Chicago, IL 60607-7061

Tamar Seideman

The Steacie Institute for Molecular Sciences, National Research Council of Canada
Ottawa K1A 0R6, Canada

Although coherent control was originally developed as a method of altering the outcome of a chemical reaction, it turns out to be also a unique spectroscopic tool. We illustrate this idea with the ionization and dissociation of HI and DI. As in our previous work,^{1,2,3,4} the parent molecule is excited coherently with three photons of frequency ω_1 and one photon of frequency $\omega_3 = 3\omega_1$. Two products, HI^+ (or DI^+) and I^+ (the latter produced by ionization of the dissociation fragment), were observed with a time-of-flight mass spectrometer. The probability of obtaining a product in channel S is given by

$$P^S = p_1^S + p_3^S + 2p_{13}^S \cos(\phi + \delta_{13}^S),$$

where p_1^S and p_3^S are, respectively, the angle averaged probabilities of the one- and three-photon processes, p_{13}^S is the amplitude of the interference term, ϕ is the relative phase of the two laser beams, and δ_{13}^S is the *phase shift* for that channel. A new experimental observable is the *phase lag*, $\Delta\delta$, which is defined as the difference between the phase shifts for a pair of channels. For example, the phase lag between ionization and dissociation of HI is given by

$$\Delta\delta(\text{HI}^+, \text{I}) = \delta_{13}^{\text{HI}^+} - \delta_{13}^{\text{I}}.$$

We explore the contributions to the phase lag from resonances coupled to one or both continua at the three photon ($3\omega_1$) level as well as those of low-lying ($2\omega_1$) resonances. We further distinguish between phase shifts produced by the phase of the asymptotic wave function (so called "molecular phases") and those produced by properties of the resonance ("resonance" or "Breit-Wigner phases"). Through a combination of experimental and theoretical studies we show that the energy and mass dependence of the phase lag is a sensitive probe of interactions in the continuum, in some cases providing information that is difficult to obtain by other methods.

¹L. Zhu, V. D. Kleiman, K. Trentelman, X. Li, and R. J. Gordon, *Science* **270**, 77 (1995).

²L. Zhu *et al.*, *Phys. Rev. Lett.* **79**, 4108 (1997).

³J. A. Fiss, L. Zhu, R. J. Gordon, and T. Seideman, *Phys. Rev. Lett.* **82**, 65 (1998).

⁴J. A. Fiss, A. Khachatrian, L. Zhu, R. J. Gordon, and T. Seideman, *Disc Faraday Soc.* (in press).

Quantum Studies of Nonadiabatic Effects in $O(^1D) + H_2 \rightarrow OH + H$

I7

Stephen K. Gray

Chemistry Division, Argonne National Laboratory, Argonne, IL 60439

Carlo Petrongolo

Department of Chemistry, University of Sienna, Pian dei Mantellini 44, I-53100 Sienna, Italy

Karen Drukker and George C. Schatz

Chemistry Department, Northwestern University, 2145 Sheridan Rd, Evanston IL 60208-3113

Abstract

A wavepacket approach to treating the electronically nonadiabatic reaction dynamics of $O(^1D) + H_2 \rightarrow OH + H$, allowing for the $1^1A'$ and $2^1A'$ potential energy surfaces and couplings, as well as the three internal nuclear coordinates, is outlined. Nonadiabatic quantum results (with total angular momentum $J = 0$) are obtained and discussed. The ab initio surfaces and couplings of Dobbyn and Knowles are used in these calculations. Several single surface calculations are carried out for comparison with the nonadiabatic results, including calculations on the $1A''$ surface. Comparisons with trajectory surface hopping calculations are included. Rate constants, based on J -shifting and related ideas, are also estimated.

Our results show that if the initial state is chosen to be effectively the $1A'$ state, for which insertion to form products occurs on the adiabatic surface, then there is very little difference between the adiabatic and coupled surface results. However, if the initial state is chosen to be effectively the $2A'$ state, the reaction dynamics is noticeably perturbed by nonadiabatic effects. A particularly interesting nonadiabatic effect occurs at low collision energies where the relevant single surface calculations are dominated by tunneling through a barrier at collinear geometries. An alternative nonadiabatic mechanism for reaction emerges that yields significantly larger reaction probabilities than would be expected on the basis of barrier tunneling. This mechanism is due to long-range nonadiabatic coupling. These reaction probabilities are still small in comparison with the $1A'$ reaction probabilities at comparable energies, and so we estimate that they lead to not more than a 10 % contribution to the thermal rate constant.

The submitted manuscript has been created by the University of Chicago as Operator of Argonne National Laboratory ("Argonne") under Contract No. W-31-109-ENG-38 with the U.S. Department of Energy. The U.S. Government retains for itself, and others acting on its behalf, a paid-up, nonexclusive, irrevocable worldwide license in said article to reproduce, prepare derivative works, dis-

Quantum Dissipative Dynamics of Surface Photoprocesses

H. Guo

Department of Chemistry, University of New Mexico, Albuquerque, NM 87131

Abstract

A major difference between chemical reactions occurring on solid surfaces and in the gas phase is the excitation and relaxation induced by the surface. Such surface-induced fluctuation and dissipation channels have either phononic or electronic origin and may have significant effects on the dynamics. In this talk, we present our recent work on reduced density matrix treatments of several surface processes stimulated by photons. In particular, we discuss a Chebyshev polynomial based short-time propagator for the Liouville-von Neumann equation and a discretization scheme based on eigenfunctions of an effective Hamiltonian. These numerical algorithms are applied to realistic dynamical models such as photon-stimulated desorption of neutral molecules from metals and atom transfer between a surface and STM tip.

Multiple surface dynamics in ICN dissociation

Gregory Hall

*Chemistry Department
Brookhaven National Laboratory
Upton, NY 11973*

The near UV dissociation of ICN continues to provide the molecular dynamics community with an opportunity to test and refine our understanding of fragmentation reactions. We now understand that UV illumination of ICN simultaneously excites parallel and perpendicular transitions to directly dissociative surfaces. Two surfaces of A' symmetry form a conical intersection slightly removed from the Franck-Condon region. Only the upper A' surface correlates to excited (2P_u) iodine atoms. Adiabatic and non-adiabatic paths combine to produce CN states in coincidence with both ground and excited iodine atoms.

We have collected a large set of CN photofragment Doppler spectra by transient frequency-modulation (FM) absorption spectroscopy, at several photolysis wavelengths and many CN rotational states. This high-resolution, low-noise, overdetermined data set allows us to test the completeness and correctness of Dixon's bipolar moment formalism for describing the coupled anisotropy of fragment velocity and angular momentum in the presence of multiple excited states and non-adiabatic couplings. We find that the observable anisotropy created by single-photon, linearly polarized photolysis and detected with single-photon, linearly polarized absorption continues to be describable in terms of five bipolar moments for each resolved velocity. The dynamical interpretation of these bipolar moments is addressed in the context of single-path dynamical functions and a multiple path interference term. For high angular momentum fragments produced in the axial recoil limit, we show that the interference term influencing measurements with linearly polarized light has a negligible effect on the Doppler profiles. When the interference term is negligible, a constraint relating three of the five bipolar moments is obtained, reducing the number of independent fitting parameters to four. Our extensive set of CN measurements can be described without systematic residuals in this reduced parameter space, and the "incoherent parameters" display many qualitatively satisfying features of the ab initio dynamical calculations. For example, the vector properties of the fast and slow components of those CN rotational levels with a bimodal speed distribution show qualitatively different patterns. They are consistent with adiabatic and non-adiabatic A' symmetry paths leading to excited $^2P_{1/2}$ I atoms, one parallel and one perpendicular, and an additional A'' symmetry path to ground state $^2P_{3/2}$ I atoms.

This work was performed at Brookhaven National Laboratory under Contract No. DE-AC02-98CH10886 with the U.S. Department of Energy and supported by its Division of Chemical Sciences, Office of Basic Energy Sciences.

NONADIABATIC MOLECULAR DYNAMICS OF CHARGE TRANSFER REACTIONS

Sharon Hammes-Schiffer

Department of Chemistry and Biochemistry, 251 Nieuwland Science Hall,
University of Notre Dame, Notre Dame, IN 46556-5670 USA
e-mail: hammes-schiffer.1@nd.edu

Multiple proton transfer and proton-coupled electron transfer reactions play a vital role in a wide range of chemical and biological processes. This talk will present mixed quantum/classical molecular dynamics methodology recently developed for the simulation of multiple charge transfer reactions in solution and in proteins. The discussion will focus on the Multiconfigurational Molecular Dynamics with Quantum Transitions (MC-MDQT) method. In this approach the transferring hydrogen atom(s) are treated quantum mechanically to incorporate quantum dynamical effects such as hydrogen tunneling. The correlation among the transferring protons and the nonadiabatic coupling between the transferring proton(s) and the active solute electrons are incorporated into the adiabatic states. A stochastic surface hopping algorithm is utilized to include nonadiabatic transitions among these adiabatic states. The MC-MDQT method allows the nonequilibrium real-time dynamical simulation of a wide range of biologically and chemically important charge transfer processes. Applications to proton-coupled electron transfer in model complexes and to proton transport along water chains will be presented.

SPECTROSCOPY AND DYNAMICS OF THE CN-H₂/D₂ VAN DER WAALS COMPLEX.

Michael C. Heaven, Yaling Chen, and Alexey Kaledin, *Department of Chemistry, Emory University, Atlanta, GA 30322*

The reaction $\text{H}_2 + \text{CN} \rightarrow \text{H} + \text{HCN}$ is a prototypical system for studies of diatom-diatom reaction dynamics. It is also of importance in the combustion of hydrocarbons in air. The reaction has a entrance channel barrier of about 1000 cm^{-1} , which permits formation of a weakly bound $\text{H}_2\text{-CN}$ complex at low temperatures. This opens the possibility that details of the reaction dynamics may be investigated by initiating reaction within the complex.

Previously, we demonstrated that the complex can be formed at low temperatures and characterized using fluorescence excitation techniques¹. A bound-free continuum spectrum was observed for the $B^2\Sigma^+ - X^2\Sigma^+$ transition, while the $A^2\Pi - X^2\Sigma^+$ system exhibited resolved rotational structure. Ground state dissociation energies of $D_0 = 38 \text{ (CN-H}_2\text{)}$ and $42 \text{ cm}^{-1} \text{ (CN-D}_2\text{)}$ were deduced from the onset of the $B-X$ continuum and the A state predissociation dynamics. Anomalous isotope effects were noted for the dissociation energies and the rotational structures of the $A-X$ bands (which were not assigned).

In recent work we have assigned the $A-X$ bands and detected bound levels of $\text{CN(B)-H}_2/\text{D}_2$. Analyses of bands associated with the CN monomer $A^2\Pi_{3/2} - X^2\Sigma^+$ 2-0 transition yielded ground state rotational constants of $B'' = 0.245 \text{ (CN-H}_2\text{)}$ and $0.229 \text{ cm}^{-1} \text{ (CN-D}_2\text{)}$. The CN(X)-H_2 constant was much smaller than would be predicted using typical van der Waals radii. A similar discrepancy, but less pronounced, was present for CN(X)-D_2 . High-level ab initio calculations predict ground state constants of $0.518 \text{ (CN-H}_2\text{)}$ and $0.292 \text{ cm}^{-1} \text{ (CN-D}_2\text{)}$ ². However, these predictions were for $J=0$ complexes. Theoretical calculations show that the zero-point levels are mixed (via Coriolis coupling) to the first excited internal rotor states. This mixing can account for the small values for the rotational constants and the anomalous isotope effects (for both D_0 and B). The rotational structure is consistent with a collinear CN-H_2 equilibrium structure for the ground state.

Electronic predissociation of $\text{CN(A}^2\Pi\text{)-H}_2/\text{D}_2$ was examined by characterizing action spectra and product state distributions. Both spin-orbit ($\text{CN(A}^2\Pi_{1/2}\text{)-H}_2 \rightarrow \text{CN(A}^2\Pi_{3/2}\text{)+H}_2$) and internal conversion ($\text{CN(A}^2\Pi_{3/2}\text{)-H}_2 \rightarrow \text{CN(X}^2\Sigma^+\text{) + H}_2$) decay channels were observed. For comparison with the predissociation data, CN(A) + H_2 collisional energy transfer was examined at low temperatures (near 10 K). The product state distributions resulting from collisions showed symmetry propensities that were not evident in the distributions resulting from predissociation. Furthermore, the symmetry propensity exhibited by spin-orbit transfer was the opposite of that seen in $A \rightarrow X$ transfer. We argue that the lack of symmetry preference in the predissociation dynamics is indicative of resonant scattering processes. The results may be explained by considering the symmetry properties of the intermolecular potential energy surfaces, and the regions of these surfaces that are sampled by predissociation and collisional transfer events.

1. Y. Chen and M. C. Heaven, *J. Chem. Phys.* **109**, 5171 (1998)
2. A. L. Kaledin, M. C. Heaven, and J. M. Bowman, *J. Chem. Phys.* **110**, 10380 (1999)

Collisions and the Dynamics of Cold Atomic Gases

Paul S. Julienne

*Physics Laboratory, National Institute of Standards and Technology, 100 Bureau Drive Stop 8423,
Gaithersburg, MD 20899-8423 USA*

Atomic collisions in the ultracold regime below a few microkelvin play a crucial role in the dynamics of a cold atomic gas or a Bose-Einstein condensate (BEC). Such gases are confined in magnetic or optical traps of finite dimension, where the De Broglie wavelength of the atoms become comparable to the trap dimension. In such traps the energy levels of the system are quantized due to the confinement, as in a large polyatomic molecule, and a "collision" between two atoms modifies the properties of bound levels of the confined system. What we think of as elastic collisions in free-space manifest themselves as a shift of energy levels in the trap. This gives rise to the mean-field shift in energy that dominates the properties of a BEC, giving it a size and mean particle energy very different from the trap ground state harmonic wavefunction. When trap confinement is very tight with a size comparable to the free-particle scattering length, as in a cell of an optical lattice, the usual delta-function approximation breaks down where the interatomic potential is expressed as a delta-function with a strength proportional to the elastic collision scattering length [1].

The interatomic interaction can be manipulated by magnetic or optical fields, which move Feshbach resonance states into the region of the collision threshold. These resonances change the phases and scattering lengths of elastic collisions. Such resonances have been shown to cause dramatic changes in BEC dynamics [2,3], due to the change in scattering length, and to lead to large losses of atoms from the trap. We explain such dynamics in terms of two models. A time-independent model explains one class of experiments in which sequential collisions result in an large effective 3-body recombination rate of the gas [4]. A time-dependent model of collisions is a magnetic field explain another class of experiments in which a field rapidly moves a resonance across the threshold region. We show that such a mechanism can be used to rapidly convert a gas of free atoms into a gas of translationally cold bound diatomic molecules [5].

The mean field interactions between atoms in a BEC give rise to a nonlinear evolution equation for the condensate wavefunction. When three condensate wavepackets collide, this nonlinearity can give rise to four wave mixing of the wavepacket momenta [6]. Thus, colliding BEC wavepackets exhibit time-dependent dynamics. We present theoretical studies of the "half-collision" version (analogous to polyatomic photofragmentation) of BEC wavepacket dynamics calculated using the time-dependent nonlinear Schrödinger equation. Nonlinear four-wave mixing of colliding BEC wavepackets has been observed experimentally [7].

Thanks are expressed to the Office of Naval Research and the Army Research Office for partial support.

- [1] E. Tiesinga and P. S. Julienne (1999).
- [2] S. Inouye, M. R. Andrews, J. Stenger, H.-J. Miesner, D. M. Stamper-Kurn, and W. Ketterle, *Nature* **392**, 151 (1998).
- [3] J. Stenger, S. Inouye, M. R. Andrews, H.-J. Miesner, D. M. Stamper-Kurn, and W. Ketterle, *Phys. Rev. Lett.* **82**, 2422 (1999).
- [4] V. A. Yurovsky, A. Ben-Reuven, P. S. Julienne, and C. J. Williams, *Phys. Rev. A*, in press (1999).
- [5] F. H. Mies, E. Tiesinga, P. S. Julienne (1999).
- [6] M. Trippenbach, Y. B. Band, and P. S. Julienne, *Opt. Express* **3**, 530 (1998).
- [7] L. Deng, E. W. Hagley, J. Wen, M. Trippenbach, Y. Band, P. S. Julienne, J. E. Simsarian, K. Helmerson, S. L. Rolston, and W. D. Phillips, "Four-wave-mixing with matter waves," *Nature* **398**, 218 (1999).

Phase and Amplitude Control of Molecular Wave Packets

Stephen R. Leone, Radek Uberna, and Zohar Amitay

JILA, University of Colorado and National Institute of Standards and Technology
Departments of Chemistry and Physics, University of Colorado
Boulder, CO 80309-0440

srl@jila.colorado.edu, <http://jilaweb.colorado.edu/~srl/>

Focusing and control of vibrational and rotational wave packets are investigated in lithium dimers using femtosecond optical pulses. Two important themes of this work are (1) the use of intermediate state selection, prior to the preparation of the wave packet, and (2) phase and amplitude control, using a liquid crystal spatial modulator to shape the electric field of the femtosecond pulses. Selection of a single state from which to launch the wave packet provides precise knowledge of the wave packet components and their amplitudes. Phase and amplitude manipulation provides a means to actively define the phases and amplitudes of as many as 10 rovibronic components in the wave packet state. These techniques permit rigorous new experiments on the dynamics of wave packet focusing and ionization control.

Using the phase control capabilities of the liquid crystal modulator, rovibronic wave packets composed of multiple excited states are prepared, each with well-defined phase. The specific limitations of the preparation of a maximum or minimum in the wave packet localization are probed. The amplitude of the maximum or minimum depends on the signs (+ or -) of the various wave packet beats in the overall preparation and detection steps. In one experiment, the signs of all the beat frequencies are found coincidentally to be positive, creating a maximum at time $t=0$. At any later time, a maximum recurrence in the wave packet amplitude can be reestablished by phase manipulation. However, amplitude minima of this same magnitude cannot be produced, since only eight quantum mechanical states are controlled by their phases, whereas 18 strong quantum beats contribute significantly to the wave packet time evolution. The limitations on the maximum and minimum spatial localization of the wave packet and the origins of the signs of the beats are considered in detail.

The method of two-level rotational coherence spectroscopy has been developed. This permits phase control of the rotational wave packets in both the preparation and probing steps. By taking advantage of single Rydberg states embedded in the continuum, phase control in the detection (probe) step has been demonstrated for the first time. Using a tunable ultrafast probe laser (OPA) and the two-level rotational wave packet signal amplitude as a means to obtain background-free measurements of the ionization, the ionization cross section for the E electronic state as a function of final vibrational state in the ion has been mapped. This cross section is highly correlated with the ionization probability as a function of internuclear distances, which changes markedly in the E state of the lithium dimer.

1. J. M. Papanikolas, R. M. Williams, P. D. Kleiber, J. L. Hart, C. Brink, S. D. Price, and S. R. Leone, *J. Chem. Phys.* **103**, 7269 (1995).
2. R. M. Williams, J. M. Papanikolas, J. Rathje, and S. R. Leone, *Chem. Phys. Lett.* **261**, 405 (1996).
3. R. M. Williams, J. M. Papanikolas, J. Rathje, and S. R. Leone, *J. Chem. Phys.* **106**, 8310 (1997).
4. J. M. Papanikolas, R. M. Williams, and S. R. Leone, *J. Chem. Phys.* **107**, 4172 (1997).
5. R. Uberna, M. Khalil, R. M. Williams, J. M. Papanikolas, and S. R. Leone, *J. Chem. Phys.* **108**, 9259 (1998).

James M. Lisy
Department of Chemistry
University of Illinois

The Interplay of Dynamics and Structure in Cluster Ions

During the past decade, there has been significant development in the spectroscopy of cluster ions. Yet, when compared to neutral cluster spectroscopy, this area is still in its infancy or at least preadolescent stage. The same analogy applies to the dynamical processes in cluster ions. There is a sharp contrast with neutral clusters in this regard, as the strong ion-neutral interaction enables significant amounts of energy to be retained in the cluster ion without unimolecular dissociation. As a result, the structural conclusions from some previous spectroscopic investigations have required revision, after the effects of internal energy were adequately accessed. This overview will briefly highlight these problems when more than one ligand or neutral molecule is bound to the ion, and present a methodology for determining the internal energy distribution of cluster ions. Using $\text{Na}^+(\text{CH}_3\text{OH})_n$ as an example, the utility of the procedure and its relevance to dynamics and structure will be demonstrated.

Hansjürgen Loesch

Fakultät für Physik, Universität Bielefeld
D-33615 Bielefeld, Germany

The brute force orientation technique is applicable to all kinds of polar molecules and is for this reason suited for systematic studies of orientational effects in reactive scattering¹. In crossed molecular beam experiments we have investigated reactions $K+IR \rightarrow KI+R$ with two classes of reagent molecules: (a) alkyl iodides and (b) aromatic iodides. Class (a) comprises methyl iodide and the molecules which result when the H atoms of CH_3I are successively substituted by methyl groups from ethyl to i-propyl to t-butyl iodide². Members of class (b) are iodobenzene³ and the three iodotoluenes which differ by the location of the methyl group from 2- to 3- to 4-iodotoluene^{3,4}.

The differential reaction cross sections in the center-of-mass (CM) frame of class (a) molecules changes from preferred backward to sideways scattering of the KI products with increasing number of methyl groups. Very striking is a conspicuous sharp forward peak that occurs only for t-butyl iodide; the mean velocity of the corresponding products amounts exactly to the stripping velocity. The CM cross sections of class (b) molecules exhibit preferred sideways (iodobenzene) and sideways/backward scattering. A very weak stripping component has been observed for iodobenzene only. Transformed to a coordinate frame that is dynamically more relevant than the CM frame the cross section of all systems exhibits backward scattering only. This uniform appearance suggests a mechanism that is common to all reaction

With brute force oriented molecules we have measured differential parallel and perpendicular steric effects. Shape and magnitude of the effects indicate in all cases a tight correlation between the directions of the C-I bond and the mean recoil velocity of the products. The extent of correlation is only weakly dependent on the number of methyl groups in the (a) class but varies significantly in the (b) class. It is tightest for iodotoluene and weakest for 2-iodotoluene. The product yield depends strongly on the orientation: it is always largest for encounters with the I-end. The yield of encounters with the R end is small (10-20%) or nearly vanishes for class (b) or (a) molecules, respectively.

The data are interpreted in terms of simple dynamical models rather than potential energy surfaces and trajectory calculations. The basic features are rationalized by the harpooning mechanism and versions of the DIPR model. The reactive asymmetry is explained via steric opacity functions and angle dependent potential energy barriers.

¹ H.J. Loesch, *Annu. Rev. Phys. Chem.* **46**, 555 (1995)

² H.J. Loesch, J. Möller, *J. Phys. Chem. A*, **102**, 9410 (1998)

³ H.J. Loesch, J. Möller, *J. Phys. Chem. A*, **101**, 7534 (1997)

Photodissociation dynamics of radicals and ions

Daniel M. Neumark
 Department of Chemistry
 University of California
 Berkeley, CA 94720
 USA

The photodissociation dynamics of the NCN and CNN radicals and the triiodide anion, I_3^- , have been investigated using complementary frequency and time-resolved experiments. All three species were studied using fast beam photofragment translational spectroscopy, and I_3^- was also probed using femtosecond photoelectron spectroscopy (FPES). Although these species are relatively small they exhibit rich spectroscopy and dynamics.

In NCN, the $\tilde{B}^3\Sigma_u^- \leftarrow \tilde{X}^3\Sigma_g^+$, $\tilde{c}^1\Pi_u \leftarrow \tilde{a}^1\Delta_g$, and $\tilde{d}^1\Delta_u \leftarrow \tilde{a}^1\Delta_g$ transitions were examined. The major dissociation products for the $\tilde{B}^3\Sigma_u^-$ and $\tilde{c}^1\Pi_u$ states are $N_2(\tilde{X}^1\Sigma_g^+) + C(^3P)$, while the $\tilde{d}^1\Delta_u$ state dissociates to $N_2(\tilde{X}^1\Sigma_g^+) + C(^1D)$. A small amount of $N(^4S) + CN(\tilde{X}^2\Sigma^+)$ is observed for the $\tilde{B}^3\Sigma_u^-$ state at photon energies greater than 4.9 eV. At all photon energies, the photofragment translational energy distributions show a resolved progression corresponding to the vibrational excitation of the N_2 photofragment. The rotational distributions of the molecular fragments suggest that the dissociation pathway for the N_2 loss channel involves a bent transition state while the $N + CN$ photofragments are produced via a linear dissociation mechanism.

The spectroscopy and photodissociation dynamics of the $\tilde{A}^3\Pi$ and $\tilde{B}^3\Sigma^-$ states of the CNN radical were also investigated. Vibronic transitions located more than 1,000 cm^{-1} above the $\tilde{A}^3\Pi \leftarrow \tilde{X}^3\Sigma^-$ origin were found to predissociate. Photofragment yield spectra for the $\tilde{B}^3\Sigma^- \leftarrow \tilde{X}^3\Sigma^-$ band between 40800 and 45460 cm^{-1} display resolved vibrational progressions with peak spacing of $\approx 1000\text{ cm}^{-1}$ corresponding to symmetric stretch 1_0^s and combination band $1_0^s 3_0^1$ progressions. The ground state products $C(^3P) + N_2$ were found to be the major photodissociation channel for both the $\tilde{A}^3\Pi$ and $\tilde{B}^3\Sigma^-$ states. The distributions for the $\tilde{B}^3\Sigma^-$ state reveal partially resolved vibrational structure for the N_2 photofragment and indicate extensive vibrational and rotational excitation of this fragment.

The FPES study of I_3^- yields the time scale of formation for the I_2^- and I products following excitation at 390 nm, and shows that the I_2^- is produced in a coherent superposition of highly excited vibrational levels. The I products appear to result from a concerted three-body process, $I_3^- \rightarrow I + I + I$. The frequency-resolved fast beam experiment provides a complementary and more complete picture of these dynamics, and in particular supports the three-body mechanism for I production. The I_2^- vibrational distribution and the I_2^-/I branching are very different from previous liquid phase results on I_3^- photodissociation in ethanol.

EXCITING DEVELOPMENTS IN THE THEORY OF REACTION DYNAMICS

117

Russell T Pack

Theoretical Division (T-12, MS B268)
Los Alamos National Laboratory
Los Alamos, NM 87545

Abstract

Progress in the theory of reaction dynamics continues to be rapid. New potential energy surfaces are being produced which are more accurate than ever before and which now contain accurate representations of multiple surfaces, conical intersections, and the nonadiabatic terms coupling different surfaces.

Classical, semiclassical, and quantum methods for treating the reaction dynamics are being pursued vigorously. The effects of conical intersections and their attendant geometric phases on the reaction dynamics are fascinating and becoming clarified. Inclusion of multiple potential surfaces in the dynamics with proper treatment of the couplings (due to intersections, spin-orbit terms, etc.) is now becoming a reality, so that nonadiabatic reactions are now being treated.

Accurate quantum reactive scattering theory (both time dependent and time independent) is being applied to larger and more complex triatomic systems and to more and more tetraatomic systems. Also, new and more reliable models are being developed to treat reactions in polyatomic systems with many atoms. Better ways, both exact and approximate, to treat high total angular momentum are being developed. New insights are being gained.

In this overview talk we will introduce the advances made by the other speakers in this session, review as many of the above developments as time permits, and also briefly describe our own work on the quantum theory of collisions involving three free bodies and its surprising implications about anomalous isotope effects and also its implication that atomic recombination reactions are dominated by true three-body collisions, not by sequential two-body collisions.

Nonadiabaticity in multidimensional systems

Robert Parson

JILA and Department of Chemistry and Biochemistry
University of Colorado at Boulder

Abstract

Most of our intuition about nonadiabatic effects in reaction dynamics is based upon our experience with simple one-dimensional problems. The speakers in this session, in contrast, will be discussing nonadiabatic processes in large molecules and condensed phases. In some cases, one can understand such processes in terms of one-dimensional pictures, provided that one chooses coordinates carefully. In others, one has to deal with phenomena that have no one-dimensional analog, such as conical intersections. In this overview I will describe, with reference to the work of the speakers, some of the concepts and techniques that have been used to sort out the complexities of multidimensional nonadiabatic dynamics. I will then discuss an example from our own research, the extremely rapid spin-orbit quenching that occurs during the UV photodissociation of solvated I_2^- . Here intuition based on one-dimensional gas-phase potential curves led to qualitatively incorrect conclusions, whereas a different one-dimensional picture, inspired by the theory of electron transfer reactions in solution, not only explained the experimental observations but predicted them in advance.

Eigenstate Resolved Chemical Reaction Dynamics

I19

Thomas R. Rizzo

Laboratoire de chimie physique moléculaire, École Polytechnique Fédérale
de Lausanne, 1015 Lausanne, Switzerland

This talk will give an overview of recent experiments that investigate and/or control the course of chemical reactions by selective preparation of individual molecular eigenstates of a reactant molecule. Methods for preparing molecules in single eigenstates at chemically significant energies as well as dynamical studies of molecules in these states will be discussed. For unimolecular dissociation studies, the states prepared should be considered resonances embedded in a dissociative continuum rather than molecular eigenstates, where coupling to the continuum contains the dynamical information. In bimolecular reactions and photodissociation studies, an eigenstate of a molecule can be initially prepared before undergoing either a collision with another molecule or further excitation to another electronic potential energy surface. In these cases, the nature of the prepared eigenstate can be chosen to control the subsequent dynamics. Examples of each scenario will be briefly mentioned.

Photodissociation Dynamics: New Developments and Challenges I20

Reinhard Schinke

Max-Planck-Institut für Strömungsforschung, D-37073 Göttingen, Germany

In this talk I will try to give an overview of the current status of the field of photodissociation. Being a theorist, new developments in treating photodissociation processes by *ab initio* methods, both in the time-independent and the time-dependent approach of quantum mechanics, will be focused on. Nevertheless, some experimental results will be presented in order to highlight the degree of sophistication, which has been achieved by now, and to illustrate the detail with which theory and experiment can be compared. A central example will be the dissociation of HNCO in the first absorption band, which has been analyzed in great detail by several experimental groups in recent years, and for which the first theoretical results (from my own research group) are becoming available now. Topics, which I plan to cover, include the construction of multi-dimensional potential energy surfaces, non-adiabatic effects during dissociation, the quantum mechanical picture of unimolecular dissociation, dissociation of molecules in strong electric fields, time resolved approaches, and dissociation in larger systems.

State Selected Unimolecular Dissociation of HOCl
Near Threshold: The $6\nu_{\text{OH}}$ Vibrational State

Amitabha Sinha

Department of Chemistry and Biochemistry
University of California-San Diego
9500 Gilman Drive
La Jolla, CA 92093-0314

ABSTRACT

The spectroscopy and unimolecular dissociation dynamics of HOCl is examined by accessing rotational resonances of the $6\nu_{\text{OH}}$ vibrational level over the $K_a=0-5$ manifolds using overtone-overtone double resonance. The spectroscopic analysis indicates that state mixing between the zero-order "bright" O-H stretching overtone state, $6\ 0\ 0$, and "dark" background vibrational levels is incomplete as the bright state only couples to roughly half of the available states. The coupling of $6\ 0\ 0$ to nearby dark states is mediated primarily by anharmonic coupling with the fourth order vibrational resonance $k_{1,223}$ playing a particularly important role through its ability to couple the $6\ 0\ 0$ state directly to the $5\ 2\ 1$ vibration and indirectly to the $4\ 4\ 2$ vibration. The measured state specific unimolecular dissociation rates for $6\ 0\ 0$ show large fluctuations with J and K_a and are substantially slower than that expected on the basis of statistical theory. The rate fluctuations in $6\ 0\ 0$ are interpreted on the basis of spectroscopic data which suggest that the fluctuations arise as a result of variation in state mixing as different dark vibrational states come in and out of resonance with the bright state for different values of J and K_a .

The cooling and trapping of atoms and atomic ions is a rapidly advancing field of fundamental science (e.g. Bose-Einstein condensation). We are attempting to extend the field to neutral molecules as well, e.g. for study of elastic, inelastic and reactive collisions in the highly quantum mechanical regime at extremely low energies. As a first step, we are employing single- and multicolor photoassociation to produce translationally ultracold $^{39}\text{K}_2$ molecules from ultracold ($\sim 300\mu\text{K}$) ^{39}K atoms confined in a magneto-optical trap.¹⁻⁷ Photoassociation of ultracold atoms (as opposed to thermal atoms) includes sharp resonances with wavelength as long-range rovibrational levels (outer turning points of tens or hundreds of Bohr) are accessed from colliding atomic pairs with 10 MHz of relative kinetic energy and only a few partial waves ($\ell = 0, 1, 2$). Potential energy curves derived from these spectra test electronic structure and long-range perturbation theory calculations of interatomic potentials. The molecules formed are translationally ultracold and rotationally cold.

Recently we have used two-color resonance enhanced multiphoton ionization to directly detect translationally ultracold molecules.⁸ These molecules are formed in $v'' = 36$ of the ground $X^1\Sigma_g^+$ state of $^{39}\text{K}_2$ following spontaneous emission from $v' \approx 191$ of the $A^1\Sigma_u^+$ state, formed in turn by one-color photoassociation of ultracold ^{39}K atoms. Currently, we are producing translationally ultracold molecules in low rovibrational levels ($v'' \leq 0, J'' \leq 3$) of the $X^1\Sigma_g^+$ state via two-color photoassociation as proposed by Band and Julienne.⁹ We plan as a further step to cool the rovibrational distribution of ground state translationally ultracold molecules produced by two-color photoassociation using laser cooling.¹⁰

We also plan to directly study free \rightarrow bound \rightarrow bound stimulated Raman photoassociation to directly produce state-selected translationally ultracold K_2 molecules as recently proposed.¹¹ Note the application of this technique to an atomic Bose-Einstein Condensate may yield a coherent beam of state-selected molecules¹² (a "molecule laser").

Both photoassociation of ultracold atoms¹³ and formation of cold molecules¹⁴ have recently been reviewed by our group.

* In collaboration with Professors Phil Gould and Ed Eyler, Drs. He Wang, John Bahns, Jason Ensher, Paul Julienne, Eite Tiesinga and Carl Williams, and Jing Li, Xiaotian Wang and Anguel Nikolov. Supported in part by the National Science Foundation.

References:

1. H. Wang, P. L. Gould and W. C. Stwalley, *Phys. Rev. A*, **53**, R1216 (1996).
2. H. Wang, P. L. Gould and W. C. Stwalley, *Z. Phys. D*, **36**, 317 (1996).
3. H. Wang, J. Li, X. T. Wang, C. J. Williams, P. L. Gould and W. C. Stwalley, *Phys. Rev. A*, **55**, R1569 (1997).
4. H. Wang, P. L. Gould and W. C. Stwalley, *J. Chem. Phys.*, **106**, 7899 (1997).
5. H. Wang, X. T. Wang, P. L. Gould and W. C. Stwalley, *Phys. Rev. Letters*, **78**, 4173 (1997).
6. H. Wang, P. L. Gould and W. C. Stwalley, *Phys. Rev. Letters*, **80**, 476 (1998).
7. X. T. Wang, H. Wang, P. L. Gould, W. C. Stwalley, E. Tiesinga and P. S. Julienne, *Phys. Rev. A*, **57**, 4600 (1998).
8. A. N. Nikolov, E. E. Eyler, X. Wang, H. Wang, J. Li, W. C. Stwalley and P. L. Gould, *Phys. Rev. Lett.*, **82**, 703 (1999).
9. Y. B. Band and P. S. Julienne, *Phys. Rev. A*, **51**, R4317 (1995).
10. J. T. Bahns, W. C. Stwalley and P. L. Gould, *J. Chem. Phys.*, **104**, 9689 (1996).
11. A. Vardi, D. Abrashkevich, E. Frishman and M. Shapiro, *J. Chem. Phys.*, **107**, 6166 (1997).
12. P. S. Julienne, K. Burnett, Y. B. Band and W. C. Stwalley, *Phys. Rev. A*, **58**, R797 (1998).
13. W. C. Stwalley and He Wang, "Photoassociation of Ultracold Atoms: A New Spectroscopic Technique," *J. Mol. Spectrosc.*, in press.
14. J. T. Bahns, P. L. Gould and W. C. Stwalley, "Formation of Cold ($T \leq 1\text{K}$) Molecules," submitted to *Adv. At. Mol. Opt. Phys.*

New Directions in Radical Photochemistry and Reaction Dynamics

Arthur G. Suits

Chemical Sciences Division MS 6-2100

Ernest Orlando Lawrence

Berkeley National Laboratory

Berkeley CA 94720 USA

Radical reaction dynamics represents an important frontier area of chemical dynamics, owing to the central role these species play in macroscopic chemical systems. Their extraordinary reactivity gives rise to well-known difficulties in preparing molecular beams of radicals, and this has hampered application of the full power of the tools of chemical dynamics to these important systems. Additional challenges in the detection of radicals and radical reaction products exist that further complicate the study of their reaction dynamics. For example, many of the most important species, from a practical point of view, are hydrocarbons with poorly characterized structures, little or no spectroscopic information, and electron-impact fragmentation patterns that preclude ready application of traditional universal detection methods. In Berkeley we have been developing and applying several methods to probe the reaction dynamics and photochemistry of radicals; two of these will be presented and discussed at the meeting. One involves the application of intense, tunable vacuum ultraviolet synchrotron undulator radiation as a *universal but selective* probe of reaction products. The second involves application of the velocity map imaging (VELMI) technique to the study of radical photochemistry and reaction dynamics. We will show that this combination of complementary universal, synchrotron-based studies with state-resolved laser imaging investigations can provide deep insight into the dynamics in these challenging systems.

Control of Molecular Dynamics: A Historical and Conceptual Overview

David J. Tannor
Department of Chemical Physics
Weizmann Institute, Rehovot, ISRAEL

The last ten years has seen an explosion of ultrafast laser technology and its uses to probe and control chemical reactions. This talk will review the four main approaches to this subject:

1. Intuitive design of pulse sequences, including pump-dump schemes, phase control over multiple pathways, and pulse chirping.
2. Variational formulation of optical control of chemical reactions, and its close relative, optimal control theory. This allows going beyond simple pulse sequences, providing a 'black box' computational scheme to design complex optimal pulse shapes and sequences via an iterative procedure.
3. Learning algorithms, including "genetic" algorithms, for iterative pulse design in a laboratory setting. Experimental examples include control of molecular fluorescence, enhancement of harmonic generation, femtosecond pulse compression, and very recently, control over photochemical branching.
4. Local optimization, in which a desired objective is forced to increase monotonically via the phase of the carrier frequency of the field. This technique has been applied to laser heating and cooling of molecules, optical paralysis (turning off multiphoton ionization) and the design of simple generalizations of STIRAP to N-level systems.

References

1. D. J. Tannor and S. A. Rice, J. Chem. Phys. 83, 5013 (1985).
2. D. J. Tannor, R. Kosloff and S. A. Rice, J. Chem. Phys. 85, 5805 (1986).
3. R. Kosloff, S. A. Rice, P. Gaspard, S. Tersigni and D. J. Tannor, Chem. Phys. 139, 201 (1989).
4. D. J. Tannor, in *Molecules in Laser Fields*, ed. A. D. Bandrauk, (Dekker; New York, 1994).

5. V. Malinovsky, Ch. Meier and D. J. Tannor, Chem. Phys. 221, 67 (1997).
6. V. Malinovsky and D. J. Tannor, Phys. Rev. A, 56, 4929 (1997).
7. D. J. Tannor, R. Kosloff and A. Bartana, Faraday Disc. 113, 1999 (submitted).
8. W. S. Warren, H. Rabitz and M. Dahleh, Science, 259, 1581 (1993).
9. P. Brumer and M. Shapiro, Scientific American, March, 1995.
10. R. J. Gordon and S. A. Rice, Annu. Rev. Phys. Chem. (1997).
11. A. Assion, T. Baumert, M. Bergt, T. Brixner, B. Kiefer, V. Seyfried, M. Strehle and G. Gerber, Science, 282, 919 (1998).

Holographic Probes of Molecular Structure and Dynamics: Nonlinear Optical Spectroscopy as a Probe of Proton Transfer and Hydrogen Bonding in Malonaldehyde

P. H. Vaccaro

Department of Chemistry, Yale University
New Haven, CT 06520-8107

The interrelated phenomena of hydrogen bonding and proton transfer represent two important aspects of molecular behavior which play crucial roles in a wide variety of chemical and biological processes. Indeed, it can be argued justifiably that the coupling and transduction of hydrons across preexisting intramolecular or intermolecular hydrogen bonds constitutes one of the most prevalent events in nature, responsible for mediating the physical properties exhibited by diverse species ranging from liquid water to *in vivo* biomolecules. The model system for quantitative investigations of these concepts is malonaldehyde, the most stable isomer of 3-hydroxy-2-propenal ($\text{HO}-\text{CH}=\text{CH}-\text{CH}=\text{O}$), which contains an intramolecular hydrogen bond that adjoins hydroxylic (proton donating) and ketonic (proton accepting) oxygen atoms. Isolated malonaldehyde exists almost completely as the chelated enol tautomer, with a finite potential barrier, having an estimated height of 2000 cm^{-1} separating two stable conformers of C_s symmetry. Although hindered, rapid interconversion between these equivalent structures can occur by means of quantum mechanical proton tunneling, thereby leading to a characteristic doubling of all rovibronic features. Rather than depending solely on the motion of the shuttling proton, the magnitude of such tunneling-induced splittings contains detailed information regarding the concomitant displacement of all other nuclei in the molecular framework as well as the redistribution of charge density among the various atoms. Consequently, vibrational and/or electronic excitation of malonaldehyde can be expected to exert a profound influence upon the overall efficiency and detailed pathway of proton migration. This talk will discuss recent experimental work designed to elucidate the electronic-state and vibrational-mode specificity of tunneling dynamics in malonaldehyde and its symmetrically-deuteriated isotopomers. In particular, building upon the background-free, absorption-like response afforded by fully resonant-enhanced variants of sub-Doppler four-wave mixing spectroscopy, ongoing laboratory efforts have successfully interrogated the weak $\tilde{A}^1B_1 - \tilde{X}^1A_1$ ($\pi^* \leftarrow n$) transition of malonaldehyde, thereby permitting the influence of electronic and nuclear degrees of freedom upon proton transfer processes to be ascertained. The insight into multidimensional tunneling dynamics gleaned from these measurements will be compared and contrasted with theoretical predictions derived from recent high-level *ab initio* calculations of potential energy hypersurfaces and related semiclassical/quantum-mechanical analyses of hydron migration.

Current issues in potential energy surfaces and dynamics: the challenge of conical intersections

A.J.C. Varandas

Departamento de Química, Universidade de Coimbra
3049 Coimbra Codex, Portugal

Abstract

We discuss recent work directed toward the understanding of vibrational spectra and reaction dynamics of small polyatomic molecules. First, we review briefly our progress on modelling potential energy surfaces which includes the extension of the double many-body expansion method to atoms of any spin multiplicity and angular momentum and the energy-switching scheme for functions of spectroscopic accuracy. Then we focus on dynamics studies which employ such potential energy surfaces. Applications cover so far several triatomic and tetraatomic systems. Although we refer briefly to studies of four-atom reactions with relevance in atmospheric chemistry and/or combustion processes which have been carried out under the premise that they occur on the ground state potential energy surface, the emphasis will be on triatomic processes involving conical intersections and hence requiring an analysis that goes beyond the usual Born-Oppenheimer approximation. Special attention will then be given to the transition state resonances of H_3 and the vibrational spectra of $^7\text{Li}_3$, which have been calculated both with inclusion and without inclusion of geometric phase effects. A novel approach toward the treatment of such effects in heteronuclear systems like HD_2 is also discussed. We conclude with some remarks on continuing challenges and an outlook on planned work.

State-resolved dynamics of NO produced by 248 nm photodissociation
of t-butyl nitrite on Ag(111)

C. Kim, W. Zhao, and J. M. White

Center for Material Chemistry
Department of Chemistry and Biochemistry
University of Texas
Austin, TX 78712

The dynamics of nitric oxide, NO, produced by 248 nm photodissociation of t-butyl nitrite, $(\text{CH}_3)_3\text{CONO}$, adsorbed on Ag(111) has been studied using the resonance enhanced multiphoton ionization time-of-flight (REMPI-TOF) technique. REMPI-TOF spectra of NO ejected from the surface are sensitive to the rotational state of NO and the surface coverage and structure of t-butyl nitrite. A REMPI-TOF spectrum of NO at high rotational states ($J > \sim 40.5$) shows a sharp peak of fast collisionless NO ejection along with an intermediate peak due to collisional energy loss of nascent NO to neighboring molecules. The collisionless peak is an evidence of direct excitation of t-butyl nitrite followed by prompt dissociation of NO. As J is lowered, the intermediate peak position changes from 60 % of the collisionless kinetic energy down to 25%. A low J ($< \sim 20.5$) spectrum shows a slow peak thermalized to the surface temperature. The experimental results support the collisional model of NO ejection previously proposed by Fieberg and White. In addition to the TOF distributions, the rotational energy, rotational polarization and electronic energy distributions of NO will be presented.

Superfluidity and Spectroscopy of Na-Doped Quantum Helium Clusters:
A Path Integral Monte Carlo Study

Akira Nakayama and Koichi Yamashita

Department of Chemical System Engineering, The University of Tokyo,

7-3-1 Hongo, Bunkyo, Tokyo 113-8656, Japan

e-mail: yamasita@chemsys.t.u-tokyo.ac.jp

The study of helium clusters has attracted a great deal of interest because of their unique finite-size quantum-liquid nature. Recent experiments on these clusters with atomic and molecular impurities doped have made it possible to conduct indirect probes of their structures [1]. These impurity-doped helium clusters are important systems for studying the solvation and dynamics of atoms and molecules interacting with a quantum environment and in finding new microscopic manifestations of superfluidity [2].

In this study, we investigate the structure of quantum helium clusters doped with a sodium atom in its ground state, excited p-state and its ion, by employing the path integral Monte Carlo method [3]. Size and temperature dependences of the cluster structure are studied. Several physical quantities such as energy, density distribution function, and superfluid fraction are calculated.

In the case of the ground state sodium atom, it is found that the atom is trapped in a dimple on the helium cluster's surface in the superfluid phase as predicted by experiments and other theoretical methods. For the sodium ion system, there is a triple layer structure in which the 'snowball' structure is formed up to the second shell. Absorption spectra for the excited Na(P) state and some other details in connection with recent experiments will be discussed.

References

1. J. P. Toennies and A. F. Vilesov, *Ann. Rev. Phys. Chem.* **49**, 1 (1998).
2. S. Grebenyev, J. P. Toennies, A. F. Vilesov, *Science*, **279**, 2083 (1998).
3. D. M. Ceperley, *Rev. Mod. Phys.* **67**, 279 (1995).

Measuring State-Resolved Differential Cross Sections Using the PHOTOLoc Technique

Richard N. Zare

Department of Chemistry, Stanford University, Stanford, CA 94305-5080.

Photoinitiated reactions analyzed by the law of cosines (PHOTOLoc) offers in favorable circumstances a means of measuring state-resolved differential cross sections for all scattering angles with high sensitivity. The photoloc technique is illustrated by applying it to the hydrogen-atom hydrogen-molecule bimolecular exchange reaction. Specifically, Brian D. Bean and Félix Fernández-Alonso have studied in detail the reaction



by coexpanding a mixture of HBr and D₂ into a vacuum chamber with a pulsed nozzle, photolyzing the HBr precursor to generate monoenergetic H atoms, and detecting the resulting HD(ν', J') products via (2+1) resonance-enhanced multiphoton ionization (REMPI). The collision energy spread is measured to be less than 50 meV. The D₂ rotational distribution is composed of a mixture of the three lowest J levels (J = 0, 1, 2) in the ratio 0.45:0.35:0.10. The angular resolution varies from about 5° for backward scattering to 15° for forward scattering. Integral cross section measurements are also readily obtained. The results will be compared to theory and with previous experimental work, particularly the H-atom Rydberg tagging studies of Schnieder et al. We find that a simple treatment that incorporates line-of-centers energetic constraints with nearly elastic specular scattering (LOCNESS model) is able to reproduce the experimental data in a qualitative manner for a wide range of scattering conditions.

Support by the National Science Foundation is gratefully acknowledged.

The SVRT model for Quantum Polyatomic Reaction Dynamics

John Z.H. Zhang

*Department of Chemistry
New York University*

ABSTRACT

In this talk, I will describe the development of a new theoretical model for practical computational study of quantum reaction dynamics involving large polyatomic molecules. The new SVRT (semi-rigid vibrating rotor target) model for polyatomic systems is a natural generalization of the exact dynamical treatment for the prototype atom-diatom and diatom-diatom reaction systems. By employing the new SVRT model, it becomes possible to carry out realistic and quantitatively accurate computational dynamics study for polyatomic reactions including atom-polyatomic, polyatomic-polyatomic, and polyatomic-surface reaction dynamics with only a limited number of mathematical degrees of freedom.

Details of the SVRT model and the time-dependent wavepacket implementation of the model to polyatomic systems will be discussed.

Daniel J. Heinzen
Dept. of Physics
The University of Texas at Austin

We have carried out studies of atomic Rb collisions at temperatures spanning the range from 1 mK to 100 nK. At the lowest temperatures the Rb gas forms a Bose-Einstein condensate (BEC). The physics of these ultracold collisions is very different from those at room temperature. Semiclassical approximations fail in this limit, and the collisions must be understood quantum mechanically. Resonance and threshold phenomena are very pronounced. In some cases, the collisions can be restricted to a single channel, in which all quantum numbers are determined. Further, it is not possible to understand the kinetics of a Bose-condensed gas in terms of isolated, two-body collisions, even though the gas is very dilute. Rather, the collision amplitudes of many pairs of atoms add coherently, and new effects such as collisional self-energy emerge. Most of our experiments have been carried out using the technique of photoassociation spectroscopy, in which we drive free-bound optical transitions in colliding pairs of atoms. With this technique, we have observed such phenomena as shape and Feshbach collision resonances. We have also carried out photoassociation experiments in a Bose-condensed Rb gas, and have observed two-photon free-bound transitions with linewidths as small as 160 kHz. These transitions provide a possible mechanism to generate a diatomic molecular BEC from an atomic BEC.

Diversity of Reactions at Surfaces

*Barbara J. Garrison
Department of Chemistry
Penn State University
University Park, PA 16802
<http://galilei.chem.psu.edu/>*

A plethora of reactions can occur at surfaces. In this overview talk a number of the possible events including adsorption, etching, surface reactions, surface-induced dissociation, sputtering and friction will be described. The binding theme will be systems that have been modeled with the Brenner hydrocarbon potential.

ABSTRACTS
OF
CONTRIBUTED PAPERS
(C1-C102)

ELECTRON CAPTURE BY H^+ colliding with Ar

Amaya-Tapia, A. Martínez, H. Hernández, R. †

Centro de Ciencias Físicas UNAM AP 18-3, Cuernavaca, Mor.

†Centro Internacional de Química, UAEM Cuernavaca, Mor.

email: jao@cco.fis.unam.mx

Electron transfer in ion-atom collisions is an important process to the understanding and controlling the properties of plasmas. Charge exchange process in the collision of a proton beam with an argon target gas has been the subject of considerable experimental effort, over a wide range of energies. The corresponding theoretical investigations have been rather scarce particularly in the keV/amu collision energy region. The close-coupling method has been extensively used for studying ion-atom collisions in the low to intermediate impact energy region. For this energy range, where the velocity of the projectile is of the same order as that of the active target electrons, various strongly coupled states play an important role in the process. This makes the close-coupling method a natural choice to account for the dynamics of the collision. We applied the recently developed (by the Kansas group) two-centre atomic orbital close-coupling method for the electron capture process to the system $H^+ + Ar \rightarrow H + Ar^+$ in the 1 - 100 keV/amu energy range. We modeled this one-electron semiclassical description to take into account the effect of the other electrons in the 3p subshell. We consider different initial and final electronic states of the ion and the target and we analyze the subshell contribution to the individual electron capture cross sections as a function of projectile's energies. The results for total capture cross sections are compared with data from the literature.

This work has been supported by CONACyT 3659P-E9607 and DGAPA IN-100392

Molecular and dissociative adsorption of nitrogen on tungsten clusters

Mats Andersson, Lotta Holmgren, Arne Rosén

Department of Experimental Physics, Chalmers University of Technology and
Göteborg University, S-412 96 Göteborg, Sweden
mats.andersson@fy.chalmers.se

We have studied the adsorption of N_2 on neutral tungsten clusters, W_{10} - W_{60} , under single-collision-like conditions in a cluster beam experiment [1]. A beam of clusters, seeded in He gas, is produced in a pulsed laser vaporization source. After skimming the beam travels through a low-pressure reaction cell where the clusters make one or a few collisions with N_2 molecules. Bare clusters and reaction products are detected with laser ionization and time-of-flight mass spectrometry. The reaction probability in a collision (S) is determined by evaluating the reaction product abundance as a function of reaction cell pressure.

The reaction probability with the first and second N_2 molecule was measured as a function of cluster size for clusters produced at room temperature (RT) and liquid-nitrogen temperature (LNT). For RT-clusters there is a strong size-selectivity, particularly in the W_{10} - W_{26} range, where the highest reaction probability $S=0.15$ - 0.2 is measured for W_{16} and W_{22} and the least reactive clusters have S close to or below the detection limit, ~ 0.01 . When the cluster source is cooled to LNT all clusters become more reactive (S up to 0.7) and the relative variations with size decrease in magnitude but persist. Also more than one N_2 can adsorb onto the LNT-clusters, which is not the case at RT. The size and temperature dependence measured in this experiment is similar to what was observed in flow-tube reactor [2].

The qualitative difference in reactivity of clusters produced at RT and LNT indicates that different reaction and binding mechanisms could be active at the two temperatures. Therefore we have employed laser-induced thermal desorption spectroscopy on the reaction products by irradiating the clusters with 4.0 -eV photons after reaction but before ionization and detection. There was practically no desorption of N_2 from the RT-clusters, while a significant fraction of the N_2 bound to the LNT-clusters desorbed. Thus, we conclude that nitrogen is very strongly bound in a dissociative state on the RT-clusters, whereas there also exist a more weakly bound molecular state on the clusters produced at LNT, and that the adsorption of molecular N_2 is much less cluster size dependent. These observations correspond qualitatively with the characteristics of nitrogen adsorption on bulk tungsten surfaces [3].

1. L. Holmgren, M. Andersson, and A. Rosén, *J. Chem. Phys.* 109, 3232 (1998).
2. S.A. Mitchell, D.M. Rayner, T. Bartlett, and P.A. Hackett, *J. Chem. Phys.* 104, 4012 (1996).
3. C.N.R. Rao and G. Ranga Rao, *Surf. Sci. Rep.* 13, 221 (1991).

Photodissociation dynamics of O_2 near 193 nm

Bernard L. G. Bakker and David H. Parker

*Department of Molecular and Laser Physics, University of Nijmegen,
Toernooiveld 1, 6525 ED Nijmegen, The Netherlands*

Abstract

The combination of (2+1) resonant multiphoton ionization and velocity map imaging has been proven to be a powerful method for investigations of photodynamical processes of diatomics[1]. It provides the determination of kinetic energy and angular distributions of the fragments allowing a full discrimination between the different decay channels.

Photodissociation of O_2 around 193 nm via the $B^3\Sigma_u^-(\nu = 4)$ state has been studied using the velocity map imaging technique and a tunable ArF excimer laser. The formed $O(^3P_2)$ were detected via (2+1) REMPI with a Nd:Yag pumped dye laser system. Also the dissociation after multiphoton excitation of O_2 has been characterized.

The spectral resonant behavior could be observed and explained. Angular and kinetic energy distributions of the formed oxygen ions and ionized $O(^3P_2)$ atoms have been recorded and analyzed.

References

- [1] D.H. Parker and A.T.J.B. Eppink, J. Chem. Phys. 107 (1997) 2357.

Energy transfer in ultracold atom-molecule collisions

N. Balakrishnan, R.C. Forrey, and A. Dalgarno

*Institute for Theoretical Atomic and Molecular Physics
Harvard-Smithsonian Center for Astrophysics
60 Garden Street, Cambridge, Massachusetts 02138*

We present results of quantum mechanical scattering calculations including full ro-vibrational coupling on the relaxation of vibrationally and rotationally excited H_2 and CO molecules in collisions with ultracold He atoms. The influence of the attractive well of the potential on the rate coefficients is investigated and is found to be qualitatively different for He-H_2 and He-CO collisions with the latter supporting a number of narrow resonances at impact energies lower than the van der Waals well depth. For both systems, the ro-vibrational transition cross sections exhibit an inverse-velocity dependence in accord with Wigner's threshold law at extremely small impact energies and the quenching rate coefficients become finite in the limit of zero temperature. The computed rate coefficients are used in an exactly solvable kinetic model to describe the decay of vibrationally excited trapped molecules due to interactions with cold atoms.

The Effect of C-H Methyl Bond Extension on CH_3CFCl_2 Photodissociation Dynamics

C5

A. Melchior, X. Chen, S. Rosenwaks and L. Bar^a

Department of Physics and ^aThe Institutes for Applied Research, Ben-Gurion

University of the Negev, Beer-Sheva 84105, Israel

Abstract

The fundamental symmetric CH_3 stretch (ν_{CH}), and the second ($3\nu_{\text{CH}}$) and third ($4\nu_{\text{CH}}$) overtones in the ground electronic state of CH_3CFCl_2 are prepared by stimulated Raman excitation and direct infrared excitation, respectively. The excited molecules are photodissociated by ~ 235 or 243.135 nm photons that further tag $\text{Cl}(^2\text{P}_{3/2})$ and $\text{Cl}(^2\text{P}_{1/2})$ [Cl^*] or H photofragments via $(2 + 1)$ resonantly enhanced multiphoton ionization. The yield of all three photofragments increases as a result of preexcitation demonstrating that the energy is not preserved in the excited bond, but rather flows to the C-Cl bond. The initial vibrational state preparation does not only enhance C-Cl and C-H bond cleavage but also affects Cl^*/Cl and $\text{H}/[\text{Cl} + \text{Cl}^*]$ branching ratios, as compared to the nearly isoenergetic one-photon ~ 235 and 193 nm photolysis of vibrationless ground state CH_3CFCl_2 , implying that it alters photodissociation dynamics.

Differential Cross Sections and Product State Distributions for the Reaction $\text{H} + \text{D}_2(v=0, J=0-2) \rightarrow \text{HD}(v'=1-3, J') + \text{D}$ near 1.6 eV Collision Energy.

Brian D. Bean, James D. Ayers, Félix Fernández-Alonso, Richard N. Zare

Using a newly constructed time-of-flight mass spectrometer with removable core-extraction masks, we measured the laboratory distribution of product speeds for the title reaction. We employ the photoloc technique (*photo*initiated reaction analyzed with the *law of cosines*) to extract differential cross sections from these measurements. In addition, we experimentally determined the distribution of product states by removing the core extraction masks and adjusting the TOF settings in order to collect all $\text{HD}(v', J')$ product ions.

The experiment in brief: A mixture of D_2 and HBr is coexpanded through a pulsed nozzle into a vacuum chamber. A tunable, linearly polarized laser intersects the expansion and creates a well-defined distribution of H-atom velocities. The H atoms react with D_2 to produce HD with a collision energy defined by the laser wavelength. Because we use (2+1) REMPI to ionize the $\text{HD}(v', J')$ products of interest we achieve complete state selectivity. The collision energy resolution is 50 meV and the spread in center-of-mass scattering angles varies from 5° - 12° (backward to forward scattering respectively).

A simple line-of-centers model can be used to describe the basic characteristics of this reaction at this energy. By supposing a direct reaction through a linear H-D-D transition state, we are able to predict the distribution of product states from the scattering maxima in the differential cross sections.



SPECTRAL
SCIENCES
INCORPORATED

C7

99 South Bedford Street, #7 Burlington, Massachusetts 01803-5169

April 27, 1999

J. J. Valentini
Dept. of Chemistry
Columbia University
3000 Broadway, MC 3120
New York, NY 10027

Dear Professor Valentini,

Below is an abstract for a poster I would like to present at the XVIIth Conference on the Dynamics of Molecular Collisions, July 18-23, 1999. If you have any questions about the work, please contact me at 781-273-4770 or at my email address, matt@spectral.com.

Sincerely,


Matthew Braunstein

Electronic Structure and Reaction Dynamics of $O(^3P) + CO(^1\Sigma^-)$ Collisions

L. S. Bernstein, M. Braunstein, W. Dimpfl, and J. W. Duff
Spectral Sciences, Incorporated
99 S. Bedford Street, Suite #7
Burlington, MA 01803

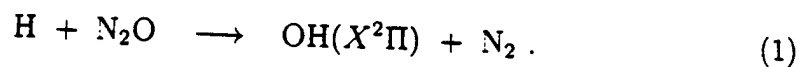
We present results of electronic structure calculations on the low-lying triplet states of CO_2 , and classical dynamics studies of $O(^3P) + CO(^1\Sigma^-)$ collisions which occur on these surfaces. Vibrational excitation of CO and "reactive exchange" of oxygen atom are important in understanding CO_2 recombination, while the deactivation of vibrationally excited $CO(^1\Sigma^-)$ by $O(^3P)$ is a critical step in the CO chemical laser. Using extensive configuration interaction calculations, we find that of the three relevant CO_2 triplet states which lead to $CO(^1\Sigma^-) + O(^3P)$ products, two are bound and one is repulsive. The two bound states have well depths of about 0.5 eV and barrier heights of about 0.25 eV. Furthermore, due to the fact that they can only decay to the singlet ground state, these triplet states have long lifetimes and should be detectable. Approximate lifetimes and spectroscopic constants for these triplet states are reported. We also have computed energies for these states at geometries important for O + CO collisions, and have fit these points to an analytic function. We have run classical trajectory calculations with these fitted potential energy surfaces and computed cross sections for reactive and non-reactive collisions up to about 4 eV. Results are compared to thermal excitation and de-excitation data and to available energy specific measurements. We find that collisional deactivation is extremely efficient, in agreement with experiment, with cross sections approaching gas kinetic at high energy. For vibrational excitation of CO by O at high collision energies, the reactive exchange channel results in extremely high excitation of CO rotational levels to produce a distinctive radiative "bandhead" signature of the nascent CO products.

The OH product state resolved stereodynamics of the reaction of
H with N₂O

M. Brouard, S.D. Gatenby, D.M. Joseph and D. Minayev

*The Physical and Theoretical Chemistry Laboratory, Department of
Chemistry, South Parks Road, Oxford, OX1 3QZ*

The stereodynamics of the reaction



has been investigated using a Doppler-resolved laser induced fluorescence technique. OH product state-resolved angular scattering and translational energy release distributions have been determined, together with OH rotational angular momentum polarizations. These observables are found to depend sensitively on OH rovibrational quantum state, and help provide valuable insight about the reaction mechanism(s). In particular, our measurements have revealed distinctly bimodal kinetic energy release distributions, which we ascribe to the operation of two microscopic mechanisms, and associate with initial H-atom attack at the terminal nitrogen and the oxygen ends of the NNO molecule.

Our most recent measurements have shown that the rotational angular momentum is aligned parallel to the OH velocity, the OH rotating in a propeller type motion. In addition, we hope to present the results of experiments aimed to determine whether the OH angular momentum distributions exhibit any *orientation*, an observable which has yet to be determined for a bimolecular reactive system.

DIFFERENTIAL CROSS SECTIONS FOR THE $F+H_2$ REACTION: A COMPARISON OF CLASSICAL TRAJECTORY RESULTS FOR TWO POTENTIAL ENERGY SURFACES

Frank E. Budenholzer and Miao-Chuan Lin

Department of Chemistry, Fu Jen Catholic University, Hsinchuang, 242 Taiwan

Classical trajectories were calculated for the $F + H_2$ reaction over two potential energy surfaces: (1) the well known Muckerman 5 surface (*Theoretical Chemistry: Advances and Perspectives* 1981,6A,1) and (2) the recent surface of Stark and Werner (*J. Chem. Phys.* 1996,104,6515). Integral cross sections, state specified cross sections, differential cross sections and product energy distributions were calculated for the two surfaces. Since the methods for calculating the trajectories and expressing differential cross sections were identical for both surfaces, the rather substantial differences in the results are clearly due to differences in the potential surfaces. The results are discussed in terms of the special characteristics of the two surfaces.

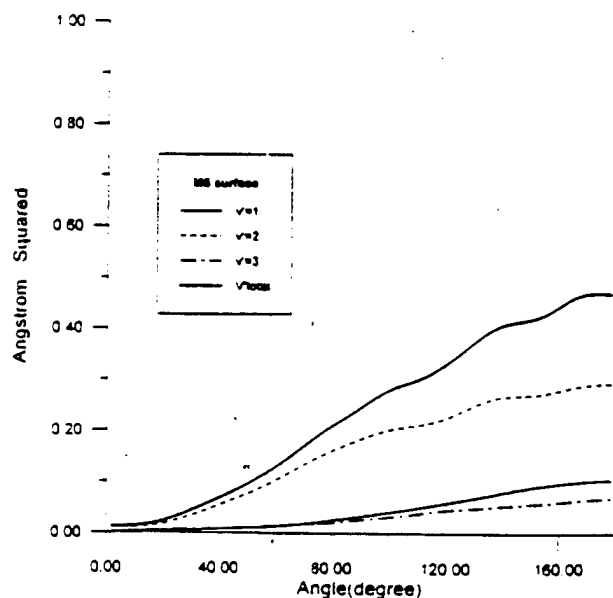


Fig. 1. Differential cross sections for the product $v' = 1, 2, 3$ vibrational states and the total differential cross section for trajectories calculated over the Muckerman 5 surface.^{*} The ordinate is in units of area \AA^2 (per steradian). The ordinate is in an-

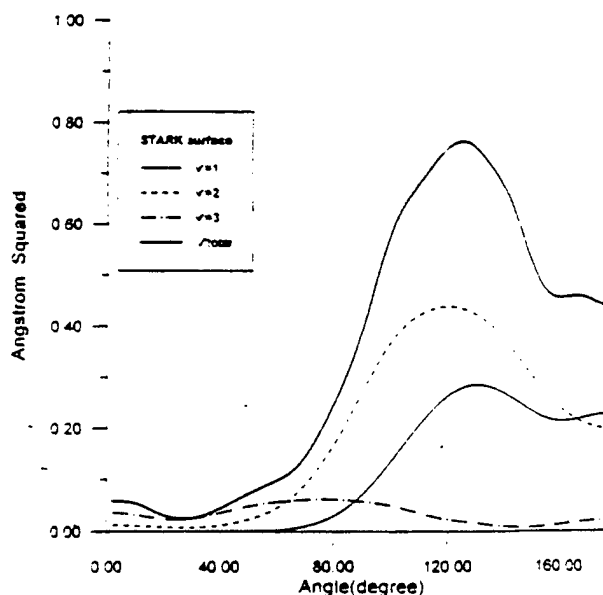


Fig. 2. Differential cross sections for the product $v' = 1, 2, 3$ vibrational states and the total differential cross section for trajectories calculated over the

Temperature Dependent Rate Constants for the Reactions of Gas Phase Lanthanides with N₂O

Mark L. Campbell*

Chemistry Department

United States Naval Academy

Annapolis, MD 21402

Abstract: The reactivity of gas phase lanthanide atoms Ln (Ln = La - Yb with the exception of Pm) with N₂O from 298 to 623 K is reported. Lanthanide atoms were produced by the photodissociation of Ln(TMHD)₃ (TMHD = 2,2,6,6-tetramethyl-3,5-heptanato ion) and detected by laser-induced fluorescence. Large variations in the reaction rate constants are observed. The bimolecular rate constants are described in Arrhenius form by: $k[\text{Ce}(^1\text{G}_4)] = (1.9 \pm 0.5) \times 10^{-10} \exp(-0.8 \pm 0.8 \text{ kJ} \cdot \text{mol}^{-1}/RT)$; $\text{Pr}(^4\text{I}_{9/2})$, $(3.6 \pm 1.2) \times 10^{-10} \exp(-8.0 \pm 1.2 \text{ kJ} \cdot \text{mol}^{-1}/RT)$; $\text{Nd}(^3\text{I}_4)$, $(3.4 \pm 0.4) \times 10^{-10} \exp(-8.8 \pm 0.5 \text{ kJ} \cdot \text{mol}^{-1}/RT)$; $\text{Sm}(^7\text{F}_0)$, $(3.2 \pm 1.1) \times 10^{-10} \exp(-11.2 \pm 1.2 \text{ kJ} \cdot \text{mol}^{-1}/RT)$; $\text{Eu}(^8\text{S}_{7/2})$, $(2.7 \pm 0.4) \times 10^{-10} \exp(-12.7 \pm 0.5 \text{ kJ} \cdot \text{mol}^{-1}/RT)$; $\text{Gd}(^9\text{D}_2)$, $(2.0 \pm 0.3) \times 10^{-10} \exp(-6.4 \pm 0.5 \text{ kJ} \cdot \text{mol}^{-1}/RT)$; $\text{Tb}(^6\text{H}_{15/2})$, $2.9 \pm 0.5 \times 10^{-10} \exp(-10.9 \pm 0.6 \text{ kJ} \cdot \text{mol}^{-1}/RT)$; $\text{Dy}(^3\text{I}_8)$, $(3.4 \pm 0.8) \times 10^{-10} \exp(-16.2 \pm 0.8 \text{ kJ} \cdot \text{mol}^{-1}/RT)$; $\text{Ho}(^4\text{I}_{15/2})$, $(2.9 \pm 0.5) \times 10^{-10} \exp(-17.1 \pm 0.6 \text{ kJ} \cdot \text{mol}^{-1}/RT)$; $\text{Er}(^3\text{H}_6)$, $(3.3 \pm 1.2) \times 10^{-10} \exp(-18.4 \pm 1.2 \text{ kJ} \cdot \text{mol}^{-1}/RT)$; $\text{Tm}(^2\text{F}_{7/2})$, $(3.5 \pm 0.6) \times 10^{-10} \exp(-19.5 \pm 0.6 \text{ kJ} \cdot \text{mol}^{-1}/RT)$; $\text{Yb}(^1\text{S}_0)$, $(2.5 \pm 0.2) \times 10^{-10} \exp(-20.2 \pm 0.3 \text{ kJ} \cdot \text{mol}^{-1}/RT)$ where the uncertainties represent $\pm 2\sigma$. The reaction barriers are found to correlate to the energy required to promote an electron out of the 6s subshell.

*Henry Dreyfus Teacher-Scholar. This research was supported by a Cottrell College Science Award of Research Corporation.

Orientation of ICN and BrCN with a Strong, Uniform Electric Field: Studies of Photodissociation Dynamics

K. J. Castle*, H. Li, and W. Kong

Department of Chemistry, Oregon State University, Corvallis, Oregon 97331-4003 USA

Email: franksk@ucs.orst.edu

Brute force orientation employs electrostatic interactions between the permanent dipole moment of a polar molecule and an external electric field. If the electrostatic interactions are strong enough to constitute a barrier to free rotation, molecules will develop a preferred orientation with their permanent dipole moments parallel to the electric field. Following dissociation of an effectively oriented system, dependence of fragment yield on the polarization direction of the dissociation laser leads to valuable information regarding the photodissociation dynamics of the system.

When more than one potential surface is accessible in a single photon process, steric control achieved via a strong uniform electric field can lead to preferential excitation of a desired transition. For example, ICN has three major potential surfaces contributing to the absorption process. Two of the surfaces are accessible through perpendicular transitions (the transition dipole moments are perpendicular to the permanent dipole of the molecule), and the third surface is accessible through a parallel transition (the transition dipole moment and the permanent dipole are parallel.) When ICN molecules are oriented in an electric field and the dissociation laser is polarized along the direction of the orientation field, the parallel transition can be preferentially excited.

This technique was used to compare the photodissociation dynamics of ICN and BrCN at photolysis wavelengths near their respective absorption maxima. Laser-induced fluorescence of the CN fragment from dissociation of ICN at 266 nm showed that this transition is nearly purely parallel in nature, while photolysis of BrCN at 213 nm showed a significant perpendicular component. Quantitative analysis was used to determine the effective transition dipole moment direction, and subsequently, the amount of perpendicular character in the transition.

Using Stretching and Bending Vibrations to Direct the Reaction of Cl Atoms with Isocyanic Acid (HNCO)

Ephraim Woods III,^a Christopher M. Cheatum, and F. Fleming Crim

Department of Chemistry

University of Wisconsin - Madison

Madison, Wisconsin 53711

Preparation of well-characterized vibrational states in the region of three quanta of N-H stretching excitation ($3\nu_1$) in isocyanic acid (HNCO) permits experimental investigation of the extent to which vibrations along the reaction coordinate and those perpendicular to it can direct the bimolecular reaction of Cl atoms with HNCO to form HCl and NCO. Angular momentum states corresponding to different amounts of a-axis rotation are well separated in energy, and perturbations by background states make each of the eigenstates a different mixture of zero-order states. Molecules in the essentially unperturbed $K = 1$ and 4 states, which are nearly pure N-H stretching excitation, react efficiently, but those in the perturbed states, $K = 0, 2$, and 3, which are a mixture of N-H stretching and bending excitation, react only half as well. Detailed analysis of resolved, perturbed eigenstates for $J = 6$ and 7 of $K = 3$ reveals the reactivity of the two interacting zero-order states separately. The less reactive zero-order state, which most likely contains only two quanta of N-H stretch and several quanta of bending excitation, reacts only 10% as well as the pure N-H stretch zero-order state.

(a) Present address: Department of Chemistry, University of North Carolina - Chapel Hill, Chapel Hill, NC 27599

Photodissociation Dynamics of Triiodide anion (I_3^-) and neutral (I_3)

Hyeon Choi, Ryan T. Bise, Alexandra A. Hoops, and Daniel M. Neumark¹

*Department of Chemistry, University of California, Berkeley, California, 94720, and
Chemical Sciences Division, Lawrence Berkeley National Laboratory, Berkeley,
California 94720.*

We have investigated the spectroscopy and dissociation dynamics of I_3^- and I_3 in the range of 290-390nm and 240-270nm, respectively, utilizing the method of fast beam photofragment translational spectroscopy. This paper reports the first photofragment yield (PFY) spectrum of I_3^- and the first electronic transition of I_3 in the gas phase. Two product mass ratios from the photodissociation of I_3^- and I_3 are observed: 1:1 and 1:2 mass ratios. Based on our detection scheme, the product channel with 1:1 mass ratio is assigned to the symmetric three-body dissociation. The $P(E_T)$ distribution with 1:2 mass ratio from the photodissociation of I_3^- shows that electronic transitions to those two absorption bands produce the $I_2^- (\tilde{X})$ and either spin-orbit ground or excited state of I. Based on our adiabatic picture, the $I_2^- (\tilde{X})$ and spin-orbit ground state of I is produced through the adiabatic process and the $I_2^- (\tilde{X})$ and spin-orbit excited of I is produced through the curve-crossing mechanism. The $P(E_T)$ distribution from the photodissociation of I_3 shows that the asymmetric three-body dissociation is a dominant process along with almost every energetically possible dissociation channel.

¹ Camille and Henry Dreyfus Teacher-Scholar

Angular Resolution in the Lyman- α Photolysis of H₂S and HCN.

C14

P. A. Cook, M. N. R. Ashfold, S. R. Langford.

School of Chemistry, University of Bristol, Bristol, UK, BS8 1TS

The Lyman- α photolysis of both H₂S and HCN (together with their deuterated isotopomers) have been studied using the technique of H atom photofragment translational spectroscopy (PTS), a time of flight (TOF) method which affords very high resolution with respect to the kinetic energy of the recoiling photofragments.

Previous studies have gone some way to addressing the question of energy disposal in these systems. However, the angular dependence of the photofragment flux, together with aspects of the branching ratios into the available electronic states of the photoproducts, remain unresolved. By coupling the H atom PTS technique to new apparatus that facilitates the study of the photolyses of such systems at a variety of photolysis laser polarisations, the anisotropy parameter ($\beta[E]$) for each system has been calculated as a function of fragment kinetic energy. Modelling of the experimental TOF profiles thus obtained gives further insight into the photofragment state distribution.

In both cases the experimental studies have been complemented by *ab-initio* calculations of the relevant potential energy surfaces.

UV Photodissociation of HN_3 : Experimental and Theoretical Studies of the $\text{H} + \text{N}_3$ Channel

C15

P. A. Cook, S. R. Langford, and M. N. R. Ashfold

School of Chemistry, University of Bristol, Bristol, United Kingdom

Recently, the technique of H atom photofragment translational spectroscopy (PTS) has been employed to study the formation of H atoms following UV excitation, at a number of wavelengths, of hydrazoic acid (HN_3) to its first electronically excited state.⁽¹⁾ From this study it is possible to conclude that the excited $^1\text{A}''$ potential energy surface (PES) possesses a significant barrier to fragmentation of approximately $\sim 4500 \text{ cm}^{-1}$. The major features of the H atom time of flight profiles thus obtained are assigned to a progression in the symmetric stretch and bend-stretch combination modes of the N_3 partner fragment.

In order to gain a further understanding of the inchoate motions of the electronically excited species that lead to such a fragment internal energy distribution, and to gain further evidence for the existence of a barrier on the $\tilde{\text{A}}^1\text{A}''$ surface, we have undertaken an ab-initio study, at the CASPT2 level, of the two implicated PESs. The surfaces thus obtained, are presented as a function of both the N-N-N and N-N-H in-plane bending co-ordinates.

¹ P. A. Cook, S. R. Langford, M. N. R. Ashfold, *Phys. Chem. Chem. Phys.*, 1999, **1**, 45-55

<http://www.chm.bris.ac.uk/pt/laser/hatom/posters/hn3poster/hn3presentation.html>

Rotationally and Electronically Inelastic Collisions of
CN($A^2\Pi$) in High Rotational Levels with Argon:
 Λ -doublet Propensities and Gateway Effects

C16

Paul J. Dagdigian and Xin Yang
Department of Chemistry
The Johns Hopkins University
Baltimore, MD 21218 USA

Rotationally and electronically inelastic transitions from specific, highly rotationally excited Λ -doublet, fine-structure levels of CN($A^2\Pi$), induced by collisions with argon, have been investigated by the optical-optical double resonance technique. High rotational levels of the CN($X^2\Sigma^+$) radical were prepared by 193 nm photolysis of BrCN diluted in slowly flowing Ar at total pressures of 0.5 – 1 Torr. After a suitable delay, individual fine-structure Λ -doublet levels of CN($A^2\Pi$, $v = 3$, $N \approx 60$) were prepared by excitation with a pulsed dye laser on various rotational lines in the $A^2\Pi - X^2\Sigma^+$ (3,0) band. Collisionally populated levels were probed after a short delay by laser fluorescence excitation in the $B^2\Sigma^+ - A^2\Pi$ (3,3) and $B^2\Sigma^+ - X^2\Sigma^+$ (3,7) bands. Absolute state-to-state rate constants were determined by comparison of the fluorescence signals for detection of the initial and final levels, and absolute total removal rate constants were obtained by following the decrease in the signal for detection of the initial level vs. the pump-probe delay.

Dramatically different final rotational state distributions were observed for collision-induced rotational transitions from initial Λ -doublet levels of A' and A'' symmetry, independent of the fine-structure label F_i . These propensities are believed to arise from approach in a "helicopter" orientation on the more attractive Ar-CN(A) A' potential energy surface, followed by curve crossing to the A'' potential energy surface correlating with the next lower rotational asymptote. The measured state-to-state rate constants compare very well with theoretical rate constants calculated by Millard Alexander (University of Maryland) in a quantum mechanical collisional treatment using *ab initio* CN-Ar potential energy surfaces computed by A. Berning and H.-J. Werner (Universität Stuttgart).

A crossing of the $A^2\Pi$ $v = 3$ F_1/f rotational/fine-structure manifold with the $X^2\Sigma^+$ $v = 7$ f manifold occurs at $N = 62$. We have investigated the importance of this "gateway" in facilitating collision-induced electronic transitions between these manifolds. The total removal rate constant for the perturbed $N = 62$ level is significantly larger than for those of neighboring unperturbed levels, indicative of the magnitude of the perturbation-assisted $A \rightarrow X$ rate constants. Moreover, the final-state distribution is strongly dependent on the identity of the initial state.

Quantum 3D calculations of the vibration-tunneling
dynamics of small metal/hydrogen clusters

JiXin Dai and Zlatko Bačić

Department of Chemistry, New York University, New York, NY 10003, U.S.A.

We present results of the theoretical investigations of the quantum dynamics of coupled anharmonic vibrations of a single hydrogen atom adsorbed on small nickel and palladium clusters. Excited H-atom vibrational states of H/M_n clusters ($M = \text{Ni, Pd}$; $n = 2 - 4$) were calculated using a 3D DVR methodology, for potential energy surfaces of Doll and co-workers,¹ based on the embedded atom method. At this stage of the investigations, the M_n subunit was treated as rigid, except for H/M_2 clusters where full-dimensional (3D) calculations were performed. The ground-state energies of H/M_2 from the 3D DVR calculations are in excellent agreement with those from DQMC calculations.¹ In addition, our calculations provide a comprehensive description of the vibrational level structure of H/M_2 clusters. The quantum 3D calculations of larger H/M_n clusters with $n = 3, 4$ (for rigid M_n), reveal intricate vibration-tunneling dynamics in excited vibrational eigenstates of the adsorbed H atom. In the case of H/M_4 , where M_4 has tetrahedral structure, the global minimum corresponds to H inside the M_4 tetrahedron, while the second, exterior isomer has H bound to the face(s) of the metal tetrahedron. Each isomer of H/M_4 has a distinct set of excited vibration-tunneling levels. Progress regarding the treatment of bigger H/M_n clusters, and attempts to include the motions of the metal atoms, will also be reported.

[1] B. Chen, M. A. Gomez, M. Sehl, J. D. Doll, and D. L. Freeman, J. Chem. Phys. 105, 9686 (1996).

Reaction Dynamics of Zr and Nb with Ethylene

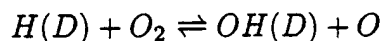
Peter Willis, Hans Stauffer, Ryan Hinrichs and Floyd Davis
Department of Chemistry and Chemical Biology
Cornell University, Ithaca NY 14853

The reactions of transition metal (M) atoms Zr and Nb with ethylene (C_2H_4) were studied using the technique of crossed molecular beams.¹ Angular and velocity distributions of MC_2H_2 products following H_2 elimination were measured at collision energies between 5 and 23 kcal/mole using electron impact and 157 nm photoionization mass spectrometry. Photodepletion studies identify that the atomic reactants are predominantly in their ground electronic states and that the observed MC_2H_2 products result primarily from reactions of these ground state atoms. Center-of-mass product angular distributions derived from the data indicate that reactions involve formation of intermediate complexes having lifetimes longer than their rotational periods. Product translational energy distributions demonstrate that a large fraction of excess available energy is channeled into product internal excitation. Wide-angle nonreactive scattering of metal atom reactants following decay of long-lived MC_2H_4 association complexes was also observed for both transition metal reactants at collision energies ≥ 9 kcal/mole, with approximately 36% of the initial translational energy converted into C_2H_4 internal excitation. At collision energies of ≤ 6 kcal/mole, nonreactive scattering of Zr from ZrC_2H_4 decay was found to be negligible, whereas this channel was clearly observed for Nb. RRKM modeling of the competition between decay of MC_2H_4 complexes back to $M + C_2H_4$ and C-H insertion forming HMC_2H_3 indicates that there exists an adiabatic potential energy barrier for $M + C_2H_4$ association in the case of Zr and that the transition state for this process is tighter than for the analogous process in $Nb + C_2H_4$. The barrier for $Zr + C_2H_4$ association is attributed to the repulsive s^2 ground state configuration of Zr, whereas for Nb the s^1 ground state configuration results in no barrier for association. The absence of decay of ZrC_2H_4 back to $Zr + C_2H_4$ at low collision energies indicates that the barrier for C-H insertion forming $HZrC_2H_3$ lies below the barrier for $Zr + C_2H_4$ association. This opens up the possibility that direct C-H insertion without initial ZrC_2H_4 formation may play an important role.

¹ P.A. Willis, H.U. Stauffer, R.Z. Hinrichs, and H.F. Davis, J. Phys. Chem. A. **103**, 3706 (1999).

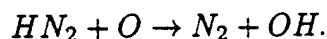
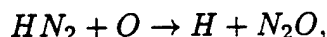
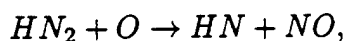
Ronald J. Duchovic, J. David Pettigrew^a, Marla Slattery^b, and James Sefton^b **C19**
Indiana University-Purdue University Fort Wayne
2101 Coliseum Blvd. East
Fort Wayne, IN 46805-1499

Previous investigations have noted that reagent vibrational excitation can influence the rate of reactions in specific ways. These effects were first noted in energy transfer processes, and later, in reactive cases as well. An initial analysis of this question has been begun by utilizing the analytic DMBE IV PES of Pastrana *et al.* (*J. Phys. Chem.*, **94**, 8073(1990)) in the VENUS trajectory code. To date, 100 000 trajectories (25 000 at each temperature, T = 1000.0 K, 2000.0 K, 3000.0 K, and 4000.0 K) for O₂ vibrational quantum numbers $v = 6, 7, 8, 9, 10$ have been completed. Comparisons between the thermal rate coefficients calculated from these trajectories and the thermal rate coefficients based on elementary statistical assumptions will be made. Because the reaction:



possesses a relatively deep energetic well corresponding to the H(D)O₂ intermediate, a distinction between short-lived and long-lived trajectories is necessary. The presence of the potential energy well may significantly attenuate the effects of reagent vibrational excitation.

Secondly, a significant number of *ab initio* studies have explored atmospheric nitrogen chemistry. However, as Bozzelli and Dean (*Int. J. Chem. Kinet.* **27**, 1097(1995)) point out, none have addressed the bimolecular reactions of the short-lived HN₂ species, in particular, O-atom reactions with HN₂. Yet, the HN₂ species has been included in the detailed kinetic models constructed to explain the Thermal De-NO_x process (J. A. Miller and C. T. Bowman, *Prog. Energy Combust. Sci.* **15**, 287(1989)). We report very preliminary investigations at the CCSD and CBS-APNO levels of theory for the reactions:



identified by Bozzelli and Dean as the most significant HN₂ bimolecular reactions. These efforts have been directed towards the construction of an accurate PES for this reaction.

Finally, several *ab initio* studies have focused on the minimum energy path region of the hydroperoxyl potential energy surface (PES) (*J. Chem. Phys.*, **88**, 6273(1988)) and the saddle point region for H-atom exchange via a T-shaped HO₂ complex (*J. Chem. Phys.*, **91**, 2373(1989)). Further, the results of additional calculations (*J. Chem. Phys.*, **94**, 7068(1991)) have been reported which, when combined with the earlier studies, provide a global description of the PES for this reaction. We report recent progress in our effort to develop a new analytic representation of the Walch *et al.* *ab initio* PES in terms of molecular parameters (bond lengths and bond angles), using a switching function formalism.

^aGraduate research assistant; ^bUndergraduate research assistant

This work has been supported by the Petroleum Research Fund of the American Chemical Society, Grant #31684-B6.

Ion Imaging O(¹D) and O(³P) Atoms From the UV Photodissociation of Ozone.

Scott M. Dylewski, Joseph D. Geiser, Paul L. Houston

Department of Chemistry
and
Field of Applied and Engineering Physics
Cornell University
Ithaca, New York, USA 14853-1301
dylewski@cornell.edu

Using the technique of ion imaging, we have studied the UV photodissociation of ozone using light from 226 nm to 320 nm. In this region, two photodissociation channels exist:

- (1) $O_3 \rightarrow O(^1D) + O_2(^1\Delta_g)$
- (2) $O_3 \rightarrow O(^3P) + O_2(^3\Sigma_g^-)$

The imaging technique readily provides both the energy and angular distributions of the fragment under study. We have previously provided results for the angular distributions of O(³P) fragments from reaction (2), and have now measured the kinetic energy distributions for several wavelengths. In addition, we have determined angular and energy distributions for reaction (1) at a select number of wavelengths.

At wavelengths above 310 nm, there is insufficient energy to produce the reaction (1), and yet O(¹D) is still observed. Imaging data indicate that the dissociation is taking place from vibrationally excited ozone molecules. Dissociation of vibrationally excited O₃ is clearly seen as low as 305 nm. At even longer wavelengths, the spin forbidden [O₃ → O(¹D) + O₂(³Σ_g⁻)] channel is observed. Exploring this region of the spectrum can give us a better understanding of the full quantum yield of O(¹D) atoms, and thus can affect models of the stratospheric chemistry.

For photon energies just above the threshold for reaction (1), the photofragments have very little translational energy. In this case, we are able to resolve individual rotational levels of the O₂(¹Δ_g, v=0) fragment. Working in collaboration with Prof. Matsumi's group, the assignment of the rotational lines has enabled us to determine a more accurate measurement of the bond dissociation energy of ozone.

Photodissociation spectroscopy of size-selected alkaline-earth ions solvated by ammonia: $\text{Sr}^+(\text{NH}_3)_n$, $\text{Sr}^+(\text{ND}_3)_n$, D_m , and $\text{Mg}^+(\text{NH}_3)_n$

James I. Lee, David C. Sperry, Anthony J. Midey, and James M. Farrar

Department of Chemistry
University of Rochester
Rochester, NY 14627

Abstract

We present a study of electronic to vibrational (E-V) energy transfer in solvated alkaline-earth cation clusters, in which metal-centered electronic transitions excite these systems above their dissociation thresholds. As cluster size increases, the absorption maxima shift from the visible through the infrared region of the spectrum. A spectral moment analysis of the absorption cross sections for $\text{Sr}^+(\text{NH}_3)_n$ shows that $\langle 0|r^2|0 \rangle$ for the radial distribution function of the valence electron in the ground state increases threefold as n increases from 1 to 9 solvent molecules, indicating increasing Rydberg character of the ground and excited states and signaling the onset of spontaneous ionization and electron solvation. For clusters of solvated Sr^+ in the size range above 10, we observe the formation of species containing up to four excess hydrogen atoms. By employing a combination of reactive scavenging methods and mass-selected spectroscopy, we identify two different kind of species. We deduce that the first excess hydrogen atom is bound to the metal core, yielding a metal hydride species. We also suggest that the second and third excess hydrogen atoms are surface-bound, in the form of solvated Rydberg radicals of the form $\text{NH}_4(\text{NH}_3)_n$. In clusters based on Mg^+ , we observe that the first solvent shell closes at $n = 3$, and an abrupt change in the absorption spectrum at $n = 4$ signals the onset of a second solvent shell. The spectra of larger clusters are consistent with a recent conjecture that solvent-based vibrational transitions borrow intensity from strongly-allowed atomic transitions.

**Experimental Probes of Calculated Potential Energy Surfaces:
H + N₂O(n,l,m) and H + O₂(v).**

Michael D. Wojcik, John Ingram, Brian Keller and T. Rick Fletcher

**Department of Chemistry
University of Idaho
Moscow, ID 83844-2343**

Recent work in our lab is focused on the title reactions at energies near the threshold of product formation. Translationally excited H atoms are produced by photolysis of CH₃SH or HI at a variety of wavelengths, while stimulated Raman excitation is used to prepare vibrationally selected N₂O (n,l,m) and O₂. The reaction products are monitored by sub-Doppler laser induced fluorescence.

The reaction cross section for H + N₂O should be dependent on reagent translational and internal energy. Since N₂O has reactive sites on both the O end (direct reaction pathway) and the N end of the molecule (indirect pathway), energy also plays a role in choosing the reaction mechanism. Experiments are described which attempt to measure and control the reaction cross section and the ratio of direct to indirect reaction pathways for H + N₂O → a) OH + N₂, or b) NH + NO as a function of translational and vibrational energy. Preliminary results indicate that the barrier height for the indirect pathway is larger than the currently accepted value.

For H + O₂(v=0), the reaction cross section, OH rotational state distribution, spin-orbit and lambda doublet ratios at a center of mass collision energy approximately 3 kcal/mol above the barrier were measured. The reaction cross section is larger than expected, and the rotational state distribution is accurately reproduced by a simple statistical model while the spin-orbit and lambda doublet ratios are strongly biased. These results are explained by a simple model of a long-lived OOH intermediate, with the angular momentum of the OOH and subsequent lambda doublet populations specified by the H + O₂ collision geometry. The large cross section might be due to resonance states accessed by the 3 kcal/mol collision energy.

A Kinetics and Product Study of the Reaction of CH_3 Radicals with $\text{O}(^3\text{P})$ Atoms using Time-Resolved Time-of-Flight Spectrometry

Christopher Fockenberg(fknberg@bnl.gov)*, Gregory E. Hall(g_hall@bnl.gov),
Jack M. Preses(preses@bnl.gov), Trevor J. Sears(sears@bnl.gov),
and James T. Muckerman(muckerma@bnl.gov)

Chemistry Department 555A, Brookhaven National Laboratory
P.O. Box 5000, Upton, NY 11973-5000

Our research is focused on determination of rates and product distributions of radical-radical reactions important to combustion systems. This type of reaction imposes challenging requirements on the experimental methods and data analysis because the recombination of two radicals frequently produces highly excited adducts that access more than one product channel. In order to fully characterize the observed reaction system, one ideally has to study the temporal evolution of all species simultaneously.

An apparatus has been constructed to observe the concentrations of multiple transient or stable species simultaneously allowing studies of radical-radical reactions in the gas phase. It consists of a tubular quartz reactor in which radicals are produced by flash photolysis and an excimer laser as a photolysis light source. The composition of the gas mixture is analyzed *in situ* by photoionizing sampled gases using the VUV emission of a hollow cathode lamp and subsequent time-of-flight mass spectrometry. A simple arrangement of grids at the entrance to the flight tube is used to interrupt the constant flux of ions by application of a combination of constant and pulsed voltages. Individual mass spectra can be taken at a repetition rate of around 20 kHz following each photolysis event. To achieve a suitable signal-to-noise ratio, signals were typically accumulated over several tens of thousands of laser shots at a pulse rate of 10 – 15 Hz.

The kinetics and product distribution for the reaction of methyl radicals, CH_3 , with ground-state, $\text{O}(^3\text{P})$ oxygen atoms, have been investigated. The radicals are produced by an excimer laser pulse ($\lambda = 193 \text{ nm}$), in the cophotolysis of acetone, CH_3COCH_3 , or bromomethane, CH_3Br , and sulfur dioxide, SO_2 , creating a homogeneous distribution of radicals along the axis of the flow reactor. In addition to the dominant product, formaldehyde (CH_2O), carbon monoxide (CO) was detected as a product with a yield of 0.17 ± 0.11 . Analysis of the rates of disappearance of methyl radicals and appearance of formaldehyde for different $\text{O}(^3\text{P})$ concentrations resulted in an overall rate coefficient for this reaction $k = (1.7 \pm 0.3) \times 10^{-10} \text{ cm}^3 \text{ molecule}^{-1} \text{ s}^{-1}$ at $T = (299 \pm 2) \text{ K}$ and $P = 1 \text{ Torr (He)}$.

Acknowledgment: This work was carried out at Brookhaven National Laboratory under Contract DE-AC02-98CH10886 with the U.S. Department of Energy and supported by its Division of Chemical Sciences, Office of Basic Energy Sciences.

Efficient Calculation of Cumulative Reaction Probabilities Using Transition State Real Wave Packet Propagation

Kelsey M. Forsythe and Stephen K. Gray

Chemistry Division, Argonne National Laboratory

Argonne, Illinois 60439

Miller and coworkers (J. Chem. Phys. 79, 4889 (1983)) introduced a rigorous formula for the cumulative reaction probability (CRP) in terms of the symmetrized flux operator. Zhang and Light (J. Chem. Phys. 104, 4544 (1996)) developed the transition wave packet approach utilizing eigenstates of the flux operator to calculate the CRP. More recently, Gray and Balint-Kurti (J. Chem. Phys. 108, 950 (1998)), by identifying relations between complex and real wavefunction components, were able to access reactive scattering quantities via solely real wavepacket propagation. We have successfully combined the transition-state wave packet method and real wavepacket propagation scheme. The former reduces the number of wavepackets to propagate and/or the required grid sizes while the latter reduces the amount of memory storage and number of operations. Additionally, we have incorporated statistical wavefunctions into the analysis reducing further the total number of propagations required to extract CRPs. Together these techniques comprise a most efficient scheme for calculating scattering probabilities. Calculations of the cumulative reaction probability and thermal rate constants for the 3-D ($J=0$) $D + H_2 \rightarrow HD + H$ and ($J=0$) $Cl + H_2 \rightarrow HCl + H$ are presented.

Theoretical Study of the Intramolecular Isotope Effect in the Reactions of $\text{Ar}^+ + \text{HD}$ using the Trajectory Surface Hopping Method

Muriel Sizun

Laboratoire des Collisions Atomiques et Moléculaires, URA du CNRS No. 281, Bat. 351,
Université Paris XI, 91405 Orsay Cedex, France

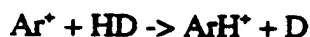
Ju-Beom Song

Department of Chemical Education, Kyungpook National University, 1370 Sankyuk-Dong,
Pook-Ku, Taegu, 702-701, South Korea

Eric A. Gislason

Department of Chemistry, University of Illinois at Chicago, 845 W. Taylor St.,
Chicago, Illinois 60607-7061

We have extended our earlier study (1) of the reactions



to gain a better understanding of the intramolecular isotope effect as a function of collision energy. We follow our earlier procedure (2) of studying each trajectory in detail to understand the reaction mechanism. The trajectories were carried out on three adiabatic potential energy surfaces derived from the DIM surfaces of Kuntz and Roach (3).

To analyze the isotope effect we have found it useful to break the reactive cross section into three factors. For the cross section for making ArH^+ this decomposition can be written:

$$Q_R(\text{ArH}^+) = Q_{\text{hit}}(\text{ArHD}) P_R(\text{ArHD}) C_{\text{m}}(\text{ArHD}).$$

Here $Q_{\text{hit}}(\text{ArHD})$ is the cross section for hitting the H end of HD, P_R is the fraction of collisions that hit the H end and give reaction (either ArH^+ or ArD^+), and $C_{\text{m}}(\text{ArHD})$ is the correction for knockout collisions, where Ar hits H first but reacts with D or vice versa. All three factors play an important role in determining the isotope effect. This analysis is carried out for these two reactions over the energy range 0.1 to 15 eV. The isotope effect is explained well by this decomposition, and we show what features of the potential energy surfaces determine this behavior.

1. M. Sizun, J. B. Song, and E. A. Gislason, *J. Chem. Phys.* **109**, 4815 (1998).
2. See, for example, J. B. Song and E. A. Gislason, *Chem. Phys.* **237**, 159 (1998).
3. P. J. Kuntz and A. C. Roach, *J. Chem. Soc. Faraday Trans. II* **68**, 259 (1972).

Theoretical analysis of pathways for fragmentation of the Na_3^+ cluster-ion in a non-adiabatic collision with He

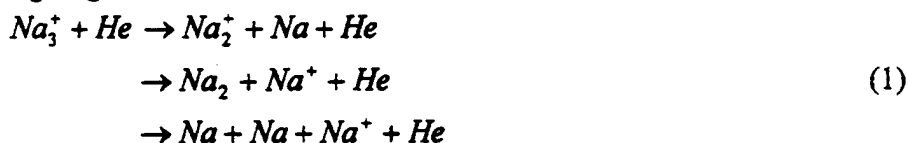
D. Babikov and E. Gislason,

Department of Chemistry, University of Illinois at Chicago,
845 West Taylor Street, Chicago, Illinois 60607-7061, USA

M. Sizun, F. Aguillon and V. Sidis,

Laboratoire des Collisions Atomiques et Moléculaires, UMR 8625,
Université de Paris Sud, Orsay, 91405, France

Fragmentation of the Na_3^+ cluster-ion in collision with He in the 100 eV (centre of mass) energy range is investigated theoretically. This follows our earlier work on the simpler He – Na_2^+ system [1]. Here we are concerned with the following fragmentation channels:



In general, the results show evidence for two different fragmentation pathways [1,2]. The first one involves an *impulsive mechanism* whereby momentum is transferred from the He atom to the atoms in the cluster. The second one involves an *electronic excitation mechanism*, which excites the cluster into a dissociative state and thereby leads to cluster break-up.

Our description of process (1) is split into two consecutive stages: the He – Na_3^+ encounter itself and the post-collisional evolution of the Na_3^+ cluster-ion. The first stage is treated semi-classically with the energy conserving trajectory (SCECT) method and involves the *frozen cluster* approximation (the Na nuclei are considered clamped while the fast He atom passes by). The results of this stage are possible electronic excitation of the cluster and/or transfer of momenta to its atoms. The second stage, which has to account for non-adiabatic transitions as a result of the movement of the Na nuclei, is handled using the trajectory surface hopping (TSH) scheme [3]. Finally, multi-differential cross sections for different fragmentation channels are calculated.

The two stages make use of *diabatic* and *adiabatic* representations, respectively. For the He – Na_3^+ potential energy surfaces and couplings an adaptation of the diatomics-in-molecules (DIM) approach incorporating *three-centre integrals* is employed.

Different fragmentation mechanisms are discussed; good agreement with experiment of ref. [2] is obtained.

Collisional effects on angular momentum orientation in acetylene for both rotationally elastic and inelastic processes

Armin D. Rudert, Jose Martin, Helmut Zacharias,
Physikalisches Institut, Universitaet Muenster, 48149 Muenster, Germany.

Wen-Bin Gao Hangzhou
Institute of Electronics Engineering, Hangzhou 310012, P.R. China,

Joshua B. Halpern,
Chemistry, Howard University, Washington DC 20059 USA},

Investigation of steric effects is a topic of growing interest. The ultimate reductionist question is how molecular orientation changes in elastic or inelastic collisions. Moreover, to study geometric constraints in reaction dynamics one must control or predict the motion and the orientation of the molecular axis prior to reaction. Stimulated Raman pumping can prepare an oriented ensemble of vibrationally excited molecules. For acetylene the theoretically calculated and the measured initial orientation, $A_0^{(1)}$, ranges between 0.7 and 0.9. A substantial part of the orientation is conserved in rotationally inelastic collisions. These results can be compared with previous measurements of collisional alignment conservation. Rotationally inelastic collisions appear to occur primarily in plane. The amount of orientation that remains after a rotationally inelastic collision is found to depend only on $|\Delta J|$. A simple model is used to calculate detailed $\langle j', m_j' | j, m_j \rangle$ transition probability matrices which match the data from both orientation and alignment transfer measurements.

Using this information one can separate orientation decay in the originally populated state due to elastic and multiple inelastic scattering. The measurements clearly show that orientation decay due to the combination of both rotationally elastic and inelastic collisions is much slower than depopulation of the prepared rotational state. Further, under the conditions of these experiments multiple scattering out of and back into the initially prepared states do not significantly affect the measurements. A second model is presented which reconciles the alignment and orientation measurements for collisional decay of both the alignment and orientation. It is shown that elastic collisions responsible for this decay are the result of rotationally elastic collisions occurring perpendicular to the plane of molecular rotation, which completely destroy any orientation or alignment, in contrast to the rotationally inelastic collisions which occur primarily in plane.

Collisional Relaxation of a Single Highly Vibrationally Excited
Level near the Dissociation Limit of $\text{SO}_2(\bar{X})$
by Quantum Beat Spectroscopy

Jun Han, Bing Xue and Hai-Lung Dai

Department of Chemistry, University of Pennsylvania, Philadelphia,
PA 19104-6323

Collisional relaxation of a single highly vibrationally excited level of $\text{SO}_2(\bar{X}^1A_1)$ by He and Ar has been studied using laser induced fluorescence quantum beat spectroscopy. Quantum interference between the optically bright rovibronic level $7_{1,6}(210)$ in the $\bar{C}(^1B_2)$ state and a highly vibrationally excited but optically dark level in the \bar{X} state, which is 44877.52 cm^{-1} above the zero point level, was used as a unique window to access the highly vibrationally excited dark level. The collisional relaxation rate coefficient for this dark level has been determined both in the temperature range of 3-12 K in supersonic expansions and at the ambient temperature. In particular, the relaxation rate coefficient by Ar at 4.9 K was determined to be $(8.3 \pm 0.8) \times 10^{-11} \text{ cm}^3 \text{ molecule}^{-1} \text{ s}^{-1}$, which is about three times larger than the value for the unperturbed isoenergetic \bar{C} state levels. The effective collisional cross-section decreases with temperature in the measured low temperature range. Ambient temperature experiments determined the effective quenching cross section (in \AA^2) of SO_2^* by collision partners He, Ar, CO_2 and SO_2 to be 87, 216, 432 and 969, respectively. The proposed collision mechanism derives contributions to the relaxation cross section from long range interactions involving electric multipole and transition dipole moments.

Quantum state-resolved reactive scattering of
 $F + CH_4 \rightarrow HF(v,J) + CH_3$:
Nascent product distributions and IR laser Dopplerimetry
in crossed supersonic jets

Warren W. Harper, Sergey A. Nizkorodov, and David J. Nesbitt

JILA, University of Colorado and National Institute of Standards and Technology and Department of Chemistry and Biochemistry, University of Colorado, Boulder, Colorado 80309-0410

State-to-state reactive scattering of $F + CH_4 \rightarrow HF(v,J) + CH_3$ has been studied using crossed supersonic jets and high-resolution ($\Delta\nu \approx 0.0001 \text{ cm}^{-1}$) IR laser direct absorption techniques. Rovibrational state-resolved HF column integrated absorption profiles are obtained under single collision conditions and converted to populations via appropriate density-to-flux transformation. Nascent rovibrational distributions in each $HF(v,J)$ state are reported. Summed over all product rotational levels, the nascent vibrational quantum state populations for $HF(v)$ ($v=3$: 0.11(1), $v=2$: 0.67(2), $v=1$: 0.19(4), $v=0$: 0.04(11)) are in excellent agreement with previous flow cell studies by Setser and coworkers. At the rotational state level, however, the current studies indicate nascent distributions for $HF(v,J)$ which are significantly hotter than previously reported, ostensibly due to greatly reduced collisional relaxation effects under crossed jet conditions. Indeed, final rotational states from $F + CH_4$ are observed up to the energetic limit (e.g. $HF(v=3, J=6)$, $HF(v=2, J=12)$), which provides experimental validation for a bent F-H-C structure at the transition state. At an even finer level of state-to-state detail, the high resolution IR profiles of HF exhibit extensive Doppler broadening that directly reflects $HF(v,J)$ translational distributions in the laboratory frame. These profiles are analyzed to yield information on state-resolved differential cross sections into $HF(v=1,2)$, which identify a propensity for forward/backward scattering ($|\cos(\theta)| \approx 1$) vs. side scattering ($|\cos(\theta)| \approx 0$) in the center of mass frame.

Understanding ortho-para conversion by using electric fields

D.A. Roozmond, B. Nagels and L.J.F. Hermans

Huygens Laboratory, Leiden University, P.O. Box 9504,
2300 RA Leiden, The Netherlands

E-mail: Hermans@molphys.leidenuniv.nl
FAX + 31 71 5275819

It has become clear over the last few years that the leading mechanism for nuclear-spin conversion in many polyatomic molecules is based on mixing of states [1]. This mixing is caused by intramolecular interactions (e.g., spin-spin or spin-rotation interaction) while the role of intermolecular collisions is merely to destroy the coherence. Of crucial importance is the energy level spacing between mixed states. By using the linear Stark effect in an external electric field, one can manipulate the M-sublevels to produce "level crossing resonances" in the conversion rate. Indeed, experiments in a static electric field have produced evidence for such resonances [2].

However, detailed information can only be derived if the conversion rate γ is measured directly as a function of field strength E . Such experiments yield the "signature" of the $\gamma(E)$ plot (analogous to absorption vs. frequency plots in spectroscopy) and make it possible to disentangle the type of intramolecular interaction involved. We have obtained such data for low pressure $^{13}\text{CH}_3\text{F}$ in a quasi-static measurement with fields up to 2500 V/cm. The signature of the $\gamma(E)$ results corresponds remarkably well with the theoretical model based on spin-spin interactions.

- [1] P.L. Chapovsky and L.J.F. Hermans, *Annu. Rev. Phys. Chem.*, 1999 (in press).
- [2] B. Nagels, N. Calas, D.A. Roozmond, L.J.F. Hermans and P.L. Chapovsky, *Phys. Rev. Lett.* **77**, 4732 (1996).

Reaction Dynamics of Ground State and Electronically Excited Neutral Transition Metal Atoms with Alkanes

Ryan Hinrichs, Hans Stauffer, Peter Willis, and Floyd Davis
Department of Chemistry and Chemical Biology
Cornell University
Ithaca NY 14853

The reactions of transition metal atoms (M) with saturated hydrocarbons such as methane, ethane, and cyclopropane are believed to be initiated by direct C-H bond insertion, without initial complex formation. Although there is considerable interest in better understanding the electronic and dynamic factors controlling the heights of potential energy barriers for such reactions, very few direct experimental studies on such systems have been carried out. Room-temperature flow cell studies indicate that first and second row ground state transition metal atoms are generally unreactive with alkanes at low collision energies due to the presence of substantial potential energy barriers for C-H or C-C insertion.¹

Using the technique of crossed molecular beams, we are studying the reaction dynamics of ground state and electronically excited transition metal atoms with alkanes. Using the seeding technique, we can study reactions having substantial potential energy barriers and, by studying the reactivity as a function of collision energy, determine barrier heights for direct comparison with theoretical predictions. Using "universal" mass detection of the chemical products and the nonreactively scattered metal atoms, we are able to gain insight into all competing channels.

To date, we have studied the nonreactive and reactive collisions between second-row transition metal atoms (Y, Zr, Nb, Mo) and several simple alkanes. In the case of Y, Zr, and Nb, insertion into the C-H bond of C_2H_6 is followed by H_2 elimination, forming MC_2H_4 . In the $Y + C_2H_6$ reaction, a second reaction channel forming $HYH + C_2H_4$ is also observed. Mo (7S) atoms, on the other hand, are found to be unreactive even up to collision energies of ~ 30 kcal/mole, implying the existence of a large potential energy barrier for the ground state reaction.² However, the metastable electronically excited Mo (5S) state, prepared by optical pumping upstream of the collision zone, is found to react on essentially every collision with methane and ethane at collision energies as low as 4 kcal/mole.

¹ J.J. Carroll, K.L. Haug, J.C. Weisshaar, M.R.A. Blomberg, P.E.M. Siegbahn, and M. Svensson, *J. Phys. Chem.* **99**, 13955 (1995).

² P.A. Willis, H.U. Stauffer, R.Z. Hinrichs, and H. F. Davis, *J. Chem. Phys.* **108**, 2665 (1998).

THE STATE-RESOLVED DYNAMICS STUDY OF S_1 ACETALDEHYDE NEAR THE DISSOCIATION THRESHOLD FOR FORMATION RADICAL PRODUCTS

C32

Cheng-Liang Huang and I-Chia Chen, Department of Chemistry, National Tsing Hua University, 101, sec. 2, Kuang Fu Road, Hsinchu, Taiwan 300, Republic of China; Chi-Kung Ni and A. H. Kung, Institute of Atomic and Molecular Sciences, Academia Sinica, P. O. Box 23-166, Taipei, Taiwan 106, Republic of China.

The state-resolved dynamics of S_1 acetaldehyde to product channels are studied via the fluorescence decay and quantum beat features. High-resolution spectra of the acetaldehyde were measured in supersonic jet in the frequency region of $31\,258 - 31\,608\text{ cm}^{-1}$. More than 15 vibronic bands in this region were observed. Fluorescence decays of levels in several bands were obtained. About 75% of measured curves display quantum beats phenomenon; hence, strong couplings between S_1 and T_1 states were expected. The decay curves from various states in band at $31\,519\text{--}31\,534\text{ cm}^{-1}$ display distinct behavior. This allows us to confirm the assignments of transitions for this band. Combined with the method of combination difference of ground electronic state, we assigned more than 70% of observed transitions in this region. Currently, complete analysis is undergoing. At $31\,569\text{--}31\,589\text{ cm}^{-1}$, various lifetimes of rotational levels of S_1 acetaldehyde were obtained, some with $\tau < 40\text{ ns}$ and some greater than 120 ns. The states with short lifetime are expected to couple with T_1 states, which is resulted from coupling to dissociation continuum. This region is about 70 cm^{-1} below the dissociation threshold measured previously. Variation of lifetime with rotational quantum number and vibrational energy will be reported.

Morphing *ab initio* potentials for intermolecular forces: a systematic study of Ne-HF

Jeremy M. Hutson and Markus Meuwly

Department of Chemistry, University of Durham, Durham, DH1 3LE, England

Abstract

A procedure for "morphing" an *ab initio* intermolecular potential energy surface to obtain agreement with experimental data is presented. The method involves angle-dependent scaling functions for both the energy and the intermolecular distance. The method is tested on the system Ne-HF, for which high-resolution infrared spectra are available. It is shown to work well even with relatively low-level *ab initio* calculations.

Several basis sets are investigated at the CCSD(T) correlation level, including various aug-cc-pVnZ basis sets and the specially-tailored Ne-HF basis set of O'Neil *et al.* All give good results after morphing, but the changes needed to match experiment are much smaller for the O'Neil basis set.

The angle-dependence of the morphing transform offers a way of evaluating the quality of the original *ab initio* potential. The O'Neil basis set can be seen to give considerably better results than the similarly sized aug-cc-pVTZ basis set. The use of MP2 calculations is also investigated: again, the MP2 potential is quite satisfactory after morphing, but requires much more modification than the CCSD(T) potential with the same basis set.

The morphing approach should be readily extendable to more complex systems.

Eley-Rideal and hot-atom reactions of H(D) atoms with D(H)-covered
Cu(111) surfaces; quantum and quasi-classical studies

Bret Jackson, Dmitrii V. Shalashilin, and Chakrapani Kalyanaraman

Department of Chemistry, University of Massachusetts, Amherst, MA 01003, USA

Mats Persson

*Department of Applied Physics, Chalmers/Göteborg University, S-412 96, Göteborg,
Sweden*

Didier Lemoine

*Laboratoire de Physique des Lasers, Atomes et Molécules, UMR CNRS, Centre d'Etudes
et de Recherches Laser et Applications, Université de Lille 1, Bâtiment P5, 59655
Villeneuve d'Ascq Cedex, France*

Abstract:

Quasi-classical molecular dynamics studies are made of H or D atoms incident from the gas phase onto D or H-covered Cu(111) surfaces. Two detailed model potential energy surfaces are used, both based on the results of extensive total energy calculations using the density functional method. The incident H (D) atoms can react directly to form HD via the Eley-Rideal mechanism, or trap onto the surface. These trapped hot atoms can react with the adsorbates to form HD, or can eventually dissipate enough energy through collisions with the adsorbates to become immobile. We also observe the formation of D₂ (H₂). Probabilities for these various processes, as well as the rotational, vibrational and translational energy distributions of the products are computed and compared with experiment. Hot atom pathways to product formation are shown to make significant contributions. One of the potentials gives excellent agreement with experiment, while the other is less successful. Fully quantum calculations are also implemented for a flat surface model which ignores corrugation effects. Reaction cross sections and product rovibrational distributions are computed using transform techniques developed for curvilinear coordinate systems.

Dissociative Adsorption at Finite Temperature: Multiconfiguration Vector
Description of the Reduced Density Matrix

Bret Jackson

*Department of Chemistry
Univeristy of Massachusetts
Amherst, MA 01003*

Abstract:

The dissociative adsorption of a diatomic molecule on a moving metal surface is described using the density matrix. By writing the full system+bath wave function in a multiconfiguration form and performing the thermal averages analytically, the reduced density matrix can be computed exactly by evolving several coupled wave vectors. The usual weak-coupling and Markov-bath assumptions are avoided. Exact and approximate calculations are implemented for the case of D_2 dissociation on a model Cu surface, at high energies and over a wide range of surface temperatures, with promising results.

V-RT Energy Transfer in Collisions between Highly Vibrationally Excited Pyrazine and CO

Quan Ju, Natalie Seiser and George W. Flynn

Department of Chemistry, Columbia University, New York, NY 10027

Collisional energy transfer between highly vibrationally excited pyrazine and CO has been explored via high resolution (0.0003 cm^{-1}) diode laser transient absorption spectroscopy. Pyrazine with a chemically significant amount of vibrational energy is prepared by 248nm excimer laser pumping to its second electronic state, followed by rapid intersystem conversion to its ground state. To understand V-RT energy transfer due to pyrazine/CO collisions, the rotational and translational degrees of freedom of CO are probed. Nascent rotational populations of CO in $J = 7 - 36$ are probed after collisions with excited pyrazine. For each of these collisionally populated rotational states, recoil velocities are also measured through Doppler spectroscopy. In addition, the field-to-state energy transfer rate constants and probabilities for pyrazine/CO collisions are determined.

Uniform Semiclassical IVR Treatment of the S -Matrix

Yosef Elran and Kenneth G. Kay*

Department of Chemistry, Bar-Ilan University, Ramat-Gan 52900, Israel

Abstract

The semiclassical Initial Value Representation (IVR) treatment of the S -matrix, developed almost three decades ago by W. H. Miller and R. A. Marcus, (MM) deserves renewed consideration. This method is potentially capable of yielding scattering amplitudes using orders of magnitudes fewer trajectories than required by more recent techniques based on semiclassical IVR expressions for the time-dependent propagator. Unfortunately, application of the MM IVR is hampered by a number of problems, including the uncertain definition of the phases appearing in the IVR integrand, the inaccuracy of the results in many cases, and the inapplicability of this technique for the treatment of reactive tunneling. In the present work, we address these problems by rederiving the MM IVR formulas from IVR expressions for the time-dependent propagator and related integral expressions for time-independent wave functions. In addition to resolving ambiguities in the original MM expressions, our work yields new formulas that require the same (relatively small) number of trajectories for convergence as the MM treatment but that are semiclassically uniform and, thus, potentially more accurate. Our approach also suggests how the MM expressions can be modified to treat reactive tunneling processes. We present preliminary numerical results that indicate some of our treatment's advantages.

LEANNE M. MILLER, THOMAS J. DOWD, and JAMES S. KELLER, Department of Chemistry and Biochemistry, University of Notre Dame, Notre Dame, IN, 45665

Ground state population depletion gratings were used to elucidate the effects of initial nuclear motion on the photodissociation dynamics of chlorine dioxide and carbon disulfide. In these experiments, the predissociative region of an ultraviolet absorption is explored by recording a hot-band spectrum of a molecule to the exclusion of all other transitions normally encountered in the range of probe frequencies employed. Our two-color variant of laser-induced grating spectroscopy permits the "tagging" of specific ground rovibrational states via well-resolved transitions that either lie below the predissociation threshold or belong to a different electronic state altogether. When a probe beam is subsequently tuned through the dissociation region, the diffraction of this beam records an absorption spectrum characterized only by vibrationally excited molecules.

The ultraviolet absorption of OClO occurs via the $A \ ^2A_2 \leftarrow X \ ^2B_1$ transition, but dissociation of OClO* proceeds on several different excited state surfaces leading to two distinct product channels. Depletion gratings were established using transitions at the red-end of the spectrum, and the effect of both bending and asymmetric stretching motion on predissociation lifetimes was determined. In carbon disulfide, the predissociative $S_3 \leftarrow S_0$ absorption was explored by tuning grating-forming beams to the frequency of a transition in the 320-nm $V \leftarrow X$ system. These latter experiments were performed in an attempt to explain the strong K -dependence of the branching to different atomic sulfur photofragment channels for this molecule. Depletion gratings which "tag" ground state levels with different quanta in the bend (ν_2) have been recorded for probe frequencies that span the predissociation threshold region of the 1B_2 state.

Speed-dependent photofragment helicity in the photodissociation of OCS at 223 nm

Zee Hwan Kim, Andrew J. Alexander, and Richard N. Zare

Department of Chemistry, Stanford University, Stanford, CA94305

Carbonyl sulfide (OCS) is photolyzed with linearly polarized 223 nm UV light and the sulfur atom ($S(^1D_2, ^3P_1, J = 1, 2)$) photofragment is detected by 2 + 1 REMPI (resonance-enhanced multiphoton ionization) with circularly polarized light. The measured orientation (helicity) of the photofragment is found to depend on the speed of the photofragment. This speed-dependent orientation of the photofragment is explained in terms of the quantum mechanical interference associated with the simultaneous excitation of the parallel and the perpendicular states that lead to the same atomic photofragment state. Especially, in the $S(^1D_2)$ product channel, only the fast component of the bimodal speed distribution shows appreciable orientation, supporting previously suggested[#] mechanism for the speed-dependent translational anisotropy of $S(^1D_2)$ photofragment in the photodissociation of OCS.

[#] Sivakumar *et al*, J. Chem. Phys. 88, 3692 (1988); Sato *et al*, J. Phys. Chem 99, 16307 (1995); Suzuki *et al*, J. Chem. Phys. 109, 5778 (1998)

Time-Resolved Studies of Energy Flow in a $\text{CH}_2\text{I}_2/\text{CCl}_4$ Solution

Dieter Bingemann, Andrew M. King, F. Fleming Crim

University of Wisconsin, Department of Chemistry, Madison, Wisconsin 53706

We study the flow of energy between vibrational modes of the CH_2I_2 molecule in a dilute solution of CCl_4 . One 100 fs pulse excites the first overtone of the CH-stretching vibration at 1.70 μm . Energy begins to flow throughout the molecule as the system begins to return to equilibrium. A second, time delayed pulse in the near UV photodissociates the CH_2I_2 molecule into its primary photoproducts, CH_2I and I. We observe an enhancement of the UV absorption as the energy flows out of the CH-stretch and into other modes that map more directly onto the dissociation coordinate, such as the CI-stretches and CI_2 -bend. The intramolecular energy redistribution occurs with a characteristic rise of about 10-20 ps, depending on photolysis wavelength. Additionally, the vibrationally excited CH_2I_2 molecule sheds its extra internal energy to the solvent as it equilibrates. We infer that the vibrational energy is redistributed among solvent motions again within 50 ps after initial vibrational excitation.

MEASUREMENTS OF TRANSITION DIPOLE DIRECTIONS USING BRUTE FORCE ORIENTATION

K. J. Castle, H. Li, and W. Kong*

Department of Chemistry, Oregon State University, Corvallis, Oregon 97331-4003 USA

Email: kongw@chem.orst.edu

Using a strong electric field and supersonic cooling, polar molecules can be oriented under the electrostatic interaction between the permanent dipole and the electric field. Dependence of absorption on the polarization direction of an excitation laser -- linear dichroism of oriented gas phase molecules -- provides information on the direction of the transition dipole moment. This paper presents results on this type of measurement. A few testing examples including in-plane transitions of diazines and other nitrogen containing compounds will be presented. Rotationally resolved out-of-plane transitions in diazines (pyridazine and pyrimidine) allowed determination of rotational temperatures of the molecular beam. The distribution function of molecular axes in an electric field was thus obtained using the linear variation method. Dependence of absorption on polarization directions of the excitation laser corroborated the perpendicular relationship between the transition dipole and the permanent dipole. In a similar manner, measurements of linear dichroism of in-plane $\pi^* - \pi$ transitions were carried out, and directions of transition dipole moments relative to the permanent dipole were thus derived. Possibilities of using this approach to study transition dipole moment directions of nucleic acid bases will be discussed.

A comprehensive theoretical treatment of orientation by electric fields will be presented. Derivations of directions for transition dipoles based on measurements of linear dichroism will be discussed. The precision of the measurement is primarily determined by the stability in rotational temperature. Calibration using known transitions such as the $\pi^* - \pi$ transition in diazines, and measurements under different orientation fields can be used for improved results.

The Composition of Metastable Noble Gas Atom Beams

Don Mueller and John Krenos

Department of Chemistry, Rutgers, the State University
610 Taylor Road, Piscataway, New Jersey 08854-8087

We will report on a novel luminescence method of determining the relative fraction f_1 of metastable noble gas atoms [$\text{Ng}^*(^3\text{P}_{J=0,2})$] produced by a supersonic noble gas source, in which excited atoms are formed by transverse electron impact at nominal electron kinetic energies [E_e] between 35 and 300 eV. The $\text{Ar}^* + \text{Xe}$ monitor system¹ is used to determine an accurate beam composition for Ar^* at $E_e = 85$ eV. The emission from Xe^* is analyzed in detail with the appropriate sum of product electronic state cross sections scaled to our quenching cross section value for $\text{Ar}^*(J=2)$ and ($J=0$).¹ Beams of Kr^* and Xe^* are produced with the same source backing pressure (number density) and E_e . The reduction in the atomic beam intensity for the heavier (slower) atoms due to velocity (mass) differences is compensated by the increased time spent by the slower atoms in the electron impact region. Since the electron excitation cross sections for Ar^* , Kr^* , and Xe^* are nearly identical at 85 eV, the intensity of the different Ng^* beams is essentially the same. Measured beam currents on a tungsten surface detector are used to determine detection efficiencies γ relative to the value of 0.20 measured by Hotop and coworkers for Ar^* detected by a graphite-covered stainless steel surface. Known cross sections for $\text{Kr}^*(J=2) + \text{Xe}$ [23.5 \AA^2 derived from Setser for $\text{Xe}^*(2p_6)$] and $\text{Xe}^*(J=2) + \text{N}_2$ [4.25 \AA^2 derived from our work for $\text{N}_2^*(B:v'=5)$] are then used to determine f_2 values for Kr^* and Xe^* at $E_e = 85$ eV. The analysis employs a γ_0/γ_2 value of 1.30 taken from Borst/Hagstrum for Kr^* and a value of 2.47 used by Borst/Ottinger for Xe^* . These ratios do not influence the values of f_2 reported at 85 eV, but are important in the second method we use to measure values at other electron impact energies. Our results at $E_e = 85$ eV are: $f_2(\text{Ar}^*) = 0.800 \pm 0.009$ ($\gamma_2 = \gamma_0 = 0.200$ assumed), $f_2(\text{Kr}^*) = 0.920 \pm 0.013$ ($\gamma_2 = 0.14_2$), and $f_2(\text{Xe}^*) = 0.904 \pm 0.020$ ($\gamma_2 = 0.026_7$).

Relative beam composition from 35-300 eV is determined by a second method. The ratio of the

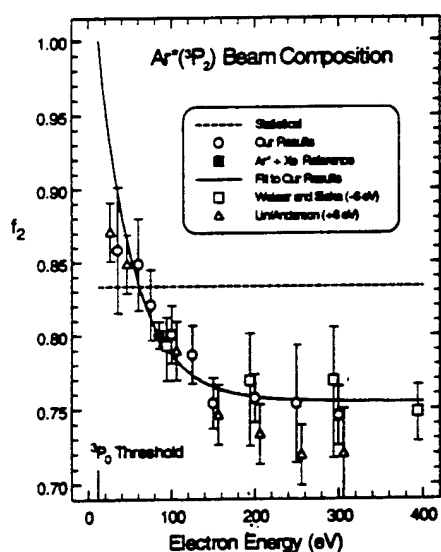


Figure 1: Beam Composition of Ar^* .

We will also report the results of experiments on the $\text{Kr}^* + \text{H}_2\text{O}$ reaction, which will be compared to our detailed experiments for $\text{Ar}^* + \text{H}_2\text{O}$. In the Ar^* system, σ_0 values drop monotonically as collision energy increases. In contrast, σ_0 values for Kr^* initially rise, reach a plateau, and then drop with increasing collision energy. This behavior can be explained by a curve-crossing model.

¹ D. Rickey and J. Krenos, *J. Chem. Phys.* **106**, 3135 (1997).

² D. Mueller and J. Krenos, *J. Phys. Chem.* **97**, 2106 (1993).

H₂ Production in the 440 nm Photodissociation of Glyoxal

L. M. Dobeck^a, H. M. Lambert, P. Pisano, W. Kong^b and P. L. Houston

Department of Chemistry and Chemical Biology
Cornell University, Ithaca, NY

^aInstitute for Computational Earth System Science
University of California, Santa Barbara

^bDepartment of Chemistry, Oregon State University at Corvallis

H₂ has been observed as a primary photoproduct in the 440 nm photodissociation of glyoxal using (2+1) REMPI detection. This is the first direct evidence of the "triple whammy channel", in which glyoxal dissociates in concerted fashion into three products: H₂ + 2 CO. H₂ rotational distributions and Doppler profiles were obtained subsequent to excitation of jet cooled glyoxal to the 8₁¹₀ band of the S₁ state. The average energy partitioned among products was determined to be 5% in rotation, 18% in vibration, and 47% in translation for H₂, leaving 31% in translation and internal energy for the 2 CO molecules. The information from the energy disposal and vector correlation measurements are discussed with reference to earlier experiments detecting CO and to *ab initio* theoretical calculations of the dissociation in the "triple whammy channel".

Adiabatic Diffusion Monte Carlo Studies for the
 Ne_nSH ($^2\Sigma^+$, $v_{\text{SH}} = 0$, $n=1,2,3,4$) van der Waals Complexes

Hee-Seung Lee, John M. Herbert and Anne B. McCoy

Department of Chemistry, The Ohio State University, Columbus, OH 43210

Two adiabatic extensions to the diffusion Monte Carlo approach (ADMC)¹ are presented. In the first, an adiabatic form of the finite field method is developed for the systematic evaluation of expectation values. In addition, an adiabatic flexible node method for calculating excited vibrational state energy is described. The above methods are tested by applying to NeSH^2 and Ar_2HCl^3 complexes where comparisons to results of variational calculation can be made. Our results show that the agreement between ADMC and variational calculation is better than 1% relative error.

Application of ADMC to the structure and spectroscopy of Ne_nSH van der Waals complexes will also be presented. The pairwise addition of Ne-SH^2 potential and Ne-Ne potential was used as a best approximation. The calculation yields ground state structure and rotational constants as well as the energies. In the case of $\text{Ne}_2\text{SH/D}$, energies and wavefunctions of excited vibrational states were also simulated using ADMC. The electronic transition ($\text{A}^2\Sigma^+ \leftarrow \text{X}^2\Pi_{3/2}$) spectra has been recorded recently for this system,⁴ but not fully assigned. As such, this work will provide valuable insights into the interpretation of complicated spectra of these very floppy systems.

¹H.-S.Lee, J.M.Herbert and A.B.McCoy, *J.Chem.Phys.* **110**,5481(1999)

²C.C.Carter, T.A.Miller, H.-S.Lee, A.B.McCoy and E.F.Hayes, *J.Chem.Phys.* **110**, 5065(1999)

³A.R.Cooper and J.M.Hutson, *J.Chem.Phys.* **98**,5337(1993)

⁴C.C.Carter and T.A.Miller (unpublished)

Detailed studies of collisional processes including energy transfer and energy pooling following the production of $\text{Ba}[6s5d(^3D_{1,2,3})]$ by pulsed laser excitation at $\lambda = 553.5 \text{ nm}$

Jie Lei

Department of Chemistry, Johns Hopkins University, Baltimore, MD 21218, USA
David Husain and Stephen Antrobus

Department of Chemistry, University of Cambridge, Cambridge CB2 1EW, U.K.
Fernando Castaño and Maria N. Sanchez Rayo

Departamento de Química Física, Universidad del País Vasco, Apartado 644,
48080 BILBAO, SPAIN.

The collisional behaviour of the low lying optically metastable state of atomic barium, $\text{Ba}[6s5d(^3D_J)]$, 1.151 eV above the $6s^2(^1S_0)$ ground state, has been investigated following the initial pulsed dye-laser excitation of atomic barium vapour at $\lambda = 553.5 \text{ nm}$ $\{\text{Ba}[6s6p(^1P_1)] \leftarrow \text{Ba}[6s^2(^1S_0)]\}$. The 3D_J state, which is not directly accessible by laser excitation, was generated via a complex set of radiative and collisional processes. It was then monitored in the 'long-time domain' by spectroscopic marker methods via transitions $\lambda = 791.1 \text{ nm}$ $\{\text{Ba}[6s6p(^3P_1)] \rightarrow \text{Ba}[6s^2(^1S_0)]\}$, $\lambda = 877.4 \text{ nm}$ $\{\text{Ba}[6s5d(^1D_2)] \rightarrow \text{Ba}[6s^2(^1S_0)]\}$ and $\lambda = 553.5 \text{ nm}$ $\{\text{Ba}[6s6p(^1P_1)] \rightarrow \text{Ba}[6s^2(^1S_0)]\}$. Time-resolved emission measurements at $\lambda = 791.1 \text{ nm}$ and $\lambda = 877.4 \text{ nm}$, which follow directly the decay profile of the 3D_J state itself, were made following collisional excitation of $\text{Ba}(^3D_J)$ to the 3P_J and 1D_2 states by He and Ba. The emission at $\lambda = 553.5 \text{ nm}$ results from the production of $\text{Ba}(^1P_1)$ arising from energy pooling to this state accompanying the $\text{Ba}(^3D_J) + \text{Ba}(^3D_J)$ self-annihilation. Rate coefficients for the decay profiles at $\lambda = 553.5 \text{ nm}$, $\lambda = 791.1 \text{ nm}$ and $\lambda = 877.4 \text{ nm}$ were thus found to be in the ratio 2:1:1 in the long-time regime where the decay of $\text{Ba}(^3D_J)$ becomes first-order. A detailed mechanism in terms of the optical and collisional processes for populating the emitting states is presented. Absolute second-order rate data for the collisional excitation of $\text{Ba}(^3D_J)$ to $\text{Ba}(^3P_J)$ by $\text{Ba}(^1S_0)$ and He, and collisional quenching by He, are presented and found to be essentially consistent with previously reported measurements of collisional relaxation from $\text{Ba}(^3P_J)$ to $\text{Ba}(^3D_J)$ by the principle of detailed balance. Various normalised integrated forms of the atomic emission intensities with $[\text{He}]$ and $[\text{Ba}]$ are tested against experimental observation to demonstrate the roles of the dominant processes in the overall mechanism. Where possible, rate data are compared with previously reported measurements including that for the mean radiative lifetime determined in this investigation, namely, $\tau_e(^3D_J) = 1.61 \text{ ms}$ and $\tau_e(^3D_1) = 502 \mu\text{s}$ which are seen to be in accord with earlier estimates.

Spectroscopic Study of Non-bonding Interactions between the Al^+ Ion and the Ar Atom

Jie Lei and Paul J. Dagdigan
Department of Chemistry
The Johns Hopkins University
Baltimore, MD 21218

The weakly bound $\text{Al}^+ - \text{Ar}$ complex has been prepared in a pulsed free jet supersonic beam and studied by laser fluorescence spectroscopy in the vacuum ultraviolet spectral region. The complex was prepared by 193 nm photolysis-ionization at the jet nozzle of trimethylaluminum seeded in argon and was probed several cm downstream by laser fluorescence excitation with tunable vuv laser radiation, prepared by 4-wave mixing in Mg vapor.

An electronic transition of the $\text{Al}^+ - \text{Ar}$ complex in the spectral region near the Al^+ ion $3s3p\ ^1P \leftarrow 3s^2\ ^1S$ resonance transition at 167.1 nm is reported. An excited-state ($v',0$) progression and the (0,1) hot band were observed. Rotational analysis revealed that these bands involved an electronic transition from the $\text{Al}^+ - \text{Ar}\ X^1\Sigma^+$ ground state to the $^1\Sigma^+$ state correlating with the $\text{Al}^+(^1P) + \text{Ar}$ asymptote. Rotational constants and upper-state vibrational constants and the dissociation energy were determined. The spectroscopic constants of the two observed $\text{Al}^+ - \text{Ar}$ electronic states are compared with those for neutral AlAr Rydberg states.

Analysis of energy transfer in collisions of azulene with He, Ar, Xe and N₂: Temperature dependence and details of transition probabilities $P(E',E)$

Uwe Grigoleit, Uwe Hold, Thomas Lenzer, Klaus Luther and Andrew C. Symonds

Institut für Physikalische Chemie, Universität Göttingen, Tammannstraße 6, 37077 Göttingen, Germany

Collisional energy transfer between highly vibrationally excited azulene molecules and the colliders helium, argon, xenon and nitrogen has been studied by means of quasiclassical trajectory calculations. A wide range of temperatures ($T = 50$ -1300 K) has been investigated for initial azulene excitation energies E between 5000 and 30000 cm⁻¹. Above roughly 300 K, the first moment of energy transfer, $\langle \Delta E \rangle$, is found to be only weakly dependent on temperature for all bath gases. However, with decreasing temperature $\langle \Delta E \rangle$ shows an pronounced increase for argon, xenon and nitrogen. The temperature at which this increase occurs is bath gas dependent and correlates directly with the potential well depth of the interacting species. This strongly suggests that energy transfer at low temperatures is enhanced due to the formation of longer-lived collision complexes. The root of the second moment of energy transfer $\langle \Delta E^2 \rangle^{1/2}$ shows a nearly linear temperature dependence except for smaller deviations at the lowest temperatures. Moreover, it is found that the observed T dependences of $\langle \Delta E \rangle$ and $\langle \Delta E^2 \rangle^{1/2}$ are fairly insensitive to the excitation energy of the azulene molecules. All findings are in agreement with recent experiments as well as theoretical studies.

Our trajectory calculations also provide detailed collisional transition probabilities $P(E',E)$. These will be compared to recent experimental $P(E',E)$ data obtained from kinetically controlled selective ionization (KCSI). The shape of the energy transfer distribution functions will be discussed, especially the contribution of various fractions of efficient collisions.

Classical Trajectory Direct Dynamics Simulations of Reactive Scattering of Ground-State Oxygen Atoms on Self-Assembled Monolayers of Thiols on Gold by Using Hybrid QM/MM Potentials: Collision Energy Dependence and Reaction Mechanisms

Guosheng Li, Sylvie B. M. Bosio and William L. Hase

Department of Chemistry, Wayne State University, Detroit, MI 48202

Reactions of atomic oxygen with hydrocarbon surfaces are important in testing and modifying surfaces of polymeric materials. Classical trajectory direct dynamics simulations were performed for the reactive scattering of triplet oxygen atoms with self-assembled monolayers of alkyl thiolates on gold surface. The surface model is the same as the one used previously[1] and consists of 35 n-hexyl thiolate molecules absorbed on a Au{111} surface comprised of a single layer of 127 gold atoms with a gold anchor atom. The force parameters are basically the same as before[1], except that the incoming oxygen atom and the top ethyl groups in the central 7 hexyl chains are treated explicitly using the PM3 method, specifically reparameterized for the $O(^3P) + C_2H_6$ reaction.

The trajectory simulations are carried out using the VENUS/MOPAC combined program[2]. Initial conditions are chosen to model experiments[3], with translational energies of 1.2, 5.0, 11.2 and 19.1 kcal/mol and a fixed incident angle of 60° . Most of the trajectories are non-reactive, with the oxygen atom exiting the surface via either an inelastic direct scattering or a trapping desorption mechanism. The translational energy distributions of the scattered oxygen atoms are in good agreement with experiment[3]. The proportion of reactive trajectories increases from 0% to 18% upon increasing the incident energy from 1.2 to 19.1 kcal/mol. The dominant reaction product is the OH radical formed by a direct reaction mechanism. Water is another product, quickly formed by abstraction of another hydrogen atom from either the same or different hydrocarbon chain by the primary OH product. Analysis of the OH product vibrational/rotational energy indicates that OH is primarily populated in a rotationally excited and ground vibrational state. When the direct dynamics trajectory is allowed to undergo a triplet-singlet transition, C_2H_5OH is formed as a reaction product, which supports the experimental observation of triplet-singlet crossing to form C-H insertion products.

- [1] S. B. M. Bosio and W. L. Hase, *J. Chem. Phys.* 1997, *107*, 9677.
- [2] G. H. Peslherbe and W. L. Hase, VENUS-MOPAC, a general chemical dynamics and semiempirical direct dynamics computer program. To be released.
- [3] D. J. Garton, T. K. Minton, M. Alagia, N. Balucani, P. Casavecchia and G. G. Volpi, *Faraday Discuss.* 1997, *108*, 387.

Classical model for complex molecular interactions

Yimin Li and John Z.H. Zhang

Department of Chemistry, New York University, New York, NY 10003, U.S.A.

Abstract

We present classical treatment to study collision dynamics in complex molecules. In the basic model the complex molecules are treated as rigid bodies and the dynamical system involves nine degrees of freedom describing the rotations of two colliding molecules and their relative translational motion. Such model allows us to construct realistic interaction potentials in a limited number of mathematical degrees of freedom for quantitative investigation of the interaction dynamics in complex molecular systems such as biological systems. The rigidity condition of the molecule can be relaxed to include some molecular motions explicitly that are important to the interaction in the dynamics calculation.

Crossed Molecular Beam Study of $O(^1D) + SiH_4$: Multiple Reaction Channels with Different Dynamics

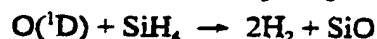
Jim J. Lin^a, Yuan T. Lee^{ab}, and Xueming Yang^a,

a. Institute of Atomic and Molecular Sciences, Academia Sinica, Taipei, Taiwan, ROC

b. Department of Chemistry, National Taiwan University, Taipei, Taiwan, ROC

Abstract

The titled reaction has been studied using a newly built crossed molecular beam apparatus with a universal detector. Angular resolved time-of-flight spectra have been measured for OH, SiO, HSiO (or SiOH), H_2SiO (or HSiOH), and H_3SiO (or H_2SiOH) products. Four distinctive channels have been identified through the analysis of the experimental data:



In the $OH + SiH_3$ channel, the angular distribution of the OH products peaks sharply at forward direction with respect to the $O(^1D)$ beam, indicating a direct reaction mechanism i.e. the lifetime of the intermediate is shorter than the rotational period. In the $H + H_3SiO$ channel, minor amount of H_3SiO products has been observed with backward angular distribution, which also suggests a direct reaction mechanism. The kinetic energy release of the $H + H_3SiO$ channel is small, therefore, the H_3SiO products are likely produced in an excited state. The $H_2 + H_2SiO$ channel and $2H_2 + SiO$ channel have close to isotropic angular distributions which may indicate that reaction intermediate has a lifetime longer than a rotational period. Other energetically possible channels, $O(^1D) + SiH_4 \rightarrow 2H + H_2SiO$ and $O(^1D) + SiH_4 \rightarrow H + H_2 + HSiO$ may also exist. This study provides an excellent example of a complicated reaction with multiple pathways, in which the universal crossed beam apparatus can get a detailed global picture of such reactions.

Time-resolved Fourier Transform Emission Spectroscopy of Highly Vibrationally Excited Pyrazine

Dong Qin, Alan B. Ritter, Gregory V. Hartland, Laura T. Letendre, Jerrell Brenner,
Dean-Kuo Liu and Hai-Lung Dai

Department of Chemistry, University of Pennsylvania, Philadelphia, Pennsylvania 19104-6323

TR-FTIRES has been used to characterize the collisional energy transfer dynamics of highly excited pyrazine initially prepared at 32460 cm^{-1} . IR emission from highly excited pyrazine is observed through six IR active modes, ν_{20b} , ν_{19b} , ν_{14} , ν_{18} , ν_{12} , and ν_{11} . A quantitative model is developed to calculate the emission spectra of pyrazine at different energies. The second-order anharmonicity constants of the observed six vibrational bands are estimated by fitting the calculated IR emission spectrum of pyrazine at 32000 cm^{-1} energy. They are further used to model the vibrational bands in TR-FTIRES spectra of excited pyrazine. The average energy content of excited pyrazine, $\langle E \rangle$, as a function of number of collisions is extracted from the emission spectra. The energy transfer rate, the energy loss per collision, $\langle \Delta E \rangle$, as a function of $\langle E \rangle$, is then derived. It is found that the energy transfer rate is similar to that of benzene and other aromatic molecules reported previously.

IR emission from levels populated by V-V energy transfer from highly excited pyrazine is also observed from TR-FTIRES spectra of pyrazine. Our result suggests that 24 vibrational modes are not equally populated during V-V energy transfer. Considering that V-V energy transfer only occurs for IR active modes. It is found that the relative importance of V-V and V-T/R during collisional quenching of highly excited pyrazine is the same in terms of the trends for the number of pyrazine excited by vibrationally excited pyrazine as a function of number of collisions.

A new continuous dynamical approach for generating the canonical ensemble

Yi Liu and Mark E. Tuckerman*

Department of Chemistry, New York University

Abstract

The new method of Generalized Gaussian Moment Thermostatting (GGMT) for generating the canonical ensemble via continuous dynamics is presented. This method is based on the idea of controlling the fluctuations of an arbitrary number of moments of the multidimensional Gaussian momentum distribution function. By applying the statistical mechanical theory of non-Hamiltonian systems introduced by M.E. Tuckerman, etc. , the new formulation is shown to generate ergodic trajectories that sample all the available phase space. Reversible integrators for the new equations of motion are derived based on a Trotter type factorization of the classical Liouville propagator. The new method, applied to a variety of simple one-dimensional model potentials, is shown to generate the correct canonical distribution functions of both position and momentum. Compared to another canonical dynamics approach, the Nosé-Hoover chain method, GGMT is demonstrated to be an efficient sampling tool not only in the model systems but also in molecular dynamics simulations of biological macromolecules.

*Also at Courant Institute of Mathematical Sciences

Rotational State-to-State Differential Cross Sections for the HCl-Ar Collision System Utilizing Velocity-Mapped Ion Imaging

K. Thomas Lorenz and David W. Chandler
Sandia National Laboratories, Livermore, CA

Fully state-resolved differential cross sections (DCS) for the j -changing collisions of HCl by Ar are presented. The technique of velocity-mapped ion imaging employed with a new crossed-molecular beam apparatus is utilized to measure the full ($\theta = 0-360^\circ$) DCS for $j=0 \rightarrow j'=1,2,\dots,6$ RIT transitions at a center-of-mass energy of 500cm^{-1} . The initial HCl rotational distribution is over 97% in the $j=0$ state, and the scattering products are state-selectively ionized via (2+1) REMPI through the E -state, allowing for the extraction of nearly state-to-state DCS's in the center-of-mass frame. These state-to-state DCS's are compared with calculated cross sections based upon the HCl-Ar $H_6(4,3,0)$ potential of Hutson [*J. Phys. Chem.* **1992**, *96*, 4237-4247]. Both the calculated and experimental cross sections agree reasonably well on the position of rainbow maxima for all Δj 's through $j_{\text{max}} = 6$. Although scattering moves from forward to backward as Δj increases, it does so non-monotonically - where a reversal occurs between $j'=2$ and $j'=3$. Images for the even Δj 's $0 \rightarrow 2$ and $0 \rightarrow 4$ are similar, and those for the odd Δj 's $0 \rightarrow 1$ and $0 \rightarrow 3$ also have similarities. These features are represented well in the calculated cross sections. However, there remain differences in the theoretical and experimental results, especially for larger Δj 's, where the calculated cross sections show a much greater angular spread than the experimental images.

Three-body decay dynamics of transient molecules

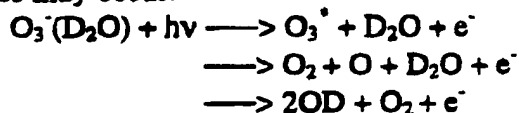
A. Khai Luong, T.G. Clements, R.E. Continetti

Department of Chemistry and Biochemistry, University of California, San Diego,
9500 Gilman Drive, La Jolla, CA 92093-0314

In recent decades, there has been increased interest in the study of three-body decay dynamics. The information gained from three-body decay dynamics may provide new insights into many gas phase processes important in atmospheric and combustion chemistry. For example, an understanding of the dissociation dynamics may provide information about the geometry, energetics and potential energy surfaces of the parent species. Furthermore, if the transition state of a three-body recombination reaction is accessed in the experiment, one may study the half reaction of the three-body recombination mechanism. Experimental studies of these systems have been limited due to the requirement to unambiguously detect at least two of the three particles originating from a single three-body decay process. Several groups have designed experiments to observe the dissociation dynamics of charged systems. In our laboratory, a recently developed apparatus allows coincident detection of an electron and multiple neutral particles from a single dissociative photodetachment event, permitting detailed studies of the kinematics of three-body dissociation processes.

A photoelectron-photofragment coincidence (PPC) technique is used to study the three-body decay processes of transient molecules formed in a fast negative ion beam. Photodetachment of a negatively charged precursor, with coincident energy analysis of the photoelectron, allows production of energy-selected transient neutral complexes. Use of a fast negative ion beam (4 keV) in conjunction with a multi-particle detector allows multiple neutral photofragments to be detected in coincidence. By measuring the positions and times-of-arrival of all the particles (one electron and three molecular fragments), the experiment yields a kinematically complete description of the three-body decay dynamics of the system of interest. The results presented will demonstrate the application of the PPC technique towards the study of three-body dissociations of $O_3(D_2O)$, produced by the photodetachment of $O_3^-(D_2O)$.

An investigation into the three-body decay dynamics of $O_3(D_2O)$ may contribute to an understanding of tropospheric and stratospheric ozone chemistry. Upon photolysis, the following processes may occur:



With the PPC technique, we can easily differentiate between the three possible pathways by analysis of the kinetic energy release of all the fragments. The results indicate that the clustering of a water molecule to ozonide stabilizes the system by approximately 0.85 eV, and that photodetachment to the triplet states of O_3 in the complex result in dissociation, with no evidence observed for quenching or intracuster reaction in the complex. Furthermore, the use of a molecular-frame differential cross section image provides insights into the possible configuration of the anion cluster.

This work was supported by the Air Force Office of Scientific Research and the David and Lucile Packard Foundation.

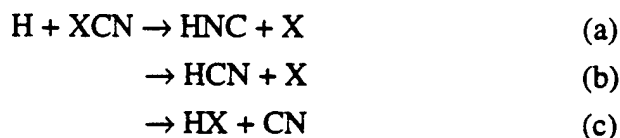
Initial Product State Distributions and Translational Energy Release for Several
Channels for the H + XCN Family of Reactions.

C55

R. Glen Macdonald

Argonne National Laboratory
Chemistry Division
Argonne, IL 60439

The reaction of translationally energetic H atoms with a series of CN containing compounds:



where X is Cl, Br or CN provides for an interesting series of reactions within related chemical environments. Various aspects of the reaction dynamics for these reactions have been investigated. The branching ratios into the two addition-elimination channels, (a) and (b), and the direct abstraction channel, (c) have been measured. Further details of the reaction dynamics, comes from the determination of the $\text{CN}(v=0;J,T)$ distribution for the abstraction channel for all three reactants. As expected for a spectator bond in a direct reactive event, $\text{CN}(v=0)$ exhibited modest rotational excitation and substantial translational energy release. Another aspect of the reaction dynamics that is under investigation is the product state distribution for the addition-elimination channels. For $\text{H} + (\text{CN})_2$, channel (a), is slightly endothermic for H atoms with 22 kcal mol^{-1} translational energy; hence, the available number of vibrational states are limited to $\text{HNC}(000)$ and $\text{HNC}(01^10)$. This enabled a complete determination of the vibrational, rotational and translational energy released into this product channel. These experiments were carried out at a total pressure of 0.1 Torr using high resolution absorption spectroscopy in the red (790 nm) to monitor CN and in the infrared (2.7 microns) to monitor HNC.

Theoretical Studies of Chemical Reactions in Clusters: Approximate treatments of quantum mechanical effects in reactions of oxygen and chlorine with HCl and Ar_nHCl

Lichang Wang, Holly B. Lavender and Anne B. McCoy

*Department of Chemistry
The Ohio State University
Columbus, OH 43210*

Abstract

Studies of chemical reactions in small clusters provide an important first step in understanding how gas phase reactivity is affected by the presence of other, loosely bound, atoms or molecules. A challenge encountered when studying reactions in clusters comes in the large number of atoms. The size makes exact quantum calculations on a system in the presence of even a single rare gas atom prohibitively expensive. In this poster, several methods for approximating quantum behaviors will be explored. These include careful sampling initial conditions for classical simulations as well as hybrid quantum/classical simulation techniques. In the latter approach, the system is divided into two parts, one that includes the degrees of freedom whose dynamics are expected to be most quantum mechanical. These are propagated using time-dependently, in the full dimensionality of the quantum sub-systems. The remaining degrees of freedom are propagated classically.

The above theoretical and computational considerations will be discussed in the context of the dynamics of reactions of atomic oxygen or chlorine with HCl and complexes of HCl with one to five argon atoms. Both bimolecular reaction dynamics and processes that are initiated from the transition state have been explored.

Molecular Beam Study of the Chemiluminescent Reaction of Manganese & Ozone: Product Distributions & Implications for Mechanism

Karen Green and John Parson

Dept. of Chemistry, The Ohio State University, 100 W. 18th Ave., Columbus, OH 43210

The electronically chemiluminescent reaction $\text{Mn} + \text{O}_3 \rightarrow \text{MnO}^* + \text{O}_2$ was investigated using a beam-gas configuration. Light from the $\text{MnO } A \ ^6\Sigma^+ - X \ ^6\Sigma^+$ transition was collected by a CCD array detector with resolutions of 0.5 and 0.1 nm. The spectrum at lower resolution (500–655 nm) encompassed the $\Delta v = -3$ to $+2$ sequences, while that at higher resolution (555.5–583.5 nm) only the $\Delta v = 0$ sequence. These two spectra were separately fitted with a non-linear least squares program to obtain vibrational and rotational distributions of the nascent MnO^* . The limited vibrational-state coverage of the higher-resolution spectrum made it unreliable for determining the vibrational state distribution, and it was useful only for characterizing the rotational distribution when $v' = 0$.

Flexible functions were built on prior distributions to model the vibrational and rotational populations:

$$P(v') = P^0(v') \exp[\lambda_{vb1} f_{v'} + \lambda_{vb2} f_{v'}^2]$$

$$P(v', N') = P^0(v', N') \exp[\lambda_{rot1} g_{N', v'} + \lambda_{rot2} g_{N', v'}^2]$$

where $f_{v'} = E_{v'}/E_{total}$, and $g_{N', v'} = E_{N'}/(E_{total} - E_{v'})$. The overall best-fit parameters were: $\lambda_{rot1} = 5.47$, $\lambda_{rot2} = 0.446$, $\lambda_{vb1} = -3.62$, and $\lambda_{vb2} = 8.48$. The best-fit vibrational excitation is somewhat less than for the prior, but the rotational excitation is considerably greater.

From Magee's equation,¹ the charge transfer was estimated to occur at short-range (Mn-O_3 separation of 0.27 nm), and models such as harpooning or Direct-Interaction-with-Product-Repulsion² are inappropriate for predicting energy disposal. A consideration of the electronic structure of reactants and products indicates that principal changes occurring in the reaction are σ electron donation from the sd_{z^2} -hybridized Mn orbital to the O_3 LUMO ($2b_1$) and π back donation from the O-O_2 $4b_2$ orbital to the Mn $3d_x$ orbital. Correlation of the orbitals involved indicates that direct access is allowed to the $\text{MnO } A \ ^6\Sigma^+ (10\sigma^{*1} 8\sigma')$ state.

This mechanism favors Mn approach perpendicular to the O_3 plane, and attributes the product's rotational excitation to O_2 -OMn repulsion arising from removal of electron density from the slightly bonding $4b_2$ orbital of O_3 . However, some rotational excitation could also be attributed to conservation of angular momentum arising from a sizeable reactive impact parameter. In order to determine if the excitation was due principally to the dynamics or kinematics, McCaffery's Quantum-Constrained-Kinematic-Model³ was used to calculate the most probable rotational quantum number for the $\text{Mn} + \text{O}_3$ reaction. The most probable rotational quantum number calculated from this model was found to be too low (29 compared to an experimental value of 83) to explain the rotational excitation of the product. This implies that the high rotational excitation observed in the $\text{Mn} + \text{O}_3$ reaction is principally a dynamic effect. The lack of significant vibrational excitation is a consequence of the short-range nature of the partial charge transfer.

¹Magee, J. L. *J. Chem. Phys.* 1940, 8, 687-698.

²Prisant, M. G.; Rettner, C. T.; Zare, R. N. *J. Chem. Phys.* 1984, 81, 2699-2712.

³McCaffery, A. J.; Truhins, K.; Whiteley, T. W. *J. Phys. B: At. Mol. Opt. Phys.*

Collision Activation of Small Peptides

Oussama Meroueh and William L. Hase

Department of Chemistry

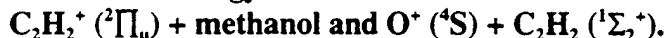
Wayne State University

Detroit, Mi 48202

May 17, 1999

Abstract

Energy transfer in the collision of small peptides with argon was studied using classical trajectory simulations at collision energies ranging from 100 to 1000 kcal/mol. High level *ab initio* calculations were performed to determine an accurate Ar-peptide intermolecular potential. The energy transfer efficiency was found to depend on several factors including the collision impact parameter, the collision energy, the size and structure of the peptides. Average energy transfer were determined for alanine and glycine polypeptides of size ranging from three to seven units. Average rotational and vibrational energy transfer were determined versus impact parameter for folded and unfolded tetraglycine. Energy was mainly transferred into the vibrational modes of the peptides and energy transfer was more efficient to the more folded peptides. The energy transfer mechanism was also studied by constraining various high and low frequency motions of the peptide. It was found that even after constraining all bending and stretching motions, so that only energy transfer to internal rotations was possible, energy transfer was still greater than 50% of the energy transfer to the unconstrained peptide. The internal energy of the peptide was monitored with time and fluctuations in the internal energy during the collisions revealed the presence of multiple collision encounters.

Ab initio Potential Energy Surfaces for Ion-Molecule Reactions:Stephan Irle, Kaori Fukuzawa and Keiji MorokumaCherry L. Emerson Center for Scientific Computation and Department of Chemistry,
Emory University, Atlanta, GA 30322

High level ab initio and density functional calculations were carried out to study the mechanism of the reaction $C_2H_2^+ + CH_3OH$ (experiment: S. L. Anderson et al., J. Chem. Phys. **108**, 7173 (1998)) for four reaction channels: hydride abstraction from methanol (HA), proton transfer from acetylene cation (PT), charge transfer (CT) and covalent complex formation (CC) channel. For the CT channel, two pathways have been found: a usual non-adiabatic pathway via A'/A" seam of crossing and a low energy adiabatic pathway through an initial intermediate; the latter may be the dominant process with favorable energies and a large impact parameter. The HA process involves a low-energy direct intermediate and a very low barrier to form $C_2H_3 + CH_2OH^+$ and is also energetically favorable. The PT processes require passage over a high-energy transition state and are not important. One of the experimentally unobserved CC channels, formation of the COCC skeleton, is energetically favorable and there is no energetic reason for it not to take place; a "dynamic bottleneck" argument may have to be invoked to explain the experiment. The increase in reaction efficiency with the CC stretch excitation may be justified by considering the TSs for two CT pathways, where the CC distance changed substantially from that in the reactant $C_2H_2^+$. Very qualitatively, the $C_2H_2^+ + CH_3OH$ potential energy surface looks more like that of the $C_2H_2^+ + NH_3$ system than the $C_2H_2^+ + CH_4$ system, because of the differences in the ionization potentials: $NH_3 \sim CH_3OH < C_2H_2 < CH_4$.

High level ab initio calculations were carried out to study in detail the early stage of the reaction: $O^+ (^4S) + C_2H_2 (^1\Sigma_g^+)$ (experiment: Y. Chiu, R. A. Dressler et al., J. Chem. Phys. **109**, 5300 (1998)) mainly for the charge transfer (CT) channels. The input channel corresponds to 4A" state in C symmetry (7A in C_1), with CT1: $O (^3P) + C_2H_2^+ (^2\Pi_u)$ and CT2: $O (^1D) + C_2H_2^+ (^2\Pi_u)$ channels below and CT3: $O (^1D) + C_2H_2^+ (^4A_2)$ just above in energy. In a very early stage of collision, the potential surface crosses with the CT2 state giving rise to a weak spin-forbidden CT process at low collision energy (~ 1 kcal/mol). At higher energy, the system goes over a transition state (barrier around 27 kcal/mol) for charge transfer with the CC stretching acting as the promotion mode to reach an intermediate, which is a weak complex Int1 between $O (^1D)$ and $C_2H_2^+ (^4A_2)$. This complex can dissociate easily to give the CT3 product. The system can further proceed over a small barrier and encounter a series of avoided crossings before reaching a strong quartet complex Int2, $[CHCHO]^+$. These avoided crossings lead to major CT1 channels, while Int2 is the starting point for further reaction channels.

This work was supported in part by AFOSR Grants (F49620-98-1-0063 and F49620-98-1-0345)

Photodissociating Trimethylamine at 193 nm to Probe Dynamics at a Conical Intersection

Nancy R. Forde, Melita L. Morton, Stephen L. Curry, S. Jarrett Wrenn and Laurie J. Butler

The James Franck Institute and Department of Chemistry

The University of Chicago

Chicago, Illinois 60637

We have studied the dynamics of the photodissociation of trimethylamine ($\text{N}(\text{CH}_3)_3$) using a crossed laser-molecular beam apparatus¹. The 5% $\text{N}(\text{CH}_3)_3$ (in He) was expanded in a supersonic jet and crossed with 193 nm laser light. The neutral photofragments were ionized and detected as a function of time-of-flight with respect to the laser pulse. After excitation to the S_2 surface, dissociation to $\text{N}(\text{CH}_3)_2 + \text{CH}_3$ follows fast internal conversion from the S_2 to the S_1 surface. Since in planar geometry (the equilibrium geometry of the S_1 surface) S_1 correlates to ground state products and S_0 correlates to $\bar{\text{A}}$ state products, the product branching into $\text{N}(\text{CH}_3)_2 (\bar{\text{X}})$ and $\text{N}(\text{CH}_3)_2 (\bar{\text{A}})$ thus allows us to investigate how internal conversion (with accompanying vibrational redistribution) influences traversal of a conical intersection in the exit channel. We compare the nonadiabatic dynamics of trimethylamine to those of ammonia² and methylamine³ previously reported. In addition, secondary dissociation before ionization produces a combination of products such as $\text{CH}_2\text{NCH}_3 + \text{H}$ and we comment on these reactions also.

¹ N.R. Forde, M.L. Morton, S.L. Curry, S.J. Wrenn and L.J. Butler, *J. Chem. Phys.*, submitted.

² For example, see the work of J. Biesner, L. Schneider, G. Ahlers, X. Xie, K.H. Welge, M.N.R. Ashfold and R.N. Dixon, *J. Chem. Phys.* **91**, 2901 (1989)

³ G.C.G. Waschewsky, D.C. Kitchen, P.W. Browning and L.J. Butler, *J. Phys. Chem.* **99**, 2635 (1995)

Wavepacket Dynamics of ICN Photodissociation Revisited

James T. Muckerman and Li Liu

Chemistry Department, Brookhaven National Laboratory, Upton, NY 11973-5000

We have attempted to extend the previous wavepacket treatments [1, 2] of ICN photodissociation on the *ab initio* potential energy surfaces of Amatatsu *et al.* [3] because non-adiabatic transitions at the avoided crossing between the $^3\Pi_{0^-}$ (A') state, which correlates diabatically to the I^* channel, and the A' component of the $^1\Pi_1$ state, which correlates diabatically to the I channel, complicate the assignment of anisotropies of selected product states. We assume that a distinct polarization (parallel or perpendicular) is associated with each element of population, and that the type of polarization is unaffected by the wavepacket dynamics. We write the time-dependent wavefunction for the system as

$$|\Psi(t)\rangle = \sum_{p=1}^2 |p\rangle \sum_{k=1}^5 |k\rangle \Phi_{kp}(t)$$

where the sum over polarization functions $|p\rangle$ can be suppressed for all but two electronic states. Note that $|\Phi_{kp}(t)\rangle$ is one component of a two-component, time-dependent nuclear wavefunction in the k th electronic state. We assume the Hamiltonian operator for the system is $\hat{H} = \hat{H}_{el} + \hat{T}_{nuc}$ and that we can express the diabatic representation of the electronic states as $\langle n|\hat{H}_{el}|k\rangle = V_{nk}$ with all off-diagonal V_{nk} equal to zero except that connecting the $^3\Pi_{0^-}$ (A') and $^1\Pi_1$ (A') electronic states. Substituting into the time-dependent Schrödinger equation and left-multiplying by $\langle n|p\rangle$ and using the orthonormality property $\langle p|p'\rangle = \delta_{pp'}$, we have

$$\frac{\partial}{\partial t} |\Phi_{np}(t)\rangle = \frac{-i}{\hbar} \sum_{k=1}^5 (\hat{T}_{nuc} \delta_{nk} + V_{nk}) |\Phi_{kp}(t)\rangle$$

which shows that the non-adiabatic coupling can transfer population only between states with the same polarization. This is the essential new feature of the present treatment, and it allows us to compute the polarization anisotropies of the I^* and I channels in ICN photodissociation as well as the rotational-state-dependent anisotropies in a given product channel.

Attempts to compare the results of these new calculations with experiment reveal deficiencies in the *ab initio* potential energy surfaces. Experimental Doppler lineshape studies by a number of workers (most recently by North, Costen and Hall) indicate that the dissociation energy of the calculated ground state is approximately 0.5 eV too small. Employing the same (incorrect) ground-state dissociation energy used in the previous calculations of Qian *et al.* introduces an artifact: the state distributions for a given photodissociation wavelength have an incorrect (spuriously high) energetic cutoff. The comparison between theoretical and experimental rotational-state-dependent anisotropy parameters also reveals serious deficiencies in the potential energy surfaces. While the theoretical description of the non-adiabatic coupling between the $^3\Pi_{0^-}$ and $^1\Pi_1$ states seems qualitatively correct, the theory appears to overestimate the relative contribution of the $^1\Pi_1$ state. Nevertheless, our approach allows us to begin to explore multiple-surface interference effects in experimental dynamics.

[1] J. Qian, D.J. Tannor, Y. Amatatsu and K. Morokuma, *J. Chem. Phys.* **101**, 9597 (1994)

[2] J.M. Bowman and R.C. Mayrhofer, *J. Chem. Phys.* **101**, 9469 (1994)

[3] Y. Amatatsu, S. Yabushita and K. Morokuma, *J. Chem. Phys.* **100**, 4894 (1994)

Acknowledgment: This work was carried out at Brookhaven National Laboratory under Contract DE-AC02-98CH10886 with the U.S. Department of Energy and supported by its Division of Chemical Sciences, Office of Basic Energy Sciences.

Torsional Motion and Antisymmetric Stretching in the Emission Spectra of Photodissociating N_2O_4

B.F. Parsons, J.A. Mueller, S.L. Curry, P.C. Ray, and L.J. Butler

*The James Franck Institute and Department of Chemistry
The University of Chicago, Chicago, IL 60637*

Dispersed emission spectra have been collected for N_2O_4 expanded in a free jet and excited at a number of wavelengths between 199.7 nm and 205 nm. Most molecules excited in this absorption band, centered at about 186 nm, dissociate directly. However, a small number emit photons before the dissociation process is complete. As the molecule begins to dissociate, good Franck-Condon overlap develops with successively higher vibrational levels of the ground electronic state, giving a series of peaks shifted from the laser line. The observed spectra show progressions in the N-N stretch and in combination bands involving the torsion and antisymmetric stretching motions. Electronic structure calculations (CIS) of the relevant excited states aid in understanding the changes experienced by the electronic wavefunction as the molecule dissociates. We reassign the torsional frequency, ν_4 , based on several bands observed in the spectra. This result is then combined with numbers from the literature¹ to obtain a gas-phase value for the N_2O_4 out-of-phase rock, ν_6 .

Previous work² on the dissociation of N_2O_4 excited at 193 nm showed production of NO_2 , with no evidence for the $\text{O} + \text{N}_2\text{O}_3$ channel. The emission experiments discussed above showed excitation of both the N-N stretch and the antisymmetric stretch motion (which indicates extension of N-O bonds, possibly leading to their dissociation). Therefore it was deemed worthwhile to reexamine the 193 nm dissociation using photofragment translational spectroscopy. The results of these experiments will be discussed in light of the information gained from the emission studies.

¹ C. Bibart and G. Ewing, *J. Chem. Phys.* **61**, 1284 (1974).

² M. Kawasaki, K. Kasatani, H. Sato, H. Shinohara, and N. Nishi, *Chem. Phys.* **78**, 65 (1983).

Kinetics of spin-orbit relaxation of the $\text{PF}(A^3\Pi_{0,1,2}, v'=0-5)$
states in He and Ar

B. Nizamov* and D. W. Setser

Department of Chemistry

Kansas State University

Manhattan, KS 66506

The spin-orbit and vibrational relaxation rates for the $\text{PF}(A^3\Pi_{0,1,2}, v' = 0-5)$ states in He and Ar have been measured by observing time and spectrally resolved emission from pulsed laser excitation of the $A^3\Pi_{0,1,2} \leftarrow X^3\Sigma^- (v',0)$ bands. The measurements were done in a flow reactor at room temperature; the $\text{PF}(X)$ molecules were produced by passing He or Ar: PF_3 mixtures through a microwave discharge. Within the experimental uncertainties, the spin-orbit relaxation constants do not depend on v' and are $k_{2,0} = 1.0 \times 10^{-11}$, $k_{2,1} = 0.40 \times 10^{-11}$, $k_{1,0} = 0.80 \times 10^{-11}$ in He and $k_{2,0} = 0.30 \times 10^{-11}$, $k_{2,1} = 1.2 \times 10^{-11}$, $k_{1,0} = 0.6 \times 10^{-11}$ in Ar. The total vibrational relaxation rate constants increase linearly with v' in both He and Ar. The vibrational relaxation mechanism can be either a conventional V - T process with $\Delta\Omega = 0$ or a simultaneous change of the vibrational and spin-orbit quantum numbers to minimize the energy defect. The ratio of the rates for the vibrational relaxation channels with $\Delta\Omega \neq 0$ to those with $\Delta\Omega = 0$ is about 2.0 in Ar and about 1.0 in He. Total collision removal rate constants were measured, and by observing the products of the vibrational relaxation it was concluded that vibrational relaxation is the major channel and quenching relaxation rates are small. The spin-orbit relaxation in He is consistent with the propensity rules; however, propensity rules do not describe spin-orbit relaxation in Ar correctly. In both He and Ar the $^3\Pi_1 \rightarrow ^3\Pi_0$ relaxation is rather fast and in Ar the $^3\Pi_1 \rightarrow ^3\Pi_0$ relaxation is much faster than the $^3\Pi_2 \rightarrow ^3\Pi_0$ and $^3\Pi_2 \rightarrow ^3\Pi_1$ relaxation. Spectroscopic investigation showed that the $A^3\Pi_0$ and $b^1\Sigma^+$ states interact strongly, and singlet - triplet interaction may explain the specificity in spin-orbit relaxation involving the $\text{PF}(A^3\Pi)$ states.

* Present address: Department of Chemistry, The Johns Hopkins University, Baltimore, MD 21218.

State-to-state reaction dynamics in $F+H_2$ studied in crossed supersonic jets

Sergey A. Nizkorodov, Warren W. Harper, William B. Chapman, Bradley W. Blackmon,
and David J. Nesbitt

*JILA, University of Colorado and National Institute of Standards and Technology and Department of Chemistry and
Biochemistry, University of Colorado, Boulder, Colorado 80309-0440*

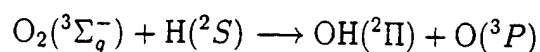
The reaction $F + n-H_2 (j = 0, 1) \rightarrow HF(v, J) + H$ is studied in a crossed jet apparatus under single collision conditions, using sensitive high-resolution direct absorption methods to probe the nascent rotational HF distributions. Reactive scattering cross sections into the $HF(v = 3, J)$ and $HF(v = 2, J)$ vibrational manifolds are obtained over a wide range of center-of-mass collision energies down to $E_{com} = 0.3$ kcal/mole, i.e. substantially below the theoretically predicted transition state barrier ($E_{barrier} \approx 1.9$ kcal/mole) for the lowest *adiabatic* $F(^2P_{3/2}) + H_2$ potential energy surface. The $HF(v = 2, J)$ cross sections agree well with the results of exact quantum calculations on the adiabatic $F(^2P_{3/2}) + H_2$ surface. On the contrary, the $HF(v = 3, J)$ cross sections decrease much more slowly with E_{com} than predicted by the theory. This observation is interpreted to result from the *non-adiabatic* $F(^2P_{1/2}) + H_2$ reaction, which becomes enhanced relative to the adiabatic $F(^2P_{3/2}) + H_2$ channel at these low collision energies, particularly for the $HF(v = 3, J)$ products lying near the reaction energetic threshold. This hypothesis is further confirmed by the observation of $HF(v = 3, J)$ rovibrational states that are *energetically inaccessible* from ground state $F(^2P_{3/2})$ atom reactions. These experimental findings show for the first time that *non-adiabatic* reactions with *spin orbit excited* $F(^2P_{1/2})$ may contribute significantly in the near threshold region, in good agreement with recent calculations by Alexander et al. (J. Chem. Phys., 1998, 109(14): p. 5710).

Time-dependent quantum mechanical calculations on $\text{H} + \text{O}_2$ for total angular momentum $J > 0$ using parallel computers

Anthony J. H. M. Meijer and Evelyn M. Goldfield

Dept. of Chemistry, Wayne State University, Detroit MI 48202

It is well known that the endothermic reaction



is a very important reaction in combustion chemistry. Consequently, a lot of experimental and theoretical work has been done on this reaction.

From a theoretical point of view the reaction is challenging. There is a deep well in the potential energy surface, corresponding to the HO_2 radical, which supports numerous bound states and gives rise to long-lived resonances. It is therefore not surprising that rigorous quantum dynamics calculations (for total angular momentum $J = 0$) have only become possible in the last five years (See, e.g., Refs. 1, 2). Calculations for $J > 0$ are even more challenging than calculations for $J = 0$, because for a specific J the calculation becomes (in principle) $2J + 1$ times more expensive than the $J = 0$ calculation.

Using a method designed for scalable parallel computers,³ we have performed calculations on the title reaction for $J > 0$, with J ranging between 1 and 25.⁴⁻⁶ We have shown that the inclusion of Coriolis coupling has a significant effect on the reaction probabilities and is needed to get accurate results. Based on our results and an interpolation scheme we are able to predict quantum mechanical cross sections and rate constants for reactions starting in the lowest ro-vibrational state.

¹ R. T Pack, E. A. Butcher, and G. A. Parker, *J. Chem. Phys.* **102**, 5998 (1995).

² D. H. Zhang and J. Z. H. Zhang, *J. Chem. Phys.* **101**, 3671 (1994).

³ E. M. Goldfield and S. K. Gray, *Comput. Phys. Commun.* **98**, 1 (1996).

⁴ A. J. H. M. Meijer and E. M. Goldfield, *J. Chem. Phys.* **108**, 5404 (1998).

⁵ A. J. H. M. Meijer and E. M. Goldfield, *J. Chem. Phys.* **110**, 870 (1999).

⁶ A. J. H. M. Meijer and E. M. Goldfield, *J. Chem. Phys.* . to be submitted.

Dynamical studies of complex molecular interactions

Nataliya Ozhegova and John Z.H. Zhang

*Department of Chemistry
New York University*

ABSTRACT

Classical dynamics studies are carried out to investigate the interaction between complex molecules. The complex molecules are currently treated as rigid rotors and the dynamics calculation is carried out in Euler angles and the distance of separation between two molecules. As a result, the interaction potential depends on six coordinates which can be constructed either by ab initio calculation or empirical forms or combination of both. This reduced dimensional approach provides a possibility to treat complex molecular interactions, such as biological and organic molecules, in a more controlled fashion with more realistic interaction potentials and longer interaction time frame.

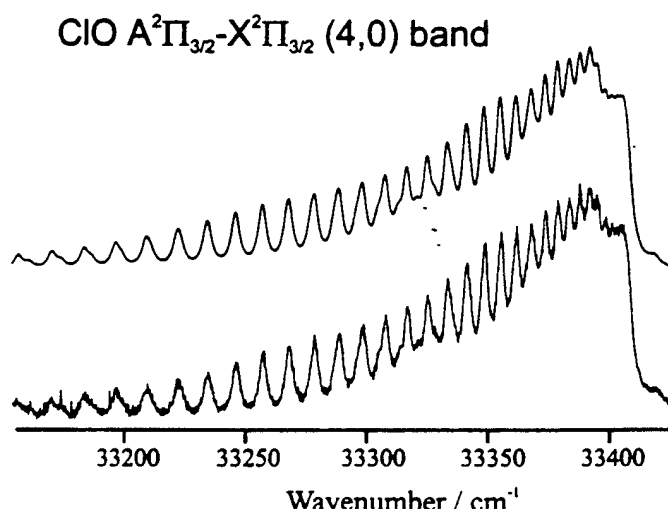
Predissociation dynamics of the ClO $A^2\Pi$ state studied by cavity ring-down spectroscopy and *ab initio* calculations.

Andrew J. Orr-Ewing, Wendy H. Howie, Ian C. Lane, and Stuart M. Newman.

School of Chemistry, University of Bristol, Bristol BS8 1TS, UK.

The UV absorption of ClO at wavelengths between 285 and 320 nm has been investigated using cavity-ring down spectroscopy. This wavelength region spans the (0,0) to (7,0) bands of the $A^2\Pi_{3/2} - X^2\Pi_{3/2}$ and $A^2\Pi_{1/2} - X^2\Pi_{1/2}$ transitions. Analysis of the spectra reveals a strong v' dependence in the linewidths of rotational features. The derived lifetimes of vibrational levels of the two spin-orbit components of the $A^2\Pi_{\Omega}$ state are markedly different at low v' .

Ab-initio calculations at the CASSCF and MRCI level have been performed on 15 valence doublet and quartet electronic states of the ClO radical in order to explore the predissociation dynamics of the $A^2\Pi_{\Omega}$ state ($\Omega = 1/2$ or $3/2$). The $X^2\Pi$, $A^2\Pi$ and $4\Sigma^-$ potentials are bound; though the latter has yet to be observed experimentally. All the other states are repulsive, and the lowest ten cross the $A^2\Pi_{3/2}$ component at energies below the $v' = 6$ vibrational level. Using arguments based on electronic configurations, candidate states for the predissociation of the $A^2\Pi_{\Omega}$ state can be selected. Simulations of the predissociation were performed by Fermi golden rule calculations for each vibrational level, using the *ab-initio* repulsive potentials and RKR curves for the $A^2\Pi_{3/2}$ and $A^2\Pi_{1/2}$ state. The vibrational dependence of the predissociation rate in the $A^2\Pi_{3/2}$ component was used to derive the magnitude of the individual couplings with the repulsive potentials. Comparison between the lifetimes of the vibrational levels in the $A^2\Pi_{3/2}$ and $A^2\Pi_{1/2}$ components restricts the principal players in the predissociation to three repulsive states: $1^4\Sigma^+_{\Omega}$, $2^4\Sigma^-_{\Omega}$ and $3^2\Pi_{\Omega}$. Coupling between the $A^2\Pi_{3/2}$ component and the $1^2\Delta$ state is also suspected. A repulsive $2^2\Sigma^+$ state is identified which is likely to be involved in the UV photodissociation of ClO.



DynaSolver: A Software Package for Quantum Reaction Dynamics Calculations with Graphical User Interface

Tong Peng, John Zhang

Department of Chemistry, New York University

Donghui Zhang

Department of Computational Science, National University of Singapore

In recent years computational chemical reaction dynamics has seen significant progresses. Many high-accuracy computational methods have been developed to treat reaction systems of fundamental importance at a very detailed level. However, we have observed that although many sophisticated methods and computational programs are developed by various research groups, it has been very difficult for people who are not very familiar with such programs to use them effectively, due to the lack of user-friendly interfaces. Especially, it is very hard for experimental researchers to take advantage of the newly developed method. As a result, communication and cooperation in this research area are hampered, and many efforts are essentially repeated.

DynaSolver is our attempt to address this problem. It aims at providing a uniform and easy-to-use modern graphical user interface to some of the most sophisticated computational programs for reaction dynamics. Some of its features include:

- Complete Graphical User Interface, complicated computations can be setup and run largely by point-and-click
- Context-sensitive help system
- Visual job controlling, monitoring
- Data visualization, including XY, 3D and contour plot and animation
- PESLIB: DynaSolver includes a modular, dynamic linking library of Potential Energy Surfaces (PESes). Its uniform and informative programming interface allows programs using PESLIB conveniently select and switch PES used. New PES can be added in without requiring programs to be relinked.

A preliminary version(0.3 Beta, 4/99) of DynaSolver is available on the Web:

<http://pl50.chem.nyu.edu/dynasolver>

Computational methods in current version include Time-dependent Wave Packet method for reactive scattering calculations for 3D atom-diatom, 6D diatom-diatom systems and 1D model systems, and tools for PES inspections. PESes coming with the package include about a dozen widely used PESes for 3-atom and 4-atom systems. Given its modular design, new methods can be easily added into the package.

PHASE SPACE OPTIMIZATION OF DIRECT PRODUCT REPRESENTATIONS

Bill Poirier* and J. C. Light,

The James Franck Institute, The University of Chicago

A new method is presented for improving the efficiency of finite basis and discrete variable representation (DVR) calculations of exact quantum mechanical quantities for molecular systems. The method relies upon a quasiclassical phase space analysis, which exploits the similarities between uniformly mixed ensembles of eigenstates and the quasiclassical Thomas-Fermi distribution, in order to generate a nearly optimal direct-product representation for an arbitrary quantum system. The quasiclassical approximation, despite being fairly crude for individual pure states, is exceedingly accurate as the number of points or basis functions becomes large. In essence, an energy cutoff criterion is applied to the Hamiltonian in phase space, which has the effect of providing just the momentum sampling required for each particular position, subject to the constraint of separability. The resultant direct-product basis is thus customized with respect to both the Hamiltonian itself, as well as the maximum energy of interest. For numerical implementations, an iterative, self-consistent-field-like algorithm based on optimal separable basis theory is suggested, typically requiring only a few reduced-dimensional integrals of the potential. Results are obtained for several model Hamiltonians, including the 2D coupled harmonic oscillator and Henon-Heiles systems. In the latter case, errors are reduced by several orders of magnitude, in comparison with an optimized sinc-function DVR of comparable size.

Spectroscopic Constants, Anharmonic Forcefields, and Bound States of HOCl and DOCl

Joseph A. Bentley^(a) and B. Ramachandran^(b)

(a) *Physical Sciences, Delta State University, Cleveland, Mississippi 38733*

(b) *Chemistry, Louisiana Tech University, Ruston, Louisiana 71272*

We report spectroscopic constants and anharmonic force fields for the HOCl and DOCl molecules in the gas phase, calculated from *ab initio* and scaled *ab initio* potential surfaces.¹ The *ab initio* calculations were performed at the CASSCF/MR-CISD levels of theory, using the highly polarized correlation consistent augmented Valence Triple Zeta (cc-pAVTZ) basis sets of Dunning. The multireference analog of the Davidson correction was used to approximate the effect of higher excitations (MR-CISD+Q). The Scaled External Correlation (SEC) method of Brown and Truhlar² was used to extract additional dynamical correlation energy from both the MR-CISD (CI/SEC) and MR-CISD+Q (CI+Q/SEC) energies. The CI, CI+Q, CI/SEC, and the CI+Q/SEC energies up to 20 000 cm⁻¹ above the HOCl minimum were fitted to polynomial expansions and the spectroscopic parameters evaluated in each case. These results are compared to those from the calculations of Koput and Peterson using significantly larger basis sets,³ the "complete basis set limit" results of Skokov *et al.*,⁴ and to available experimental results. It is seen that applying the SEC scaling to CI or CI+Q energies obtained using a moderate basis set (cc-pAVTZ) is a viable alternative to the use of extremely large basis sets.

We also present the results of accurate quantum bound state calculations on these forcefields as well as a global fit to the MRCI+Q/SEC energies. A comparison of these bound state energies with the results of Skokov *et al.*, experimental values, and those from calculations on an earlier *ab initio* surface by Hernandez *et al.*⁵ will also be presented.

References

1. H. Zhang, B. Ramachandran, J. Senekowitsch, and R.E. Wyatt, *J. Mol. Struct. (Theochem)*, in press.
2. F.B. Brown and D.G. Truhlar, *Chem. Phys. Lett.* 117 (1985) 307.
3. J. Koput and K.A. Peterson, *Chem. Phys. Lett.* 283 (1998) 139.
4. S. Skokov, K.A. Peterson, and J.M. Bowman, *J. Chem. Phys.* 109 (1998) 2662.
5. M. Hernandez, C. Redondo, A. Laganá, G.O. de Aspuru, M. Rosi, and A. Sgamellotti, *J. Chem. Phys.* 108 (1996) 2710.

Dynamics of the $O(^3P) + HCl$ reaction: Roles of the $^3A''$ and the $^3A'$ Electronic States C71

B. Ramachandran

Chemistry, Louisiana Tech University, Ruston, Louisiana 71272

The title reaction is studied using quasiclassical trajectory (QCT) propagation¹ and Variational Transition State Theory (VTST)² on potential energy surfaces for the $^3A''$ and the $^3A'$ electronic states. The $^3A''$ surface is based on a recent fit to scaled *ab initio* (MR-CISD+Q) energies and appears to reproduce many of the experimental results for this system better than previous realistic potential surfaces for this system.³ The $^3A'$ state, which is degenerate with the $^3A''$ at collinear and asymptotic geometries but lies above it elsewhere, is modeled by an extended LEPS function. Thermal rate coefficients are computed on these potential energy surfaces using VTST,² and detailed state-to-state cross sections are computed using QCT propagation methods.¹

We present comparisons of calculated (using VTST) and experimental thermal rate coefficients in the range 293–1483 K. The state-resolved product rotational distributions obtained from QCT propagation are compared to the measurements of Zhang *et al.*⁴ QCT differential cross-sections on the two potential energy surfaces and an analysis of the energy disposal will also be presented.

References

1. B. Ramachandran, E. A. Schrader III, J. Senekowitsch, and R.E. Wyatt, *J. Chem. Phys.* (submitted).
2. T.C. Allison, B. Ramachandran, J. Senekowitsch, D.G. Truhlar, and R.E. Wyatt, (work in progress).
3. H. Koizumi, G.C. Schatz, and M.S. Gordon, *J. Chem. Phys.* **95**, 6421 (1991); T.C. Allison, B. Ramachandran, J. Senekowitsch, D.G. Truhlar, and R.E. Wyatt, *J. Mol. Struct. (Theochem)* **454**, 307 (1998).
4. R. Zhang, W.J. van der Zande, M.J. Bronikowski, and R.N. Zare, *ibid.* **94**, 2704 (1991).

Ultraviolet Photodissociation Dynamics of the Hydrogen Halides

C72

Paul M. Regan, Stephen R. Langford, Daniela Ascenzi,
Phillip A. Cook, Andrew J. Orr-Ewing and Michael N.R. Ashfold

School of Chemistry, University of Bristol, England

Hydrogen halide molecules, HX (X = I, Br, Cl), provide an excellent opportunity to investigate systems in which photodissociation may involve more than one electronically excited state. In such cases, the initial excitation can populate more than one Born-Oppenheimer (BO) state, and (non-adiabatic) transitions between BO states may occur as the parent molecule fragments. Both of these processes depend on couplings between potential energy surfaces, and the HX series allows an assessment of the relative influence of the spin-orbit coupling on the photofragmentation process. Experimental measurements of the branching fraction (Γ) between the two accessible spin-orbit product channels [$\text{H} + \text{X}(^2\text{P}_j)$; $J = 3/2, 1/2$], and the angular distribution of products (β), as a function of excitation energy, proves sufficient to understand the photodissociation mechanisms of the different hydrogen halides.

To this end, the technique of H Rydberg atom time-of-flight (HRTOF) spectroscopy has been applied to characterise Γ and β across the first ultraviolet (UV) absorption bands of HI and HBr. The same method has been used to determine Γ for the accessible region ($201 \text{ nm} \leq \lambda \leq 210 \text{ nm}$) of the UV absorption band of HCl. A drastically different wavelength-dependence for Γ is predicted for DCl and we present the first measurements of Γ for DCl photolysis at long wavelengths ($200 \text{ nm} \leq \lambda \leq 220 \text{ nm}$). These results were obtained using resonance enhanced multiphoton ionization with TOF mass spectrometry to detect nascent $\text{Cl}(^2\text{P}_j)$ photofragments. Recent quantum mechanical, *ab initio* calculations of the photodissociation of HCl and DCl [Lambert *et al.* J. Chem. Phys. **108**, 4460] are shown to be in excellent agreement with the experimental determinations of Γ .

SPCTROSCOPY AND DYNAMICS OF ALKALI-METAL ATOMS AND
OLIGOMERS ATTACHED TO LARGE HELIUM CLUSTERS

J. Reho, J.P. Higgins, K.K. Lehmann, and G. Scoles

Princeton University, Princeton, NJ 08544

Helium cluster isolation spectroscopy is an exciting spectroscopic technique in which a very cold (0.4K) supersonic beam of liquid He droplets (each averaging $\sim 10^4$ He atoms) is used as an ultracold matrix for the study of dynamic processes in simple diatomic and triatomic systems. Our studies have focused on alkali-metal atoms and oligomers bound to the He cluster surface which experience desorption after electronic excitation. We have found that Na^*He and K^*He exciplexes are formed on the He cluster surface after optical excitation of Na or K atoms bound to the cluster. Time-correlated single photon counting has been combined with frequency-resolved measurements to form a rather complete picture of the formation and dynamics involved in the exciplex formation and desorption from the cluster surface. These studies have helped us to understand the role played by the cluster in the reaction dynamics of excited dopants and we have successfully modeled the measured formation dynamics for several exciplex systems.

Further, the He cluster selects "high spin" (van der Waals) states of oligomers over their low spin (*i.e.*, chemically bound) counterparts. These high spin dimers and trimers are difficult to probe in the gas phase. In studying such species, we have focused on the alkali-metal trimers and dimers as they represent "simple" hydrogen-like systems. Work focusing on the rates of desorption and unimolecular decomposition of quartet Na trimers and K triplet dimers on He clusters will be presented in which photo-induced fundamental chemical reaction dynamics at ultracold temperatures have been initiated and probed using the He cluster matrix.

Jason C. Robinson^{a,b}, Weizhong Sun^{a,b}, Osman Sorkahbi^b, Fei Qi^b, Arthur G. Suits^b and Daniel M. Neumark^{a,b}

^a*Department of Chemistry, University of California, Berkeley, CA 94720, and*

^b*Chemical Sciences Division, Lawrence Berkeley National Laboratory, Berkeley, CA 94720*

The dissociation dynamics of anisole (methoxybenzene, C₆H₅OCH₃) have been probed by a variety of techniques. As shown in reaction 1, thermal decomposition studies indicate that anisole produces phenoxy and methyl radicals via cleavage of the O-CH₃ bond.^{1,2} The phenoxy radical can further decompose to the cyclopentadienyl radical and CO, as indicated in reaction 2.



Indeed, the production and decomposition of the phenoxy radical deserves investigation, considering that mechanisms for the combustion of species such as benzene and toluene generally involve the phenoxy radical. IRMPD studies at low laser flux produce phenoxy and n-pentyl radicals exclusively, while at higher flux, the decomposition of phenoxy is observed.³ Evidence for a ladder-switching process, wherein the molecule is ionized and dissociated following further absorption, has been observed in fragmentation of the anisole ion following MPI in the 3-5 eV range.⁴ Dissociation of anisole at 193 nm has been previously investigated using flash photolysis⁵ and photofragment translational spectroscopy (PTS).⁶ The flash photolysis studies monitor the production of phenoxy radical, while the PTS studies provide angle-resolved lab-frame velocity distributions and, using forward convolution, the center-of-mass-frame translational energy distributions for the photofragments.

In this experiment, we employ PTS on a crossed molecular beams machine set up for photodissociation studies. The anisole sample is heated and seeded in a continuous supersonic helium beam before crossing at 90° with 193 nm light from an ArF excimer laser. The recoiling photofragments are ionized with tunable synchrotron radiation (5-30 eV) from the Chemical Dynamics Beamline at the LBNL Advanced Light Source.

Previous PTS studies using electron impact ionization indicate a multitude of possible channels are produced from the 193 nm dissociation of anisole.⁶ However, in the current study we observed photofragments for $m/z = 15$, 28, 65, and 93, corresponding to CH₃, CO, C₅H₅, and C₆H₅O respectively. Photofragments for $m/z = 15$, 65, and 93 were ionized using 11 eV radiation, while photofragments for $m/z = 28$ were ionized using 15.5 eV radiation. Scattering angles from 10° to 40° were used for each mass. The velocity distributions indicate that anisole dissociates via several pathways.

¹ Pecullan, M.; Brezinsky, K.; Glassman, I. *J. Phys. Chem. A* **1997**, *101*, 3305-3316.

² Lin, C.-Y.; Lin, M. C. *J. Phys. Chem.* **1986**, *90*, 425-431.

³ Schmoltner, A. M.; Anex, D. S.; Lee, Y. T. *J. Phys. Chem.* **1992**, *96*, 1236-1240.

⁴ Stiller, S.W.; Johnston, M. V. *J. Phys. Chem.* **1985**, *89*, 2717-2719.

⁵ Kajii, Y.; Obi, K. *J. Chem. Phys.* **1987**, *87*, 5059-5063.

⁶ Schmoltner, A. M. Ph.D. Thesis, University of California, Berkeley, 1989.

Dissociative recombination of CO^{2+}

C. P. Safvan, M. J. Jensen, H. B. Pedersen and L. H. Andersen
Institute of Physics and Astronomy, University of Aarhus, DK-8000 Aarhus C, Denmark
 (May 12, 1999)

C75

The dissociative recombination of a doubly charged molecular ion (CO^{2+}) has been studied for the first time using the heavy ion storage ring ASTRID. Absolute cross sections have been measured for the formation of ($\text{C} + \text{O}^+$) and ($\text{C}^+ + \text{O}$) have been measured for electron energies ranging from 0 to 100 eV.

Multiply charged diatomic molecular cations are in general, unstable towards dissociation because their vibrational levels are embedded in the dissociative continuum, and as a consequence they are difficult to study from both experimental and theoretical points of view. Some molecular dications have lifetimes of less than a few μs , but other ions like CO^{2+} have been shown to have long lifetimes (due to barriers against dissociation) that enable us to perform advanced experimental studies in storage rings, which require time for injection, acceleration and data accumulation.

CO^{2+} ions were produced in an electron impact ion source and injected into the storage ring at an energy of 300 keV. They were then accelerated to 5.9 MeV in approximately 2.5 s which allows most of the electronically and vibrationally excited species formed in the ion source to decay. The fast beam of CO^{2+} was then merged with an adiabatically expanded, magnetically confined electron beam, whose energy could be varied.

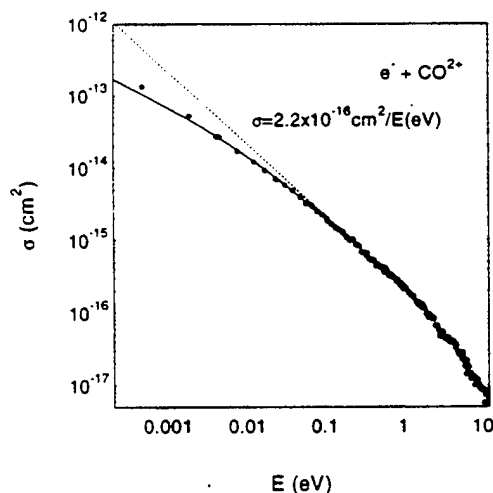
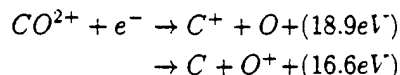


FIG. 1. Absolute cross-sections ($\sigma = \langle v\sigma \rangle / v$) for the formation of either C or O. The dashed curve shows a $1/E$ dependence. Due to the finite energy resolution a deviation from $1/E$ occurs at low energy as calculated by the solid curve which has $kT_{\perp} = 22$ meV and $kT_{\parallel} = 0.5$ meV.

The neutral products formed in the reaction



pass undeflected through the bending magnets of the storage ring and were detected by a large solid state detector.

Figure 1 shows the absolute cross sections for the formation of either C or O, and figure 2 shows the partial rates for the formation of C and O fragments.

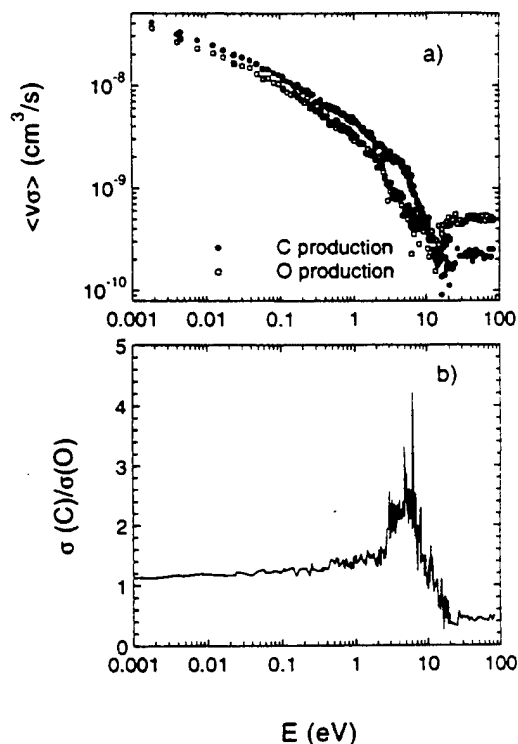


FIG. 2. a) Rate coefficients for the formation of C and O. b) The ratio of C and O formation as a function of the energy.

The total cross section shows a $1/E$ dependence upto ~ 20 eV. The increase in the O production around 2 eV is close to the barrier height of CO^{2+} . The increase in C and O production after 10 eV are due to dissociative excitation processes. Further theoretical efforts are necessary for a quantitative understanding of the processes taking place.

This work has been supported by the Danish National Research Foundation through the Aarhus Center for Atomic Physics (ACAP).

Storage ring studies of the dissociative recombination of He_2^+

C. P. Safvan, M. J. Jensen, L. H. Andersen

Institute of Physics and Astronomy, University of Aarhus, DK-8000, Aarhus C, Denmark

Xavier Urbain

Département de Physique, Université catholique de Louvain, B-1348 Louvain-la-neuve, Belgium

C76

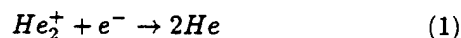
Dissociative recombination of He_2^+ is an important source for the production of excited atomic He. This process has therefore been the subject of intense investigation for the past three decades. The unfavorable positions of the relevant potential energy curves of the He_2^+ and He_2^{2+} predict very low reaction rates for ro-vibrationally cold molecular ions and low energy electrons, in agreement with the presently accepted value of $\alpha \leq 5 \times 10^{-10} \text{cm}^3 \text{s}^{-1}$ [1].

However, large discrepancies between various experimental studies could be explained only qualitatively by invoking highly non-equilibrium distributions of vibrational and rotational states of the molecular ion [2]. Indeed, all the known mechanisms (three-body association, associative ionization etc) for the formation of He_2^+ ions lead to an inverted ro-vibrational distribution [3].

The kinetics of the internal energy relaxation of the molecular ions therefore determines the time evolution of the decaying helium plasma studied in afterglow experiments. In order to follow the relaxation dynamics, and the dependence of the rates of dissociative recombination on the internal energy content of the ion, we have carried out the first ever storage ring study of dissociative recombination of He_2^+ .

He_2^+ ions were produced in a plasma (Nielsen) ion source and injected into the heavy ion storage ring ASTRID at 150 keV. Both $^4\text{He}_2^+$ and $^3\text{He}^4\text{He}^+$ ions were produced and accelerated to 0.726 MeV/amu within the storage ring in approximately 3.65s. In the case of the asymmetric $^3\text{He}^4\text{He}^+$, the ro-vibrationally hot ions produced in the ion source are able to cool down by radiative cascade.

The accelerated beam was then merged with an adiabatically expanded, magnetically confined electron beam in one of the arms of the storage ring. The neutral atoms produced in the reaction



pass undeflected through the bending magnets of the storage ring and are detected by a large (4×6 cm) solid state detector.

Figure 1 shows the cross sections measured for reaction 1 as a function of the electron energy. The cross section for $^4\text{He}_2^+$ decreases monotonously with increasing relative energy and shows no time dependence. For $^3\text{He}^4\text{He}^+$ the cross section exhibits a peak structure around 6 eV which

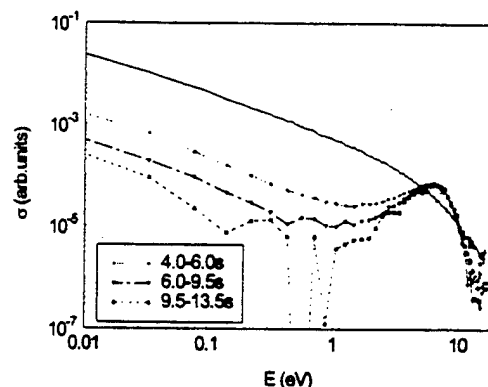


FIG. 1. Cross sections for the dissociative recombination of $^4\text{He}_2^+$ and $^3\text{He}^4\text{He}^+$ as a function of the electron energy. For $^3\text{He}^4\text{He}^+$ the cross sections are shown as measured at various times

is attributed to a direct transition (Franck-Condon) to a manifold of repulsive He_2^{2+} states. This structure remains constant throughout the experimental time window implying full vibrational relaxation. At low energies the cross section for $^3\text{He}^4\text{He}^+$ dramatically decreases with time (as measured from the time of production), indicating that cold He_2^+ molecular ions do not recombine significantly with low energy electrons.

As a consequence of the above observations, we can conclude that the recombination signal at low energies arises almost completely due to rotational excitation of the ground vibrational state of $^3\text{He}^4\text{He}^+$.

This work has been supported by the Danish National Research Foundation through the Aarhus Center for Atomic Physics (ACAP).

- [1] R. Deloche, P. Monchicourt, M. Cheret and F. Lambert *Phys. Rev. A* **13** (1976) 1140
- [2] V. A. Ivanov, N. P. Penkin, and Yu. E. Skoblo *Opt. Spectrosc. (USSR)* **54** (1983) 552
- [3] J. S. Cohen *Phys. Rev. A* **13** (1976) 86

The cross section for $\text{H} + \text{H}_2\text{O}(04)^+ \rightarrow \text{OH} + \text{H}_2$ diverges at zero translational energy

G.C. Schatz¹, G. Wu¹, G. Lendvay², De-Cai Fang³ and L. B. Harding³

¹Department of Chemistry, Northwestern University
Evanston, IL 60208-3113

²Institute of Chemistry, Chemical Research Center,
Hungarian Academy of Sciences
H-1525 Budapest, P.O.Box 17.

³Theoretical Chemistry Group, Argonne National Laboratory
Argonne, IL 60439

The dynamics of the collisions of H atoms with vibrationally excited H_2O were studied using quasiclassical reactive and quantum mechanical nonreactive scattering calculations using a recently developed potential surface from Ochoa and Clary. The trajectory calculations show that this endoergic reaction is activated for water in its vibrational ground state and with one quantum of OH stretch, but excitation by two or more OH stretch quanta results in diverging cross sections at low translational energy. The reactive rate coefficients are therefore very large for these states, being a significant fraction of the gas kinetic rate coefficient. This behavior is qualitatively different from what is obtained using the I5 surface of Isaacson, or the often used WDSE surface which show activated behavior even for excitation as high as $(04)^+$. To verify the accuracy of the OC surface, we have performed high quality *ab initio* calculations for $\text{H} + \text{H}_2\text{O}$, considering geometries in the reagent region that correspond to high OH stretch excitation, and we find that the OC surface is qualitatively correct, although it has too long a range in its attractive tail. New trajectory results based only on the *ab initio* surface produce somewhat smaller cross sections.

Our quantum calculations of the total inelastic rate coefficients for collisions with water initially excited in OH stretch overtone states give values for the OC surface that are comparable in magnitude with the reactive rate coefficients for the same states. This suggests that in the recent measurements by Smith and coworkers of the rate coefficients for total loss of excited water, reaction and vibrational energy transfer are of comparable importance.

Three dimensional wavepacket calculation of the $\text{NH}_3^+ + \text{H}_2 \rightarrow \text{NH}_4^+ + \text{H}$ reaction

C78

François Aguillon and Muriel Sizun
Laboratoire des Collisions Atomiques et Moléculaires, UMR 8625 ,
Bât. 351, Université Paris XI, 91405 Orsay Cedex, France

In the untitled polyatomic chemical reaction Zare et al.⁽¹⁾ have studied experimentally the effect of vibrational excitation of the umbrella mode of ammonium on the dynamics .

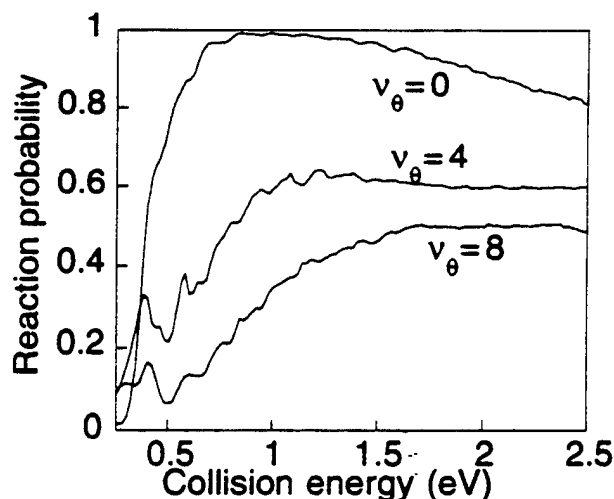
We present here as a first step a reduced dimensionality dynamical study of this reaction. In our model only the degrees of freedom necessarily involved in the reaction are taken into account : the umbrella mode of the ammonium v_θ , the relative distance $\text{NH}_3^+ - \text{H}_2$, the interatomic distance of H_2 . The system stays in C_{3v} symmetry during the whole process. The study becomes equivalent to the study of a collinear exchange of an hydrogen atom between two centers in presence of the active umbrella mode v_θ



where A is an "atom" of mass $= 3m_{\text{H}}$. The product molecule NAH^+ is a constraint molecule NH_4^+ with only two degrees of freedom.

The electronic potential energy surface is determined at the MCSCF level taking into account the constraints described above. The coordinates used for the dynamics are the collinear hyperspherical coordinates (ρ, ϕ) and the umbrella angle θ . The wavefunction is sampled on a grid (ρ, ϕ, θ) . The time dependent Schrödinger equation is solved using the Lanczos method.

Total reaction probabilities as a function of the energy collision ($0 < E_{\text{coll}} < 3\text{eV}$) and the v_θ quantum number are shown below.



State resolved reaction probabilities will be presented at the conference.

ABSTRACT**Fitting Classical Microcanonical Unimolecular Rate Constants to a Modified RRK Expression: Anharmonic and Variational Effects****Kihyung Song***Department of Chemistry, Korea National University of Education, Chongwon,
Chungbuk 363-791 Korea***William L. Hase***Department of Chemistry, Wayne State University, Detroit, Michigan 48202*

Classical RRKM (i.e., microcanonical) rate constants are often calculated for analytic potential energy surfaces (PESs) developed to represent unimolecular decomposition reactions. The values for these rate constants reflect the complete anharmonicities of the PESs. A common procedure is to fit these rate constants with the expression of RRK theory, which is the harmonic limit of classical RRKM theory. These RRK fits often give values for s significantly less than $3n-6(5)$, which are not meaningful, since anharmonic rate constants are represented with a harmonic model. In this work different schemes are proposed for introducing anharmonic and also variational transition state effects into the RRK expression. These modified RRK schemes allow one to fit classical anharmonic RRKM rate constants with $s=3n-6(5)$. The fits give information about the importance of anharmonicity in the unimolecular reactant's density of states and the transition state's sum of states.

Hans U. Stauffer, Ryan Z. Hinrichs, Peter A. Willis, and H. Floyd Davis

Department of Chemistry and Chemical Biology

Cornell University

Ithaca, NY 14853

Reactions of ground state Y atoms with acetylene (C_2H_2) are thought to be initiated either by formation of a π -bonded addition complex (*i.e.*, YC_2H_2) or a C-H insertion complex (*i.e.*, HYC_2H). These initially formed complexes can subsequently decay back to $Y + C_2H_2$ reactants or proceed through competing hydrogen atom loss (forming $YC_2H + H$) and molecular hydrogen elimination (forming $YC_2 + H_2$) channels.

We have studied $Y + C_2H_2$ reactions at several collision energies ($\langle E_{\text{coll}} \rangle = 6\text{--}25$ kcal/mol) under well-defined single collision conditions using a rotatable source crossed molecular beams apparatus. The velocity distributions of the neutral YC_2H and YC_2 reaction products and inelastically scattered Y atom reactants are detected as a function of scattering angle using 157 nm photoionization mass spectrometry. The $YC_2H + H$ channel is only observed to occur above a collision energy threshold of 21.5 ± 2.0 kcal/mol. Since formation of this channel is fully spin-allowed and involves simple Y-H bond fission in the intermediate HYC_2H complex, it is unlikely that any significant potential energy barrier is present in excess of the reaction endoergicity. From detailed studies of the $Y + C_2H_2$ and $Y + C_2D_2$ reactions, we thus conclude that the collision energy threshold observed for the H or D atom loss channel results from the energetic threshold for reaction, yielding $D_0(Y\text{-}CCH) = 110.2 \pm 2.0$ kcal/mol. This dissociation energy is slightly lower than a recent theoretical prediction. At all studied collision energies, the $YC_2 + H_2$ channel as well as decay of long-lived YC_2H_2 or HYC_2H complexes back to reactants is observed. Decay back to reactants is found to transfer 40–50% of the initial relative translational energy into C_2H_2 internal excitation. Product translational energy distributions for the H_2 elimination channel demonstrate that a substantial fraction of excess energy available to $YC_2 + H_2$ products is channeled into relative translational energy. We have also studied analogous H_2 elimination channels in reactions of Zr and Nb with C_2H_2 at $\langle E_{\text{coll}} \rangle = 6.0$ kcal/mol. In contrast to the behavior observed for $YC_2 + H_2$ products, the H_2 elimination product translational energy distributions for these reactions are found to peak near zero kinetic energy. This suggests a significant potential energy barrier exists in the exit channel of the $YC_2 + H_2$ elimination step, whereas no exit channel barrier exists in forming $ZrC_2 + H_2$ and $NbC_2 + H_2$.

**Studies of Inelastic and Reactive Collision Dynamics
Using High Resolution H atom TOF Spectroscopy**

Brian Strazisar, Cheng Lin and Floyd Davis
Department of Chemistry and Chemical Biology
Cornell University
Ithaca NY 14853

We have recently assembled a fixed-source, rotatable detector crossed molecular beams apparatus for studies of inelastic and reactive bimolecular collision dynamics. Although our long-term goal is to study elementary reactions relevant to combustion chemistry, we have begun with a relatively simple system in order to evaluate the sensitivity and resolution of the apparatus: $\text{H} + \text{DCI} \rightarrow \text{HCl} + \text{D}$. Although this reaction has been studied by several groups using a variety of methods, there have been no studies in which both product angular and velocity distributions have been determined.

A fast photolytic beam of H atoms is produced by UV photodissociation of HI. This beam crosses a DCI beam at 90 degrees and the resulting D atom products are detected as a function of scattering angle using the Rydberg tagging method. Current progress on this project will be discussed.

FLUORESCENCE QUANTUM YIELD MEASUREMENT BY CAVITY RING DOWN SPECTROSCOPY : APPLICATION TO CaBr AND CaI RADICALS

J. ROSTAS and G. TAIEB

Laboratoire de Photophysique Moléculaire du CNRS, Bat. 210

Université de Paris Sud 91405 ORSAY France

The $A^2\Pi - X^2\Sigma^+$ and $B^2\Sigma^+ - X^2\Sigma^+$ of CaBr and CaI, and the $D^2\Sigma^+ - X^2\Sigma^+$ transitions have been recorded simultaneously by Laser Induced Fluorescence and by Cavity Ring Down techniques. The radicals are formed in a standard Broida oven, where calcium metallic vapor is reacting with vapor pressure of bromine and iodine liquid organic compounds. Laser excitation is obtained by a Nd-YAG pumped dye laser (15 Hz, 1mJ, 10 ns), detected through a monochromator used as a band pass filter for the LIF, and simultaneously by PM for the CRD signal. Labview programming is used for data acquisition.

The technique is able to give information on both :

- Relaxation of vibrational and rotational levels of the upper electronic state of the transitions
- Non radiative channels like energy transfer or predissociations of the upper electronic state.

Results on the A-X and B-X systems will show that quantitative information can be extracted from analysis of the spectra on the vibrational and rotational relaxation processes. Data on the D-X transition of CaI will put evidence of predissociation of the D state.

Semiclassical Calculation of Cumulative Reaction Probabilities C83

Sophya Garashchuk^a and David J. Tannor^b

^a *Department of Physics, Department of Chemistry & Biochemistry, University of Notre Dame,
Notre Dame, IN 46556, USA*

^b *Department of Chemical Physics, Weizmann Institute of Science, Rehovot, 76100, Israel
(May 28, 1999)*

Abstract

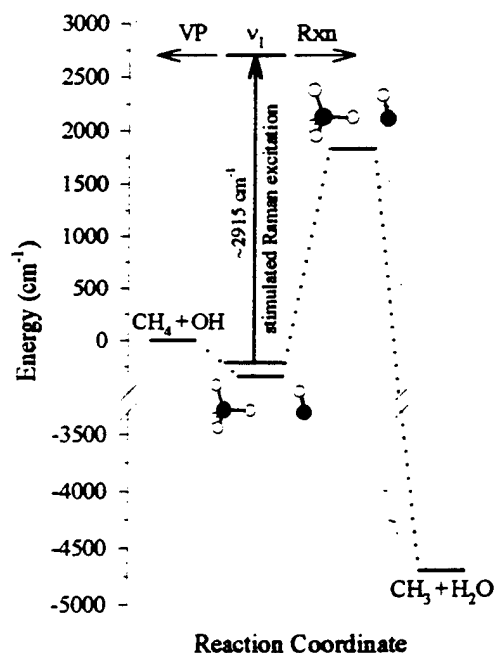
Calculation of chemical reaction rates lies at the very core of theoretical chemistry. The essential dynamical quantity which determines the reaction rate is the energy-dependent cumulative reaction probability, $N(E)$, whose Boltzmann average gives the thermal rate constant, $k(T)$. Converged quantum mechanical calculations of $N(E)$ remain a challenge even for 3- and 4-atom systems, and a longstanding goal of theoreticians has been to calculate $N(E)$ accurately and efficiently using semiclassical methods. Here we present a variety of methods for achieving this goal, by combining semiclassical initial value propagation methods with a reactant-product wavepacket correlation function approach to reactive scattering. The correlation function approach, originally developed for transitions between asymptotic internal states of reactants and products, is here reformulated using wavepackets in an arbitrary basis, so that $N(E)$ can be calculated entirely from trajectory dynamics in the vicinity of the transition state. This is analogous to the approaches pioneered by Miller for the quantum calculation of $N(E)$, and leads to a reduction in the number of trajectories and the propagation time. Numerical examples are presented for both one-dimensional test problems and for the collinear hydrogen exchange reaction.

Vibrational and Electronic Excitation of CH₄-OH Reactant Complexes

Maria Tsiouris, Martyn D. Wheeler, and Marsha I. Lester
 Department of Chemistry, University of Pennsylvania
 Philadelphia, PA 19104-6323

Abstract

Weakly bound complexes composed of the CH₄ and OH reactants have been stabilized in a shallow well in the entrance channel to the CH₄ + OH → CH₃ + H₂O reaction, notwithstanding the low activation barrier to reaction. The CH₄-OH reactant complexes have been identified by electronic spectroscopy in the OH A²Σ⁺ - X²Π (1,0) and (0,0) spectral regions as well as by stimulated Raman excitation in the vicinity of the symmetric stretch (ν₁) of CH₄. The spectroscopic studies enable the CH₄ + OH interaction potential to be probed with unprecedented detail. The electronic and/or vibrational excitation of CH₄-OH can also induce inelastic and/or reactive scattering dynamics between the partners under the restricted geometry conditions imposed by the complex. Stimulated Raman excitation of the C-H stretching mode supplies enough energy to surmount the activation barrier and initiate reaction or, alternatively, to break the weak intermolecular bond (see figure). Vibrational activation of the reactive C-H stretching mode is expected to significantly enhance reactivity by driving the reactants towards the transition state. Ongoing experiments are exploring the inelastic and/or reactive scattering dynamics upon vibrational activation of various modes in the CH₄-OH reactant complexes.



Eigenstates as a Probe of Gas-Surface Reactivity

L. B. F. Juurlink, R. R. Smith, P. R. McCabe, C. L. DiCologero, and A. L. Utz

Department of Chemistry and

W.M. Keck Foundation Laboratory for Materials Chemistry

Tufts University

Medford, MA 02155

Eigenstate-resolved studies of gas-surface reactivity provide a detailed view into the dynamics of direct dissociative chemisorption. Such experiments permit a direct comparison of how energy deposited into different coordinates affects reactivity, and they shed light on the key features of the potential energy surface governing gas-surface reactivity. Probing the reactivity of individual eigenstates is particularly important in the study of polyatomic reagents, where different internal vibrational modes may differ significantly in their ability to couple to the reaction coordinate and promote reactivity.

We have recently developed a new experimental technique that uses infrared laser excitation of molecules in a supersonic molecular beam to select the reagent's vibrational and rotational quantum state. The state-selected molecules then impinge on a well-characterized surface housed in an ultrahigh vacuum chamber, and Auger electron spectroscopy quantifies the extent of dissociative chemisorption.

Our initial studies focus on the reactivity of methane on the Ni(100) surface. We find that methane molecules excited to the $v=1$ level of the antisymmetric C-H stretching vibration, ν_3 , are up to 1600 times more reactive than are molecules in the $v=0$ level. Over a translational energy range from 16 to 68 kJ/mol, the sticking probability for these molecules increases from 3×10^{-5} to 2×10^{-2} . While this reactivity enhancement is significant, a comparison with the results for a thermal distribution of vibrational states indicates that ν_3 does not dominate the reactivity of a thermal distribution of vibrational states. Our experiments also permit a direct comparison of how vibrational and translational energy promote dissociative chemisorption. We find that excitation of ν_3 is less effective than an equivalent amount of translational energy directed along the surface normal.

Marc C. van Hemert and Rob van Harreveldt.

Leiden Institute of Chemistry, Gorlaeus Laboratories, Leiden University
PO Box 9502, 2300RA Leiden, Netherlands.

The lowest triplet state of water has never been observed directly in absorption experiments. Early electron impact experiments put the transition around 7.2 eV, approximately 0.25 eV below the $\tilde{\text{A}}^1\text{B}_1$ band maximum. Recently transitions to this triplet state have been invoked by Schröder et al. ⁽¹⁾ to interpret the order of magnitude difference between experimental ⁽²⁾ (12) and theoretical (>100) OD/OH branching ratio for HOD at the very low excitation energy corresponding to 193 nm. In this poster we present the completely ab initio calculation of the triplet absorption spectra of H_2O and its isotopomers and of the branching ratio.

First, new 3D potential energy surfaces were calculated for the ground state X^1A_1 and for the excited $\tilde{\text{A}}^1\text{B}_1$, B^1A_1 , D^1A_1 and $\tilde{\text{a}}^3\text{B}_1$ states. The Wuppertal-Bonn MRDCI code was used for this purpose. Further, the transition dipole moment functions for the X to $\tilde{\text{A}}$, X to B and X to D transitions were determined. The $\tilde{\text{A}}$ state surface was slightly adjusted such that the numerous experimental direct and vibrationally mediated photodissociation spectra were reproduced quantitatively. The adjustment incorporates a scaling that depends exponentially on the bond lengths. Also a solid shift (0.19 eV) of the ab initio potential to higher energies is made. This shift is necessary because electronic structure calculations always underestimate the ground state dissociation energy. The $\tilde{\text{a}}$ state surface was adjusted with the same parameters as used for the $\tilde{\text{A}}$ state. At the ground state equilibrium geometry the energy gap between the singlet and triplet surfaces is 0.4 eV, slightly larger than the value of 0.25 eV reported by Schröder et al.

In order to determine the amount of triplet character in the ground state and the amount of singlet character in the $\tilde{\text{a}}$ excited state, spin-orbit coupling matrix elements were calculated at a series of geometries at and around the ground state equilibrium geometry. For the ground state only interaction with the $\tilde{\text{a}}^3\text{B}_1$ state was considered, while for the $\tilde{\text{a}}^3\text{B}_1$ state also interaction with the nearby B^1A_1 and D^1A_1 states was taken into account. The spin-orbit coupling was calculated from the MRDCI wave functions with the full Breit-Pauli Hamiltonian. The effective transition dipole was derived in a first order perturbation theory approximation from the spin-orbit couplings, the X to B and X to D transition dipoles and the X and $\tilde{\text{a}}$ permanent dipoles, and the energy gaps.

The potential energy surfaces and the (effective) transition dipole moments were used in a standard 3D wave packet program ⁽³⁾ to obtain fragment resolved spectra in absolute units, both for the $\tilde{\text{A}}$ and for the $\tilde{\text{a}}$ state of HOD. In the poster we will show the spectra and the resulting OD/OH branching ratios over a large wavelength range. At 193 nm our ab initio value is 20, close to the experimental value of 12 +/- 8. Similar calculations were performed for a comparison of the H_2O and D_2O photodissociation cross sections. At 193 nm we find a cross section ratio of 80, also close to the experimental value of 64 +/- 10. The very recent, and sometimes surprising, experimental results for far off resonance photodissociation in vibrationally excited H_2O ⁽⁴⁾ will be discussed as well.

1. T. Schröder, R. Schinke, M. Ehara and K. Yamashita, J. Chem. Phys. 109, 6641 (1998).
2. D.F. Plusquellic, O. Votava and D.J. Nesbitt, J. Chem. Phys. 109, 6631 (1998).
3. G.J. Kroes, E.F. van Dishoeck, R.A. Beärda and M.C. van Hemert, J. Chem. Phys. 99, 228 (1993).
4. O. Votava, D.F. Plusquellic and D.J. Nesbitt, J. Chem. Phys. 109, 6631 (1998).

Quantum Dynamics for Polyatomic Reaction on Surface

Dunyou Wang and John Z.H. Zhang

Department of Chemistry, New York University, New York, NY 10003

ABSTRACT

We present a quantum dynamical model for reaction of a polyatomic molecule on a rigid surface. In this model, the reacting molecule is treated as a semi-rigid vibrating rotor target (SVRT). The exact SVRT model for polyatomic reaction on a rigid surface is completely described by seven degrees of freedom which is realistic for rigorous numerical computation. In this poster, We use a more accurate adiabatic SVRT (ASVRT) reaction model, in which the change of the internal structure as a function of the reactive coordinate is treated as adiabatically. The time-dependent wavepacket method has been used for numerical computation of the ASVRT model for H_2O on metal surface.

Ab Initio Quantum Dynamics Study of Reaction $\text{CH}_3 + \text{H}_2$
 $\longrightarrow \text{CH}_4 + \text{H}$

Ming L. Wang and John Z.H. Zhang

Department of Chemistry, New York University, New York, NY 10003, USA

*The Center for Theoretical and Computational Chemistry, Dalian Institute of Chemical Physics,
Chinese Academy of Science, Dalian, 116023, China*

(May 6, 1999)

Abstract

We present a detailed *ab initio* quantum dynamics study of the title reaction by applying a previously proposed SOFA fitting of potential energy surface (PES) from calculated *ab initio* points. To make the quantum dynamics calculation tractable, we treat the CH_3 radical as a pseudo atom which reduces the reaction system to a three-dimension atom-diatom system. *Ab initio* calculations at the QCISD/6-311g(d,p) level are carried out to generate potential energies at discrete points. These discrete points are used to generate potential energies at quadrature points that are used in dynamics calculation through sequential one dimension fitting approach (SOFA). Time-dependent quantum wavepacket method is employed to carry out dynamics calculation to yield reaction probabilities. The calculated cross section and rate constants are scaled by a geometry factor related to the effective reaction cone in order to take into account the the rotational effect of CH_3 . It is shown that the scaled rate constants are in good agreement with experimental results at a wide range of temperature with an effective cone angle of 26° .

**Multiphoton ionization and *ab initio* calculation studies of the
hydrogen-bonded clusters $C_4H_5N-(H_2O)_n$**

Xiuyan WANG , Yue LI, Xianghong LIU, Nanquan LOU

*State Key Laboratory of Molecular Reaction Dynamics, Dalian Institute of Chemical Physics,
Chinese Academy of Sciences, Dalian 116023, P.R.China*

In this paper the multiphoton ionization of the hydrogen-bonded clusters $C_4H_5N-(H_2O)_n$ was studied using a time-of-flight mass spectrometer at 355nm and 532nm laser wavelengths. At both wavelengths, a series of $C_4H_5N-(H_2O)_n^+$ and the protonated products $C_4H_5N-(H_2O)_nH^+$ were obtained. The two-photon resonance ionization processes at 355nm make the ion intensities of pyrrole and the clusters obviously more abundant than at 532nm. *Ab initio* calculations show that in the protonated products, the proton prefers to link with α -C of pyrrole rather than with the N atom. The production of the protonated products needs an intracuster proton transfer reaction. The protonated products obtained at 532nm are suggested to arise from an intracuster penning ionization or a charge transfer process. The abnormally higher intensities of photofragments $C_4H_4N-(H_2O)_n^+ (n \geq 1)$ than $C_4H_4N^+$ are attributed to the stabilization effects of the cluster formation on the dissociation products $C_4H_4N^+$ of the pyrrole molecule.

Molecular Beam Studies of $O(^1D) + N_2O \rightarrow 2 NO$

C90

Michael S. Westley, Patrick J. Pisano and Paul L. Houston
Department of Chemistry and Chemical Biology
Cornell University

The reaction $O(^1D) + N_2O \rightarrow 2 NO$ is thought to be the primary source of stratospheric NO and also important in combustion. The exothermicity of the reaction (-341 kJ/mol) results in the excitation of a large manifold of the rovibrational states of the products. We are studying this reaction using crossed molecular beams with REMPI/TOFMS detection, with the capability to image the angular dependence of the state selected NO products. Currently, integrated state selected signal has been observed using both molecular beams. A simpler experiment, where the reaction occurs at the exit of one of the nozzles and the products are then expanded in a molecular beam and detected downstream, has allowed measurement of the vibrational populations of the product NO. These measurements will provide useful information on the dynamics of the reaction as well as indicating the product states with the highest population for detection and possible imaging in the crossed beam configuration.

MODE-SELECTIVE DECAY DYNAMICS OF ENTRANCE CHANNEL COMPLEXES

MARTYN D. WHEELER, MICHAEL W. TODD, DAVID T. ANDERSON,
and MARSHA I. LESTER

Department of Chemistry, University of Pennsylvania, Philadelphia, PA 19104-6323, USA

PAUL J. KRAUSE and DAVID C. CLARY

Department of Chemistry, University College London, London, WC1H 0AJ, UK

The OH + H₂ reaction provides a prototypical example of a hydrogen abstraction reaction involving hydroxyl radicals to form water in atmospheric and combustion environments. The work presented here describes a novel approach to studying this fundamental reaction system by initiating reactive or inelastic scattering events under restricted orientation conditions imposed by the formation of a molecular cluster. Weakly-bound complexes composed of *ortho*-H₂ and OH have been stabilized in a shallow well in the entrance channel to reaction. Infrared or stimulated Raman excitation of either the OH or H₂ partners provides sufficient energy to surmount the low barrier to reaction or, alternatively, break the weak in the intermolecular bond, thereby providing access to both inelastic and reactive scattering dynamics. The ensuing mode-selected decay dynamics have been monitored in both time- and frequency-resolved experiments by detecting inelastically scattered OH X ²Π (v, j) products arising from vibrational predissociation. The experimental results reveal substantial differences in the lifetimes of vibrationally excited *o*-H₂-OH as well as OH X ²Π (v, j) product distributions. These results illustrate the qualitatively distinct dynamics subsequent to excitation of different intramolecular modes of *o*-H₂-OH. The vibrational predissociation dynamics have also been calculated in full dimensionality with a time-dependent wavepacket technique using a potential energy surface derived from high quality *ab initio* calculations. A direct comparison of the experimental results and theoretical calculations is presented. In addition, the likelihood of inducing chemical reactions upon vibrational activation of *o*-H₂-OH will be discussed.

HIGH-RESOLUTION INFRARED SPECTROSCOPY OF Ar-OH

MARTYN D. WHEELER, R. TIMOTHY BONN, and MARSHA I. LESTER

Department of Chemistry, University of Pennsylvania, Philadelphia, PA 19104-6323. USA

An infrared-ultraviolet (IR-UV) double-resonance scheme has been employed to probe the vibrational spectroscopy of Ar-OH in the region of the OH fundamental stretch ($2.8\ \mu\text{m}$). Using an optical parametric oscillator Ar-OH is prepared with one quantum of OH stretch ($\nu_{\text{OH}} = 1$), while a UV laser promotes Ar-OH ($\nu_{\text{OH}} = 1$) to the excited *A* electronic state resulting in laser-induced fluorescence signal. Transitions have been observed from ground state Ar-OH ($\nu_{\text{OH}} = 0$, $K=3/2$) to the pure OH fundamental stretch ($\nu_{\text{OH}} = 1$, $K=3/2$) and the first combination band ($\nu_{\text{OH}} = 1$, $K=1/2$) involving intermolecular bending excitation. The pure fundamental stretching band gives rise to PQR rotational structure typical of a parallel band of a molecule containing unquenched orbital angular momenta. The OH fundamental stretch of Ar-OH in its ground electronic state is shifted $0.64\ \text{cm}^{-1}$ to lower energy from that in free OH. The combination band shows a rather more complicated rotational band structure due to the large splitting between rotational levels with the same total angular momentum and opposite parity in the excited intermolecular bending state. The experimental determination of the parity splitting provides a direct measure of the splitting between the *A'* and *A''* potential energy surfaces in the non-linear configurations accessed by the excited intermolecular bend. The experimental results are found to be in near quantitative agreement with recent bound state calculations on a new high-level *ab initio* potential energy surface. A direct comparison of the observed energy level structure of the $K=1/2$ state with these calculations will be presented.

Ion Imaging and Wave Packet Studies of the Photodissociation Dynamics of IBr.

E. Wrede, A. Brown, A.J. Orr-Ewing, and M.N.R. Ashfold

School of Chemistry, University of Bristol. U.K.

The visible and UV spectroscopy as well as photochemistry of diatomic interhalogens (such as BrCl, Br₂, or IBr) is highly complex as a large number of excited electronic states are involved. In particular IBr has attracted special interest, because the avoided crossing between its $B(^3\Pi_{0+})$ and $B'(0^+)$ excited states is of *intermediate* strength, *i.e.* neither an adiabatic nor diabatic picture of these states is suitable. Whereas recent femtosecond pump-probe experiments and corresponding wave packet calculations concentrate on the nonadiabatic dynamics of the avoided crossing the aim of this work is an overall picture of the IBr photolysis including all the excited states accessible with a single photon in the visible and near-UV wavelength region.

Experimentally, the photofragment ion imaging technique was used to investigate IBr photolysis in the wavelength range from 600 nm down to 267 nm. Angular and velocity distributions of both the Br and I fragments either in their $X(^2P_{3/2})$ ground or $X(^2P_{1/2})$ spin-orbit excited state were measured. The extracted anisotropy parameters β and branching fractions $X^*/(X+X^*)$ provide quantitative information about the excitation to and the nonadiabatic couplings between the different states involved in the photolysis process.

In order to describe the photodissociation dynamics theoretically, wave packet calculations have just been carried out on the multiple, coupled potentials, the results of which will be presented at the conference for comparison with the experiment. It turns out that the IBr potential curves are not well known in particular in the unbound region of interest for this study. Fortunately, the additional experimental information available from the ion imaging study could be used to improve the repulsive walls of the low lying excited states.

The Hydrogen Exchange Reaction: Experimental and Theoretical Cross Sections and the Influence of the Geometrical Phase Effect.

B. Niederjohann, E. Wrede^{*}, K. Seekamp-Rahn[†], L. Schnieder[‡],
K.H. Welge

Fakultät für Physik, Universität Bielefeld, Germany

F.J. Aoiz, L. Bañares, J.F. Castillo, B. Martínez-Haya
Departamento de Química Física, Universidad Complutense, Madrid, Spain

V.J. Herrero

Instituto de Estructura de la Materia (CSIC), Madrid, Spain

The hydrogen exchange reaction has now been studied over seven decades and still serves as a model system to develop theoretical methods to calculate the dynamics of chemical reactions. In recent years high resolution experimental results as well as fully converged 3-dimensional quantal calculations have become available for this prototype chemical reaction, both of them allowing a very detailed comparison between experiment and theory.

The $\text{H} + \text{D}_2(v = 0, j = 0) \rightarrow \text{HD}(v', j') + \text{D}$ isotopic variant has been investigated experimentally by determining rovibronically state resolved differential cross sections for a wide range of collision energies: from near the threshold up to slightly above the minimum energy for the conical intersection of the two lowest potential energy surfaces ($0.52 \leq E_{\text{col}} \leq 2.67$ eV). In comparison with theoretical results the high resolution data obtained in a crossed molecular beam experiment enabled the assessment of both the theoretical methods to calculate the dynamics and the underlying potential energy surfaces used.

The possible influence of the first excited electronic state on the dynamics has been discussed intensively in recent years. In particular the Geometric Phase effect due to the conical intersection has been predicted to become important even at relatively low energies, although there is no real experimental evidence so far, that this is indeed the case. Furthermore, the high resolution experimental data can be very well reproduced by quantum calculations *not* including the Geometric Phase effect. A detailed quasiclassical trajectory study was carried out to estimate the contribution of this effect to the cross sections.

^{*}present address: *School of Chemistry, University of Bristol, U.K.*

[†]present address: *Medizinische Fakultät, Universität Tübingen, Germany*

[‡]present address: *Zentrum für medizinische Forschung, Tübingen, Germany*

Quantum 3D calculations of intermolecular vibrations of
tetracene-Rg and pentacene-Rg (Rg = He, Ar) dimers

Minzhong Xu and Zlatko Bačić

Department of Chemistry, New York University, New York, NY 10003, U.S.A.

We have performed accurate calculations of the van de Waals (vdW) vibrational levels of tetracene-Rg and pentacene-Rg (Rg = He, Ar) dimers, using the previously developed quantum 3D DVR methodology.¹ The intermolecular potential energy surfaces of these complexes were modeled by a sum of atom-atom Lennard-Jones pair potentials, while tetracene and pentacene are treated as rigid. The IPESs of tetracene-Rg and pentacene-Rg have multiple minima along the long molecular axis; 3 and 4 minima for tetracene-He and pentacene-He, respectively, and 2 and 3 minima for tetracene-Ar and pentacene-Ar, respectively. These corrugated potential landscapes give rise to intricate vibration-tunneling dynamics, which differs qualitatively from that of the related 2,3-dimethylnaphthalene-Rg dimers (Rg = He, Ar) studied previously,^{2,3} whose IPESs exhibit a single minimum above (and below) the aromatic ring plane. The wave functions of the excited eigenstates of the vdW dimers involving He are extensively delocalized over the multiple potential minima, resulting in appreciable tunneling splittings. Comparison is made to the experimental data available for these dimers.

- [1] M. Mandziuk and Z. Bačić, *J. Chem. Phys.* **98**, 7165 (1993); [2] A. Bach, S. Leutwyler, D. Sabo, and Z. Bačić, *J. Chem. Phys.* **107**, 8781 (1997); [3] M. Mandziuk, Z. Bačić, T. Droz, and S. Leutwyler, *J. Chem. Phys.* **100**, 52 (1994).

Electron solvation dynamics in $\Gamma(\text{Xe})_n$ and $\Gamma(\text{H}_2\text{O})_n$ using femtosecond photoelectron spectroscopy

C96

Martin T. Zanni, C. Frischkorn, Alison V. Davis, and Daniel M. Neumark

Department of Chemistry, University of California, Berkeley, California, 94720

L. Lehr and R. Weinkauff

Institut für Physikalische und Theoretische Chemie, Technische Universität München, Germany

Anions solvated in polar solutions typically exhibit distinct bands in the ultraviolet that are denoted charge-transfer-to-solvent bands (CTTS). These states involve detachment of the solute anion to nearby solvent molecules and serve as precursor states to fully solvated electrons. We have investigated the dynamics of the CTTS states in $\Gamma(\text{Xe})_n$ and $\Gamma(\text{H}_2\text{O})_n$ clusters in an effort to learn about the size-dependent properties of these states.

For excitation into the $^2\text{P}_{1/2}$ CTTS state in $\Gamma(\text{Xe})_{11}$, we find a lifetime of 547 fs that increases to 1142 fs in $\Gamma(\text{Xe})_{38}$. For the smallest cluster studied here, $n=6$, the $^2\text{P}_{3/2}$ CTTS state has a lifetime greater than 225 ps. Therefore, spin-orbit autodetachment is responsible for the decay of the upper state. No evidence for solvent reorganization is observed in the photoelectron spectra, which indicates that the cluster geometries of the initial $\Gamma(\text{Xe})_n$ and CTTS states are similar.

In contrast, excitation of the $^2\text{P}_{3/2}$ CTTS state in $\Gamma(\text{H}_2\text{O})_n$ clusters exhibits non-adiabatic dynamics and solvent reorganization. For $\Gamma(\text{D}_2\text{O})_4$, the electron is excited into a dipole bound state where the electron resides mostly on the outside of the water cluster. For $n=5$ and larger, however, the solvent reorganizes to stabilize the electron inside the cluster. Thus $n=5$ represents the smallest cluster analog of electron solvation.

Kesheng Xu^a and Jingsong Zhang^{a,b,*}^aDepartment of Chemistry and ^bAir Pollution Research Center
University of California, Riverside, CA 92521-0403

ABSTRACT

A vinyl radical (C_2H_3) beam is produced by photolysis of vinyl bromide precursors in a He mixture with 193-nm ArF excimer laser radiation and subsequent supersonic expansion and cooling. Photodissociation of vinyl radical via its first excited \tilde{A}^2A'' state is studied by using high- n Rydberg-atom time-of-flight (HRTOF) technique. TOF spectra of the H atom product have been measured at both 366.2 and 327.2 nm photolysis wavelengths, and center-of-mass (CM) translational energy distributions of the H atom and acetylene photofragments are derived. Average CM product translational energy is small; two extensive and highly inverted vibrational progressions of the C_2H_2 product (most likely acetylene C-C stretch and its combination band with C-H bend, with vibrational quanta up to 7) are identified. By utilizing the polarized photolysis radiation at 366.2 and 327.2 nm, anisotropic and energy-dependent angular distributions of the H-atom product have been observed, indicating a short excited \tilde{A}^2A'' state lifetime (less than a rotational period) at these excitation wavelengths. Implication of the C_2H_2 vibrational state distribution and photodissociation dynamics of C_2H_3 in the first excited \tilde{A}^2A'' state are discussed.

* e-mail: jszhang@ucrcl.ucr.edu

Rotationally inelastic scattering of CO

Ao Lin, Antonis P. Tsakotellis,
Stiliana Antonova, Paresh Ray,
and George C. McBane

Department of Chemistry
The Ohio State University
Columbus, OH 43210

Abstract

Rotationally inelastic scattering of CO with several atomic and molecular partners has been studied in crossed supersonic beams with state-selective detection. Experiments have been done that determine integral and differential cross sections and alignment moments. Comparisons with quantum scattering calculations and discussions of qualitative classical (polarization, rotational rainbows) and quantum (interference structure) effects will be presented.

Gas phase deep-ultraviolet photochemistry of phenylacetylene using photofragment translational spectroscopy

Osman Sorkhabi, Fei Qi, Abbas H. Rizvi, and Arthur G. Suits

Chemical Sciences Division, Lawrence Berkeley National Laboratory, University of California, Berkeley, CA 94720

Abstract: The gas phase ultraviolet photochemistry of phenylacetylene was studied at 193 nm. The only primary fragments characterized were for m/e 26 and m/e 76. The m/e 26 fragment has been identified as acetylene and m/e as either (E)-3-Hexene-1,5-diyne or (Z)-3-Hexene-1,5-diyne. Some of the m/e 76 molecules were found to decompose to 1,3,5-hexatriyne and molecular hydrogen. From the energetic threshold for this process, a heat of formation of 160 ± 3 kcal mol⁻¹ was calculated for 1,3,5-hexatriyne. Angular distribution measurements yielded an isotropic distribution for this channel, thus, suggesting that this process occurs on a time scale longer than several periods of rotation. An exhaustive search yielded no evidence for the radical channel - phenyl + ethynyl and the atomic hydrogen elimination channel.

***Photodissociation Dynamics of H₂O: Dynamical Interference
and Resonance***

D. W. Hwang, X. F. Yang, S. Harich, J. J. Lin and X. Yang

Institute of Atomic and Molecular Sciences, Academia Sinica, Taipei, Taiwan

and

R. N. Dixon

School of Chemistry, University of Bristol, Bristol, England

Abstract

Photodissociation of H₂O at 121 and 157 nm has been studied using the H atom Rydberg tagging time-of-flight technique. Vibrational and rotational state distributions have been measured for the OH product from H₂O photodissociation at these two excitation wavelengths. Experimental results indicate that H₂O photodissociation at 121 nm mainly produces highly rotationally excited OH in the ground electronic state with little vibrational excitation, while H₂O photodissociation produces vibrationally excited OH product with little rotational excitation. Dynamical inference effect In addition, dissociation channel to the OH A²Σ state and the triple dissociation process have been clearly observed. Very interesting dynamical resonance phenomenon has also been observed in the HOD photodissociation at 121.6 nm. The photodissociation studies at 157 nm indicate that the relative populations for the high vibrationally excited OH(*v* ≥ 2) products from 157 nm excitation measured by the LIF technique are significantly underestimated, suggesting that LIF as a technique to quantitatively measure vibrational distributions of reaction product OH is seriously flawed. The experimental results presented here for H₂O photodissociation give us an excellent example for unimolecular dissociation, which also provide us a solid test ground for a quantitative picture of this important system.

State-to-state Dynamics of Atom + Polyatom Abstraction Reactions.

A.Srivastava, C.A.Picconatto and J.J.Valentini

Department of Chemistry, Columbia University, New York, New York 10027

Abstract

We report measurements of the H_2 product quantum state distributions and absolute cross section for the $H + C_6H_{12} \rightarrow H_2 (v', J')$ reaction at a collision energy of 1.6 eV using 2+1 REMPI spectroscopy. Comparison with state-to-state dynamics results previously obtained for the kinematically and energetically similar $H + CD_4 / C_2H_6 / C_3H_8 \rightarrow H_2 (v', J')$ is presented.

Photoinduced Reactions in $(\text{HCl})_2$ *C.A. Picconatto, A. Srivastava and J.J. Valentini*

Department of Chemistry, Columbia University, New York, New York 10027

Abstract

We have performed experiments measuring the state distribution of HCl photofragments produced from the photolysis of HCl dimer. We form the clusters by supersonic expansion through a pulsed nozzle of a 10% HCl in Ar mixture. Great care is taken in characterizing the performance of the expansion to assure the signal results from the dimer. An excimer laser photolyzes the reactants with a 193 nm pulse and the products (HCl) are probed at short time delay via resonance enhanced multi-photon ionization (REMPI). The experiments are performed under collisionless conditions.

We find the distribution to be extremely cold with very little transfer of energy to either rotation or vibration of the HCl molecule. Signal from $v'=1$ is at the detection limit and linear surprisal analysis of the ground state distribution yields an extremely large rotational parameter of $\Theta_r = 110(20)$.

AUTHOR INDEX FOR INVITED AND CONTRIBUTED TALKS

(I stands for Invited Talks and C stands for Contributed Talks)

<u>NAME</u>	<u>POSTER#</u>
Aguillon, François	C26, C78
Alexander, Andrew J.	C39
Amaya-Tapia, A.	C1
Amitay, Zohar	I13
Andersen, L.H.	C75, C76
Anderson, David T.	C91
Andersson, Mats	C2
Antonova, Stiliana	C98
Aoiz, F.J.	C94
Ascenzi, Daniela	C72
Ashfold, M.N.R.	C14, C15, C72, C93
Ayers, James D.	C6
Babikov, D.	C26
Bacic, Zlatko	I1, C17, C95
Bakker, Bernard L.G.	C3
Balakrishnan, N.	C4
Balint-Kurti, Gabriel	I2
Bañares, L.	C94
Bar, I.	C5
Bean, Brian D.	C6
Bentley, Joseph A.	C70
Bernstein, L.S.	C7
Bingemann, Dieter	C40
Bise, Ryan T.	C13
Blackmon, Bradley W.	C64
Bonn, R. Timothy	C92

Bosio, Sylvie B.M.	C48
Braunstein, M.	C7
Brenner, Jerrell	C51
Brouard, M.	C8
Brown, Alexander	I2, C93
Budenzholzer, Frank E.	C9
Butler, Laurie J.	I3, C60, C62
Campbell, Mark L.	C10
Castillo, J.F.	C94
Castle, K.J.	C11, C41
Chandler, David W.	C53
Chapman, William B.	C64
Cheatum, Christopher M.	C12
Chen, I-Chia	C32
Chen, X.	C5
Chen, Yaling	I11
Choi, Hyeon	C13
Clary, David C.	C91
Clements, T.G.	C54
Continetti, R.E.	C54
Cook, Phillip A.	C14, C15, C72
Crim, F. Fleming	C12, C40
Curry, Stephen L.	C60, C62
Dagdigian, Paul J.	I4, C16, C46
Dai, Hai-Lung	C28, C51
Dai, JiXin	C17
Dalgarno, A.	C4
Davis, Alison V.	C96
Davis, Floyd	C18, C31, C80, C81
DiCologero, C.L.	C85

Dimpfl, W.	C7
Dobeck, L.M.	C43
Dixon, R.N.	C100
Dowd, Thomas J.	C38
Drukker, Karen	I7
Duchovic, Ronald J.	C19
Duff, J.W.	C7
Dylewski, Scott M.	C20
Elran, Yosef	C37
Fang, De-Cai	C77
Farrar, James M.	C21
Fernández-Alonso, Félix	C6
Fiss, Jeanette A.	I6
Fletcher, T. Rick	C22
Flynn, George W.	C36
Fockenberg, Christopher	C23
Forde, Nancy R.	C60
Forrey, R.C.	C4
Forsythe, Kelsey M.	C24
Frischkorn, C.	C96
Fukuzawa, Kaori	C59
Füsti-Molnár, László	I2
Gao, Wen-Bin	C27
Garashchuk, Sophya	C83
Garrison, Barbara	I32
Gatenby, S.D.	C8
Geiser, Joseph D.	C20
Gerber, Gustav	I5
Gislason, Eric A.	C25, C26
Goldfield, Evelyn M.	C65

Gordon, Robert J.	I6
Gray, Stephen K.	I7, C24
Green, Karen	C57
Grigoleit, Uwe	C47
Guo, H.	I8
Hall, Gregory	I9, C23
Halpern, Joshua B.	C27
Hammes-Schiffer, Sharon	I10
Han, Jun	C28
Harding, L.B.	C77
Harich, S.	C100
Harper, Warren W.	C29, C64
Hartland, Gregory V.	C51
Hase, William L.	C48, C58, C79
Heaven, Michael C.	I11
Heinzen, Daniel J.	I31
Herbert, John M.	C44
Hermans, L.J.F.	C30
Hernández, R.	C1
Herrero, V.J.	C94
Higgins, J.P.	C73
Hinrichs, Ryan	C18, C31, C80
Hold, Uwe	C47
Holmgren, Lotta	C2
Hoops, Alexandra	C13
Houston, Paul L.	C20, C43, C90
Howie, Wendy H.	C67
Hunag, Cheng-Liang	C32
Hutson, Jeremy M.	C33
Hwang, D.W.	C100

Ingram, John	C22
Irle, Stephan	C59
Jackson, Bret	C34, C35
Jensen, M.J.	C75, C76
Joseph, D.M.	C8
Ju, Quan	C36
Julienne, Paul S.	I12
Juurlink, L.B.F.	C85
Kaledin, Alexey	I11
Kalyanaraman, Chakrapani	C34
Kay, Kenneth G.	C37
Keller, Brian	C22
Keller, James S.	C38
Khachatrian, Ani	I6
Kim, C.	I27
Kim, Zee Hwan	C39
King, Andrew M.	C40
Kong, W.	C11, C41, C43
Krause, Paul J.	C91
Krenos, John	C42
Lambert, H.M.	C43
Lane, Ian C.	C67
Langford, Stephen R.	C14, C15, C72
Lavender, Holly B.	C56
Lee, Hee-Seung	C44
Lee, James I.	C21
Lee, Yuan T.	C50
Lehmann, K.K.	C73
Lehr, L.	C96
Lei, Jie	C45, C46

Lemoine, Didier	C34
Lendvay, G.	C77
Lenzer, Thomas	C47
Leone, Stephen R.	I13
Lester, Marsha	C84, C91, C92
Letendre, Laura T.	C51
Li, Guosheng	C48
Li, H.	C11, C41
Li, Yimin	C49
Li, Yue	C89
Light, J.C.	C69
Lin, Ao	C98
Lin, Cheng	C81
Lin, Jim J.	C50, C100
Lin, Miao-Chuan	C9
Lisy, James M.	I14
Liu, Dean-Kuo	C51
Liu, Li	C61
Liu, Xianghong	C89
Liu, Yi	C52
Loesch, Hansjürgen	I15
Lorenz, K. Thomas	C53
Lou, Nanquan	C89
Luong, A. Khai	C54
Luther, Klaus	C47
Macdonald, R. Glen	C55
Martin, Jose	C27
Martínez, H.	C1
Martínez-Haya, B.	C94
McBane, George C.	C98

McCabe, P.R.	C85
McCoy, Anne B.	C44, C56
Meijer, Anthony J.H.M.	C65
Melchior, A.	C5
Melin, Junia	I2
Meroueh, Oussama	C58
Meuwly, Markus	C33
Midey, Anthony J.	C21
Miller, Leanne M.	C38
Minayev, D.	C8
Morokuma, Keiji	C59
Morton, Melita L.	C60
Muckerman, James T.	C23, C61
Mueller, Don	C42
Mueller, J.A.	C62
Nagels, B.	C30
Nakayama, Akira	I28
Nesbitt, David J.	C13, C29, C64
Neumark, Daniel M.	I16, C13, C74, C96
Newman, Stuart M.	C67
Niederjohann, B.	C94
Nizamov, B.	C63
Nizkorodov, Sergey A.	C29, C64
Orr-Ewing, Andrew J.	C67, C72, C93
Ozhegova, Nataliya	C66
Pack, Russell T	I17
Parker, David H.	C3
Parson, John	C57
Parson, Robert	I18
Parsons, B.F.	C62

Pedersen, H.B.	C75
Peng, Tong	C68
Persson, Mats	C34
Petrongolo, Carlo	I7
Pettigrew, J. David	C19
Picconatto, C.A.	C101, C102
Pisano, Patrick J.	C43, C90
Poirier, Bill	C69
Preses, Jack M.	C23
Qi, Fei	C74, C99
Qin, Dong	C51
Ramachandran, B.	C70, C71
Ray, P.C.	C62
Ray, Paresh	C98
Regan, Paul M.	C72
Reho, J.	C73
Ritter, Alan B.	C51
Rizvi, Abbas H.	C99
Rizzo, Thomas R.	I19
Robinson, Jason C.	C74
Roozemon, D.A.	C30
Rosén, Arne	C2
Rosenwaks, S.	C5
Rostas, J.	C82
Rudert, Armin D.	C27
Safvan, C.P.	C75, C76
Schatz, G.C.	I7, C77
Schinke, Reinhard	I20
Schnieder, L.	C94
Scoles, G.	C73

Sears, Trevor J.	C23
Seekamp-Rahn, K.	C94
Sefton, James	C19
Seideman, Tamar	I6
Seiser, Natalie	C36
Setser, D.W.	C63
Shalashilin, Dmitrii V.	C34
Sidis, V.	C26
Sinha, Amitabha	I21
Sizun, Muriel	C25, C26, C78
Slattery, Marla	C19
Smith, R.R.	C85
Song, Ju-Beom	C25
Song, Kihyung	C79
Sorkahbi, Osman	C74, C99
Sperry, David C.	C21
Srivastava, A.	C101, C102
Stauffer, Hans	C18, C31, C80
Strazisar, Brian	C81
Stwalley, William C.	I22
Suits, Arthur G.	I23, C74, C99
Sun, Weizhong	C74
Symonds, Andrew C.	C47
Taieb, G.	C82
Tannor, David	I24, C83
Todd, Michael W.	C91
Truhins, Kaspars	I6
Tsakotellis, Antonis P.	C98
Tsiouris, Maria	C84
Tuckerman, Mark E.	C52

Uberna, Radek	I13
Urbain, Xavier	C76
Utz, A.L.	C85
Vaccaro, P.H.	I25
Valentini, James J.	C101, C102
van Harreveld, Rob	C86
van Hernet, Marc C.	C86
Varandas, A.J.C.	I26
Wang, Dunyou	C87
Wang, Lichang	C56
Wang, Ming L.	C88
Wang, Xiuyan	C89
Weinkauff, R.	C96
Welge, K.H.	C94
Westley, Michael S.	C90
Wheeler, Martyn D.	C84, C91, C92
White, J.M.	I27
Willis, Peter A.	C18, C31, C80
Wojcik, Michael D.	C22
Woods III, Ephraim	C12
Wrede, E.	C93, C94
Wrenn, S. Jarrett	C60
Wu, G.	C77
Xu, Kesheng	C97
Xu, Minzhong	C95
Xue, Bing	C28
Yamashita, Koichi	I28
Yang, X.	C100
Yang, X.F.	C100
Yang, Xin	C16

Yang, Xueming	C50
Zacharias, Helmut	C27
Zanni, Martin T.	C96
Zare, Richard	I29, C6, C39
Zhang, Donghui	C68
Zhang, Jingsong	C97
Zhang, John Z.H.	I30, C49, C66, C68, C87, C88
Zhao, W.	I27
Zhu, Langchi	I6

List of Participants

A. Amaya-Tapia
Centro de Ciencias Fisicas
UNAM
Cuernavaca, Mor., Mexico

Mats Andersson
Department of Experimental Physics
Chalmers University of Technology
and Göteborg University
S-412 96 Göteborg, Sweden

James D. Ayers
Department of Chemistry
Stanford University
Stanford, CA 94305

D. Babikov
Department of Chemistry
University of Illinois at Chicago
Chicago, IL 60607

Zlatko Bacic
Department of Chemistry
New York University
New York, NY 10003

Bernard L.G. Bakker
Department of Molecular
and Laser Physics
University of Nijmegen
6525 ED Nijmegen, Netherlands

N. Balakrishnan
Institute for Theoretical Atomic
and Molecular Physics
Harvard-Smithsonian Center
for Astrophysics
Cambridge, Massachusetts 02138

Gabriel G. Balint-Kurti
School of Chemistry
University of Bristol
Bristol, BS8 1TS UK

I. Bar
Department of Physics and the
Institutes for Applied Research
Ben-Gurion University of the Negev
Beer-Sheva 84105, Israel

Brian D. Bean
Department of Chemistry
Stanford University
Stanford, CA 94305

Joseph A. Bentley
Physical Sciences
Delta State University
Cleveland, MS 38733

Matthew Braunstein
Spectral Sciences, Incorporated
99 S. Bedford Street, Suite #7
Burlington, MA 01803

M. Brouard
The Physical and Theoretical
Chemistry Laboratory
Department of Chemistry
Oxford, OX1 3QZ UK

Frank E. Budenholzer
Department of Chemistry
Fu Jen Catholic University
Hsinchuang, 242 Taiwan, R.O.C.

Laurie J. Butler
Department of Chemistry
University of Chicago
Chicago, IL 60607

Zhengting Cai
Jinan, Shangdong 250100
People's Republic of China

Mark L. Campbell
Chemistry Department
United States Naval Academy
Annapolis, MD 21402

K.J. Castle
Department of Chemistry
Oregon State University
Corvallis, OR 97331

Christopher M. Cheatum
Department of Chemistry
University of Wisconsin-Madison
Madison, WI 53711

Hyeon Choi
Department of Chemistry
University of California
Berkeley, CA 94720

List of Participants

Phillip A. Cook
School of Chemistry
University of Bristol
Bristol, BS8 1TS UK

Paul J. Dagdigan
Department of Chemistry
The Johns Hopkins University
Baltimore, MD 21218

JiXin Dai
Department of Chemistry
New York University
New York, NY 10003

Floyd Davis
Department of Chemistry and
Chemical Biology
Cornell University
Ithaca, NY 14853

Ronald J. Duchovic
Indiana University-Purdue
University Fort Wayne
Fort Wayne, IN 46805

Scott M. Dylewski
Department of Chemistry and Field of
Applied and Engineering Physics
Cornell University
Ithaca, NY 14853

James M. Farrar
Department of Chemistry
University of Rochester
Rochester, NY 14627

T. Rick Fletcher
Department of Chemistry
University of Idaho
Moscow, ID 83844

Christopher Fockenberg
Chemistry Department 555A
Brookhaven National Laboratory
Upton, NY 11973

Kelsey M. Forsythe
Chemistry Division
Argonne National Laboratory
Argonne, IL 60439

Barbara Garrison
Department of Chemistry
Penn State University
University Park, PA 16802

Gustav Gerber
Physikalisches Institut
Universität Würzburg
97074 Würzburg, Germany

Eric A. Gislason
Department of Chemistry
University of Illinois at Chicago
Chicago, IL 60607

Evelyn Goldfield
Department of Chemistry
Wayne State University
Detroit, MI 48202

Stephen Gomez
Department of Chemistry
Cornell University
Ithaca, New York
14853

Robert J. Gordon
Department of Chemistry
University of Illinois at Chicago
Chicago, IL 60607

Stephen K. Gray
Chemistry Division
Argonne National Laboratory
Argonne, IL 60439

Hua Guo
Department of Chemistry
University of New Mexico
Albuquerque, NM 87131

Gregory Hall
Department of Chemistry
Brookhaven National Laboratory
Upton, NY 11973

Joshua B. Halpern
Department of Chemistry
Howard University
Washington, D.C. 20059

List of Participants

Sharon Hammes-Schiffer
Department of Chemistry and
Biochemistry
University of Notre Dame
Notre Dame, IN 46556

Jun Han
Department of Chemistry
University of Pennsylvania
Philadelphia, PA 19104

Warren W. Harper
JILA, University of Colorado and
National Institute of Standards and
Technology and Department of
Chemistry and Biochemistry,
University of Colorado
Boulder, CO 80309

Michael C. Heaven
Department of Chemistry
Emory University
Atlanta, GA 30322

Maxmilian Heckscher
University of Wisconsin-Madison
Madison, WI 53706

Daniel J. Heinzen
Department of Physics
University of Texas at Austin
Austin, TX 78712

L.J.F. Hermans
Huygens Laboratory
Leiden University
2300 RA Leiden, Netherlands

Ryan Hinrichs
Department of Chemistry and
Chemical Biology
Cornell University
Ithaca, NY 14853

Kenji Honma
Department of Material Science
Himeji Institute of Technology
Kamigori, Hyogo, Japan

Cheng-Liang Huang
Department of Chemistry
National Tsing Hua University
Hsinchu, Taiwan 300, R.O.C.

Jeremy M. Hutson
Department of Chemistry
University of Durham
Durham, DH1 3LE, England

Bret Jackson
Department of Chemistry
University of Massachusetts
Amherst, MA 01003

Charles Jaffé
Department of Chemistry
West Virginia University
Morgantown, WV 26506

Quan Ju
Department of Chemistry
Columbia University
New York, NY 10027

Paul S. Julienne
Physics Laboratory
National Institute of Standards
and Technology
Gaithersburg, MD 20899

Kenneth G. Kay
Department of Chemistry
Bar-Ilan University
Ramat-Gan 52900, Israel

James S. Keller
Department of Chemistry
and Biochemistry
University of Notre Dame
Notre Dame, IN 45665

Zee Hwan Kim
Department of Chemistry
Stanford University
Stanford, CA 94305

Andrew M. King
Department of Chemistry
University of Wisconsin
Madison, WI 53706

W. Kong
Department of Chemistry
Oregon State University
Corvallis, OR 97331

List of Participants

John Krenos
Department of Chemistry
Rutgers, the State University
Piscataway, NJ 08854

H.M. Lambert
Department of Chemistry and
Chemical Biology
Cornell University
Ithaca, NY 14853

Hee-Seung Lee
Department of Chemistry
The Ohio State University
Columbus, OH 43210

Jie Lei
Department of Chemistry
The Johns Hopkins University
Baltimore, MD 21218

Thomas Lenzer
Institut für Physikalische Chemie
Universität Göttingen
37077 Göttingen, Germany

Stephen R. Leone
JILA, University of Colorado and
National Institute of Standards and
Technology and Department of
Chemistry and Biochemistry,
University of Colorado
Boulder, CO 80309

Guosheng Li
Department of Chemistry
Wayne State University
Detroit, MI 48202

Yimin Li
Department of Chemistry
New York University
New York, NY 10003

Jim J. Lin
Institute of Atomic and Molecular
Sciences, Academia Sinica
Taipei, Taiwan, R.O.C.

James M. Lisy
Department of Chemistry
University of Illinois
Urbana, IL 61801

Dean-Kuo Liu
Department of Chemistry
University of Pennsylvania
Philadelphia, PA 19104

Yi Liu
Department of Chemistry
New York University
New York, NY 10003

Hansjürgen Loesch
Fakultät für Physik
Universität Bielefeld
D-33615 Bielefeld, Germany

K. Thomas Lorenz
Sandia National Laboratories
Livermore, CA

A. Khai Luong
Department of Chemistry and
Biochemistry
University of California, San Diego
La Jolla, CA 92093

R. Glen Macdonald
Argonne National Laboratory
Chemistry Division
Argonne, IL 60439

George C. McBane
Department of Chemistry
The Ohio State University
Columbus, OH 43210

Anne B. McCoy
Department of Chemistry
The Ohio State University
Columbus, OH 43210

Anthony J. H. M. Meijer
Department of Chemistry
Wayne State University
Detroit, MI 48202

Oussama Meroueh
Department of Chemistry
Wayne State University
Detroit, MI 48202

List of Participants

Keiji Morokuma
Cherry L. Emerson Center for
Scientific Computation
and Department of Chemistry
Emory University
Atlanta, GA 30322

Melita L. Morton
The James Franck Institute and
Department of Chemistry
The University of Chicago
Chicago, IL 60637

James T. Muckerman
Chemistry Department
Brookhaven National Laboratory
Upton, NY 11973

J.A. Mueller
The James Franck Institute and
Department of Chemistry
The University of Chicago
Chicago, IL 60637

Daniel M. Neumark
Department of Chemistry
University of California
Berkeley, CA 94720

B. Nizamov
Department of Chemistry
Kansas State University
Manhattan, KS 66506

Sergey A. Nizkorodov
JILA, University of Colorado and
National Institute of Standards and
Technology and Department of
Chemistry and Biochemistry,
University of Colorado
Boulder, CO 80309

Andrew J. Orr-Ewing
School of Chemistry
University of Bristol
Bristol BS8 1TS, UK

Nataliya Ozhegova
Department of Chemistry
New York University
New York, NY 10003

Russel T Pack
Theoretical Division
Los Alamos National Laboratory
Los Alamos, NM 87545

John Parson
Department of Chemistry
The Ohio State University
Columbus, OH 43210

Robert Parson
JILA, University of Colorado and
National Institute of Standards and
Technology and Department of
Chemistry and Biochemistry,
University of Colorado
Boulder, CO 80309

Tong Peng
Department of Chemistry
New York University
New York, NY 10003

Carl Picconatto
Department of Chemistry
Columbia University
New York, NY 10027

Patrick Pisano
Department of Chemistry
and Chemical Biology
Cornell University
Ithaca, NY 14853

Bill Poirier
The James Franck Institute
The University of Chicago
Chicago, IL 60637

Jack M. Preses
Chemistry Department
Brookhaven National Laboratory
Upton, NY 11973-5000

B. Ramachandran
Department of Chemistry
Louisiana Tech University
Ruston, LA 71272

List of Participants

Paul M. Regan
School of Chemistry
University of Bristol
Bristol, BS8 1TS UK

J. Reho
Department of Chemistry
Princeton University
Princeton, NJ 08544

Thomas R. Rizzo
Laboratoire de chimie physique
moléculaire
École Polytechnique Fédérale de
Lausanne
Lausanne, Switzerland

Jason C. Robinson
Department of Chemistry
University of California and
Chemical Sciences Division
Berkeley National Laboratory
Berkeley, CA 94720

Celeste M. Rohlfing
National Science Foundation
Arlington, VA 22230

Eric Rohlfing
U.S. Department of Energy
Office of Energy Research
Division of Chemical Sciences
Germantown, MD 20874

C. P. Safvan
Institute of Physics and Astronomy
University of Aarhus
DK-8000 Aarhus C, Denmark

G. C. Schatz
Department of Chemistry
Northwestern University
Evanston, IL 60208-3113

Reinhard Schinke
Max-Planck-Institut für
Strömungsforschung
D-37073 Göttingen, Germany

Amitabha Sinha
Department of Chemistry and
Biochemistry
University of California-San Diego
La Jolla, CA 92093

Muriel Sizun
Laboratoire des Collisions Atomiques
et Moléculaires
Universite Paris XI
91405 Orsay Cedex, France

Kihyung Song
Department of Chemistry
Korea National University
of Education
Chongwon, Chungbuk 363-791, Korea

Osman Sorkhabi
Chemical Sciences Division
Lawrence Berkeley National
Laboratory
Berkeley, CA 94720

Abneesh Srivastava
Department of Chemistry
Columbia University
New York, NY 10027

Hans U. Stauffer
Department of Chemistry and
Chemical Biology
Cornell University
Ithaca, New York 14853

Brian Strazisar
Department of Chemistry and
Chemical Biology
Cornell University
Ithaca, New York 14853

William C. Stwalley
Department of Chemistry
University of Connecticut
Storrs, CT 06269

Arthur G. Suits
Chemical Sciences Division
Lawrence Berkeley National
Laboratory
Berkeley, CA 94720

Weizhong Sun
Department of Chemistry
University of California
and Chemical Sciences Division
Lawrence Berkeley National
Laboratory
Berkeley, CA. 94720

List of Participants

G. Taieb
Laboratoire de Photophysique
Moléculaire du CNRS
Université de Paris Sud
91405 Orsay, France

Xiaofeng Tan
Department of Chemistry
The Johns Hopkins University
Baltimore, MD 21218

David J. Tannor
Department of Chemical Physics
Weizmann Institute of Science
Rehovot, 76100 Israel

Maria Tsiouris
Department of Chemistry
University of Pennsylvania
Philadelphia, PA 19104

A.L. Utz
Department of Chemistry
and W.M. Keck Foundation
Laboratory for Materials Chemistry
Tufts University
Medford, MA 02155

P.H. Vaccaro
Department of Chemistry
Yale University
New Haven, CT 06520

James J. Valentini
Department of Chemistry
Columbia University
New York, NY 10027

Marc C. van Hemert
Leiden Institute of Chemistry
Gorlaeus Laboratories
Leiden University
2300RA Leiden, Netherlands

A.J.C. Varandas
Departamento de Química
Universidade de Coimbra
3049 Coimbra Codex, Portugal

Dunyou Wang
Department of Chemistry
New York University
New York, NY 10003

Ming L. Wang
Department of Chemistry
New York University
New York, NY 10003

Xiuyan Wang
State Key Laboratory of Molecular
Reaction Dynamics
Dalian Institute of Chemical Physics
Chinese Academy of Sciences
Dalian 116023, P.R.C.

Michael S. Westley
Department of Chemistry
Cornell University
Ithaca, NY 14853

Martyn D. Wheeler
Department of Chemistry
University of Pennsylvania
Philadelphia, PA 19104

J.M. White
Center for Material Chemistry
and Department of Chemistry
and Biochemistry
University of Texas at Austin
Austin, TX 78712

E. Wrede
School of Chemistry
University of Bristol
Bristol, BS8 1TS UK

Minzhong Xu
Department of Chemistry
New York University
New York, NY 10003

Koichi Yamashita
Department of Chemical
System Engineering
The University of Tokyo
113-8656 Tokyo, Japan

Sangwoon Yoon
Department of Chemistry
University of Wisconsin-Madison
Madison, WI 53706

Martin T. Zanni
Department of Chemistry
University of California
Berkeley, CA 94720

List of Participants

Richard N. Zare
Department of Chemistry
Stanford University
Stanford, CA 94305

Jianming Zhang
Department of Chemistry
and Biochemistry
Montana State University
Bozeman, MT 59717

Jingsong Zhang
Department of Chemistry and
Air Pollution Research Center
University of California, Riverside
Riverside, CA 92521

John Z.H. Zhang
Department of Chemistry
New York University
New York, NY 10003

AIR FORCE OFFICE OF SCIENTIFIC
RESEARCH (AFOSR)
NOTICE OF TRANSMITTAL TO DTIC. THIS
TECHNICAL REPORT HAS BEEN REVIEWED
AND IS APPROVED FOR PUBLIC RELEASE
IN ACCORDANCE WITH AFR 190-12. DISTRIBUTION IS
UNLIMITED
YOUNG MANN
STINFO PROGRAM MANAGER